

INFORMATION TO USERS

This manuscript has been reproduced from the microfilm master. UMI films the text directly from the original or copy submitted. Thus, some thesis and dissertation copies are in typewriter face, while others may be from any type of computer printer.

The quality of this reproduction is dependent upon the quality of the copy submitted. Broken or indistinct print, colored or poor quality illustrations and photographs, print bleedthrough, substandard margins, and improper alignment can adversely affect reproduction.

In the unlikely event that the author did not send UMI a complete manuscript and there are missing pages, these will be noted. Also, if unauthorized copyright material had to be removed, a note will indicate the deletion.

Oversize materials (e.g., maps, drawings, charts) are reproduced by sectioning the original, beginning at the upper left-hand corner and continuing from left to right in equal sections with small overlaps.

Photographs included in the original manuscript have been reproduced xerographically in this copy. Higher quality 6" x 9" black and white photographic prints are available for any photographs or illustrations appearing in this copy for an additional charge. Contact UMI directly to order.

**Bell & Howell Information and Learning
300 North Zeeb Road, Ann Arbor, MI 48106-1346 USA
800-521-0600**

UMI[®]

QUALITATIVE INVESTIGATIONS OF SOLUTIONS TO
EINSTEIN'S FIELD EQUATIONS ADMITTING A
KINEMATIC SELF-SIMILARITY

By
Patricia M. Benoit

SUBMITTED IN PARTIAL FULFILLMENT OF THE
REQUIREMENTS FOR THE DEGREE OF
DOCTOR OF PHILOSOPHY
AT
DALHOUSIE UNIVERSITY
HALIFAX, NOVA SCOTIA
MARCH 1999

© Copyright by Patricia M. Benoit, 1999



National Library
of Canada

Acquisitions and
Bibliographic Services

395 Wellington Street
Ottawa ON K1A 0N4
Canada

Bibliothèque nationale
du Canada

Acquisitions et
services bibliographiques

395, rue Wellington
Ottawa ON K1A 0N4
Canada

Your file Votre référence

Our file Notre référence

The author has granted a non-exclusive licence allowing the National Library of Canada to reproduce, loan, distribute or sell copies of this thesis in microform, paper or electronic formats.

The author retains ownership of the copyright in this thesis. Neither the thesis nor substantial extracts from it may be printed or otherwise reproduced without the author's permission.

L'auteur a accordé une licence non exclusive permettant à la Bibliothèque nationale du Canada de reproduire, prêter, distribuer ou vendre des copies de cette thèse sous la forme de microfiche/film, de reproduction sur papier ou sur format électronique.

L'auteur conserve la propriété du droit d'auteur qui protège cette thèse. Ni la thèse ni des extraits substantiels de celle-ci ne doivent être imprimés ou autrement reproduits sans son autorisation.

0-612-49244-3

Canada

DALHOUSIE UNIVERSITY

FACULTY OF GRADUATE STUDIES

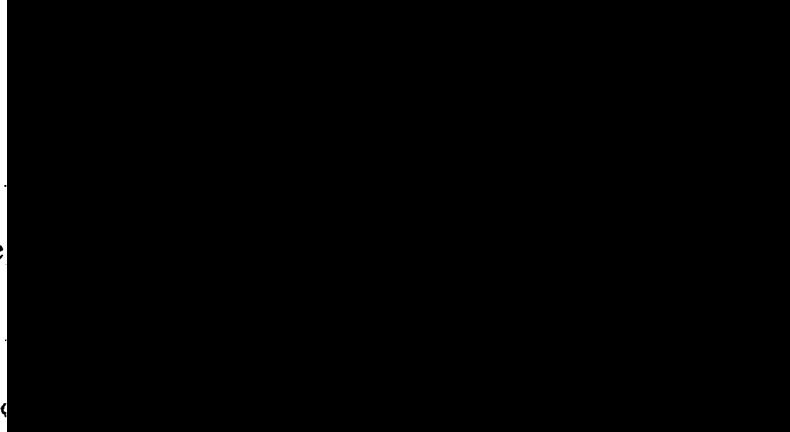
The undersigned hereby certify that they have read and recommend to the Faculty of Graduate Studies for acceptance a thesis entitled "Qualitative Investigations Of Solutions To Einstein's Field Equations Admitting A Kinematic, Self-Similarity"

by Patricia Benoit

in partial fulfillment of the requirements for the degree of Doctor of Philosophy.

Dated: March 26, 1999

External Examiner
Research Supervisor
Examining Committee



DALHOUSIE UNIVERSITY

Date: January 1999

Author: Patricia M. Benoit

**Title: Qualitative Investigations of Solutions to Einstein's
Field Equations Admitting a Kinematic
Self-Similarity**

Department: Mathematics Statistics and Computing Science

Degree: Ph.D. Convocation: May Year: 1999

Permission is herewith granted to Dalhousie University to circulate and to have copied for non-commercial purposes, at its discretion, the above title upon the request of individuals or institutions.



Signature of Author

THE AUTHOR RESERVES OTHER PUBLICATION RIGHTS, AND NEITHER THE THESIS NOR EXTENSIVE EXTRACTS FROM IT MAY BE PRINTED OR OTHERWISE REPRODUCED WITHOUT THE AUTHOR'S WRITTEN PERMISSION.

THE AUTHOR ATTESTS THAT PERMISSION HAS BEEN OBTAINED FOR THE USE OF ANY COPYRIGHTED MATERIAL APPEARING IN THIS THESIS (OTHER THAN BRIEF EXCERPTS REQUIRING ONLY PROPER ACKNOWLEDGEMENT IN SCHOLARLY WRITING) AND THAT ALL SUCH USE IS CLEARLY ACKNOWLEDGED.

Contents

List of Tables	vii
List of Figures	viii
Abstract	xi
1 Introduction and Background	1
1.1 Self-Similarity	2
1.1.1 Self-Similarity in Cosmology	3
1.1.2 Kinematic Self-Similarity	6
1.2 Brief Survey of Techniques in Dynamical Systems	11
1.3 Outline of Work	19
2 Einstein's Field Equations with Kinematic Self-Similarity	21
2.1 Comparison to Cahill and Taub's Derivations	24
2.2 Plane and Hyperbolic Symmetry	26
2.3 Algebraic Structure	28
3 Physical Self-Similarity for Spherically Symmetric Metrics	30
3.1 Special Subcase: $M_1 = 0$	31
3.1.1 Zeroth Order geodesic solutions	35
3.2 Special Subcase: $M_2 = 0$	36
3.2.1 Static Models	37

3.2.2	Zeroth Type static solutions	40
4	Qualitative Behaviour of Governing Equations	41
4.1	Shear-Free Solutions: $x_2 = 0$	45
4.1.1	Curvature Dominated Solutions: $x_4 \rightarrow \pm\infty$	49
4.1.2	Shear-free solutions in the full four-dimensional space	53
4.2	Plane Symmetric Solutions: $x_4 = 0$	54
4.3	Physical Nature of Asymptotic Solutions	76
4.3.1	Finite Singular Points	76
4.3.2	Infinite Singular points	78
4.4	Summary of the Dynamics	81
5	Infinite Kinematic Self Similarity	87
5.1	Reduction of the EFEs in full	87
5.2	Qualitative Analysis	90
5.2.1	Subcase: $x_2 = 0$	93
5.2.2	Subcase: $x_4 = 0$ - Plane Symmetry	95
5.3	Description of Asymptotic Solutions	102
5.3.1	Finite Singular Point Asymptotic States	103
5.3.2	Infinite Singular Point Asymptotic States	103
5.4	Physical Self-Similarity for Infinite KSS	105
5.4.1	Case I: $x_3 = 0$	105
5.4.2	Case II: $x_1 = 0$	106
5.4.3	Case III: $x_4 + 2x_1x_3 + x_1^2 = 0$	108
5.5	Summary	108
6	Anisotropic Fluids	109
6.1	Geodesic Models	112
6.1.1	Perfect Fluid Models	113
6.1.2	Solutions with $S + \dot{S} = 0$	114
6.2	Special Cases	115

6.2.1	Case A: Dimensional Constants	115
6.2.2	Case B: Equations of State	116
6.3	Analysis of Special Cases	117
6.4	Discussion	121
6.5	Other Models	123
7	Discussion	125
7.1	Phase Space and Dynamics	125
7.2	Physical Self-Similarity	126
7.3	Physical Considerations: Equation of State and Energy Conditions . .	129
7.4	Remarks	132
7.5	Brief comments on future work	134
A	Investigation of Eigenvalue Algebra	136
	References	140

List of Tables

4.1	Finite Singular Points for equations (4.1)-(4.4).	43
4.2	Classification of the Infinite Singular Points of the system of equations (4.5)-(4.8)	44
4.3	Finite Singular Points for equations (4.11)-(4.12).	46
4.4	Classification of Local dynamics for finite singular points of (4.11)-(4.12).	48
4.5	Summary of finite singular points for plane symmetric solutions with non-zero shear.	83
5.1	Finite Singular Points for equations (5.22)-(5.25).	92
5.2	Invariant regions of the space (x_1, x_2, x_3) for the system (5.40)-(5.42).101	
6.1	Classification of Finite Singular Points for equations (6.36)-(6.37) 118	

List of Figures

4.1	Phase portrait of spherically symmetric solutions with zero shear . . .	50
4.2	Phase portrait of plane symmetric solutions with zero shear	51
4.3	Phase portrait of hyperbolically symmetric solutions with zero shear .	52
4.4	Local Dynamics of the singular point \mathbf{Q}	56
4.5	Eigenvalues for the singular point \mathbf{R}_+	58
4.6	Eigenvalues for the singular point \mathbf{R}_+	58
4.7	Eigenvalues for the singular point \mathbf{R}_-	59
4.8	Local dynamics of the singular point \mathbf{R}_+	60
4.9	Local dynamics of the singular point \mathbf{R}_-	61
4.10	Dynamics on the infinite boundary for the plane symmetric solutions	62
4.11	Dynamics on the infinite boundary for the plane symmetric solutions	63
4.12	Plot of isocline surfaces for the system (4.26)-(4.28)	65
4.13	Direction fields for plane symmetric solutions with positive shear . . .	68
4.14	Numerically generated orbits for the region U_4	69
4.15	Numerically generated orbits for the region U_6	70
4.16	Direction fields for plane symmetric solutions with negative shear . .	72
4.17	Numerically generated orbits for the region U_9	73
4.18	Numerically generated orbits for the region U_7	74
4.19	Numerically generated orbits for the region U_{11}	75
4.20	Schematic of the path of generic orbits for plane symmetric solutions with positive shear	84

4.21	Schematic of the path of generic orbits for plane symmetric solutions with negative shear	85
5.1	Phase portrait of the Poincare transformation of system (5.35)- (5.36)	96
5.2	Phase portrait of the Poincare transformation of system (5.45)- (5.46)	98
5.3	Phase portrait of the Poincare transformation of system (5.45)- (5.46)	99
5.4	Phase portrait of the Poincare transformation of system (5.47)- (5.48)	100
6.1	Phase portraits for the system (6.39)/(6.40)	120

To Jennie.

Abstract

We will show that the perfect fluid Einstein field equations in the case of spherical, plane and hyperbolic symmetry reduce to an autonomous system of ordinary differential equations when a spacetime is assumed to admit a kinematic self-similarity (of either the second or zeroth kind). The qualitative properties of solutions of this system of equations, and in particular their asymptotic behaviour, will be investigated. Some details of the nature of kinematic self-similarity will be discussed to demonstrate the importance of various subcases of the full model. In particular, the geodesic subcase and a subcase containing the static models will be examined in detail. Exact solutions in these important subcases will be given and their asymptotic behaviour fully discussed. Exact solutions admitting a homothetic vector (i.e., a self-similarity of the first kind) will be shown to play an important role in describing the asymptotic behaviour of the kinematic self-similar models. The mathematical techniques developed in the examination of perfect fluid solutions will then be applied to the case of an anisotropic fluid. The special case of kinematic self-similarity of infinite type will also be discussed.

Acknowledgements

I would like to take this opportunity to thank those people whose assistance and presence have made the completion of this work possible.

First and foremost I would like to thank my supervisor, Dr. Alan Coley. His assistance and patience both through the work and the writing of this thesis has been most appreciated. In addition I would like to thank him for his meticulous reading of my work, and his genuine concern for my professional development and future successes.

In addition, I would like to thank the graduate coordinators who have helped smooth the administrative "waters," namely Dr. Thompson, Dr. Sutherland and Dr. Keast. A graduate coordinator can make a big difference, and I thank each of you for the care with which you do your jobs. In addition, I must thank my brother David for his endless computer support.

I greatly acknowledge the financial support of the Natural Sciences and Engineering Research Council, the Sumner Foundation and Dalhousie University. Without financial support, this work, most certainly, could not have been completed.

Finally, on a more personal note I would like to thank those people whose emotional support have helped throughout my years at Dalhousie. My friends have been constant throughout these years, so: To my "skating buddies," many thanks for making me laugh and letting me vent; to my fellow students, Andrew, Hossien and Robert, "Merci" for the endless support; and to Jeff and Bill, "Grazie" for the smiles and for being the ever-present support that you are. And lastly, and most importantly, to my family whose love is never failing my humble thanks.

Chapter 1

Introduction and Background

The primary goal of cosmology is to describe the large-scale structure of our Universe. In 1915 Einstein developed the Theory of General Relativity which provides the necessary mathematical framework to begin an investigation of possible models of the Universe. The theory provides a link between the geometry of the Universe (imposed by the gravitational field) and the matter (or the fluid) which makes up the Universe. In natural units, $c = 8\pi G = 1$, this theory results in a system of governing equations, referred to as Einstein's Field Equations (EFEs), which read:

$$G_{ab} = T_{ab}, \tag{1.1}$$

where G denotes the Einstein tensor and T the matter tensor.

The EFEs represented by equation (1.1) are in general a system of ten highly non-linear partial differential equations (PDEs) in four independent variables. The complexity of these equations presents a great deal of computational challenges, which has left the theory lacking any "general solutions". At the same time, however, equations (1.1) provide the study of cosmology with a vast and diverse set of solutions which model the possible evolution of the Universe. The various cosmological models which have been studied over the years have typically resulted from an initial set of assumptions on the content of the fluid and/ or the geometry which are consistent with the astronomical observations of the present state of our Universe. These assumptions

result in a simplification of the system (1.1), and in each case may give rise to special solutions, or classes of solutions.

Once classes of solutions to the EFEs are found a variety of mathematical methods have been used to investigate their nature. These methods include, though are not limited to (Wainwright and Ellis, 1997):

1. Topological Methods
2. Numerical Methods
3. Perturbation Methods
4. Qualitative Methods

In particular, qualitative methods focuses on the examination of the evolution of classes of solutions with emphasis on their asymptotic states (past, future, and intermediate) which is of special importance in cosmology theory. The mathematical theory of dynamical systems has provided support to these investigations. Dynamical systems theory originated with the work of Poincare (see, for example, Guckenheimer and Holmes, 1983), with special focus on the study of autonomous ordinary differential equations (ODEs). A summary of dynamical systems theory will be given in section 1.2.

The work of this thesis involves the study of a class of solutions of the EFEs using a dynamical systems approach. An initial assumption of generalised self-similarity is made, which allows the EFEs to reduce to a self consistent system of autonomous ODEs. The details of the assumption of self-similarity and its role in cosmology will now be discussed.

1.1 Self-Similarity

Similarity solutions of DEs are those solutions which are found by assuming that the DEs are invariant under particular continuous transformations. While these solutions

are not *general* solutions of the DEs, they are, however, important because they often represent intermediate asymptotics of the system (for more details see section 1.2). In general, similarity solutions which are *self-similar* are those which are invariant under scaling transformations of the independent variables. The scaling transformations form a Lie group. The infinitesimal transformation of this group then defines the infinitesimal generator, from which the invariants of the group action can be determined. The use of these properties of Lie groups to the simplification of differential equations has been outlined in various texts (see Ovsianikov [1982] for a formal treatment, and Hui [1985] for an outline of the method). The invariants of the Lie group then represent invariants of the differential equation. When the solutions of the differential equations are restricted to be in the form of the invariants, the equations simplify. Solutions to these simplified equations are then called *similarity solutions*

Geometrically, given a differentiable manifold the existence of self-similarity can be intrinsically defined in terms of the metric components which define the manifold. In particular, the infinitesimal generator (now referred to as the self-similar generator) and the invariants (now referred to as the similarity variable) can be defined through the metric. These definitions will be discussed in the next section.

1.1.1 Self-Similarity in Cosmology

Geometrically, self-similarity refers to the situation in which the spatial distribution of the characteristics of motion remains similar to itself at all times. Solutions possessing this symmetry in classical (Newtonian) theory were investigated by Barenblatt and Zel'dovich (1972) where they showed that self-similar solutions represent solutions of degenerate problems in which all dimensional constant parameters from the initial or boundary conditions vanish or become infinite. Cases in which the form of the self-similar asymptotics can be obtained from dimensional considerations alone were termed "self-similar solutions of the first kind." In Newtonian hydrodynamics self-similar solutions occur when the functions used in the definitions of all physical quantities depend on the similarity variable $x/l(t)$ where x and t are the independent

variables of the system and $l(t)$ is a time dependent scale. In the case in which the asymptotics are obtained from dimensional considerations only, the function $l(t)$ is simply the identity function $l(t) = t$. In all cases, this functional dependence then results in a reduction of the number of independent variables for the governing equations.

The reduction of the number of independent variables implies a reduction in the complexity of the governing equations. It is this reduction in complexity that provided the initial motivation for the study of self-similar solutions. More physical motivation came as a result of the realization that self-similar solutions describe the "intermediate-asymptotic" behaviour of solutions when they are in the region which no longer depends on the initial and/ or boundary values, even though the system may be far from its state of equilibrium (Barenblatt and Zel'dovich, 1972).

Since the pioneering work of Sedov in 1946, the study of self-similar solutions has played an important role for many physical phenomenon, including the study of strong (nuclear) explosions (Sedov, 1946 and 1967; Taylor, 1950) and a thermal wave (Zel'dovich and Kompaneets, 1950; Barenblatt, 1952; Zel'dovich and Raizer, 1963). Similarity solutions are also of interest within general relativity. For example, an explosion in a homogeneous background produces fluctuations that may be complicated initially, but they may tend to be described more closely by a simpler spherically symmetric similarity model as time evolves (Sedov, 1967), and this applies even if the explosion takes place in an expanding cosmological background (Schwartz et al., 1975; Ikeuchi et al., 1983).

In cosmology, the expansion of the Universe from the big bang (and the collapse of a star to a singularity) might (both) exhibit self-similarity in some form since it might be expected that the initial conditions "are forgotten" in some sense. Indeed, the possibility that (at least in some circumstances) fluctuations naturally evolve (via the EFEs) to a self-similar solution in the non-linear regime from initially more complicated initial conditions have been studied by several authors previously (see Coley, 1996 and Coley and Carr, 1998).

Cahill and Taub (1971) were the first to study similarity solutions within the framework of general relativity. They did so in the cosmological context and under the assumption of a spherically symmetric distribution of a self-gravitating perfect fluid, in which the energy-momentum tensor is given by

$$T_{ab} = (\mu + p)u_a u_b + p g_{ab}, \quad (1.2)$$

where u^a is the normalised fluid 4-velocity and μ and p are, respectively, the density and pressure. They assumed that the solution was such that the dependent variables are essentially functions of a single independent variable constructed as a dimensionless combination of the independent variables (r and t , and the solution is invariant under the transformation $\bar{t} = at$, $\bar{r} = ar$; a constant) and that the model contains no other dimensional constants; in other words, the assumption of "self-similarity of the *first kind*".

Cahill and Taub (1971) showed that the existence of a similarity (of the first kind) in this situation could be invariantly formulated in terms of the existence of a homothetic vector. A proper homothetic vector (HV) in a given spacetime is a vector field ξ which satisfies (after a constant rescaling)

$$\mathcal{L}_\xi g_{ab} = 2g_{ab}, \quad (1.3)$$

where g_{ab} is the spacetime metric and \mathcal{L} denotes Lie differentiation along ξ . From (1.3) we have that

$$\mathcal{L}_\xi G_{ab} = 0. \quad (1.4)$$

From dimensional considerations, in the case of self-similarity of the first kind and if the source of the gravitational field is a perfect fluid, the physical quantities transform according to (Cahill and Taub, 1971)

$$\mathcal{L}_\xi u^a = -u^a, \quad (1.5)$$

and

$$\mathcal{L}_\xi \mu = -2\mu, \quad \mathcal{L}_\xi p = -2p. \quad (1.6)$$

From these equations it follows that

$$\mathcal{L}_{\xi}T_{ab} = 0, \quad (1.7)$$

which is consistent with the EFEs (1.1). Indeed, in the case of a perfect fluid it follows that (Cahill and Taub, 1971; Eardley, 1974) equations (1.5) and (1.6) result from equations (1.3) [through eqns. (1.1), (1.4) and (1.7)] so that the physical quantities transform appropriately. The term "geometric" self-similarity will be used to indicate that the geometry terms (or terms of the metric tensor) remain self-similar to themselves through the evolution (and equation (1.3) holds), and the term "physical" self-similarity will be used to indicate that the physical (or matter) variable (in the case of a perfect fluid, the energy density and pressure) remain self-similar (and equations (1.6) hold). Hence in this case of a perfect fluid "geometric" self-similarity and "physical" self-similarity coincide. However, this need not be the case (cf. Coley, 1997).

The existence of self-similar solutions of the first kind is related to the conservation laws and to the invariance of the problem with respect to the group of similarity transformations of quantities with independent dimensions. In this case a certain regularity of the limiting process in passing from the original non-self-similar regime to the self-similar regime is implicitly assumed. However, in general such a passage to this limit need not be regular, whence the expressions for the self-similar variables are not determined from dimensional analysis of the problem alone. Solutions are then called *self-similar solutions of the second kind*. Characteristic of these solutions is that they *contain dimensional constants* that are not determined from the conservation laws (but can be found by matching the self-similar solutions with the non-self-similar solutions whose asymptotes they represent) (Barenblatt and Zel'dovich, 1972).

1.1.2 Kinematic Self-Similarity

Self-similarity in the broadest sense refers to the general situation in which a system is not restricted to be strictly invariant under the relevant group action, but merely

to be appropriately rescaled. The basic condition characterising a manifold vector field ξ as a self-similar generator (Carter and Henriksen, 1991) is that there exist constants d_i such that for each independent physical field Φ^i ,

$$\mathcal{L}_\xi \Phi_A^i = d_i \Phi_A^i, \quad (1.8)$$

where the fields Φ_A can be scalar (e.g., μ), vectorial (e.g., u_a) or tensorial (e.g., g_{ab}). In general relativity the gravitational field is represented by the metric tensor g_{ab} , and an appropriate definition of "geometrical" self-similarity is necessary. In the seminal work by Cahill and Taub (1971) the simplest generalisation was effected whereby the metric itself satisfies an equation of the form (1.8), namely ξ is a HV, this evidently corresponding to Zel'dovich's similarity of the first kind.

However, in general relativity it is not the energy-momentum tensor itself that must satisfy (1.8), but each of the physical fields making up the energy-momentum tensor must separately satisfy an equation of the form (1.8). In the case of a fluid characterised by the timelike congruence u_a the energy-momentum tensor can be uniquely decomposed with respect to u_a (Ellis, 1971), and each of these uniquely defined components (each of which has a physical interpretation in terms of the energy, pressure, heat flow and anisotropic stress as measured by an observer comoving with the fluid) must separately satisfy an equation of the form (1.8). In the same way, if the metric can be uniquely, physically, and covariantly decomposed then the homothetic condition can be replaced by the conditions that each uniquely defined component must satisfy (1.8), maintaining self-similarity. For example, in the case of a fluid, the metric can be decomposed uniquely in terms of u_a , through the projection tensor

$$h_{ab} = g_{ab} + u_a u_b, \quad (1.9)$$

into parts h_{ab} and (minus) $u_a u_b$. The projection tensor represents the projection of the metric into the 3-spaces orthogonal to u^a (i.e., into the rest frame of the comoving observers), and if u_a is irrotational these 3-spaces are surface forming, the decomposition is global, and h_{ab} represents the intrinsic metric of these 3-spaces.

It is arguments similar to these, and, more importantly, a detailed comparison with self-similarity in a continuous Newtonian medium, that has led Carter and Henriksen (1989) to the covariant notion of *kinematic self-similarity* in the context of relativistic fluid mechanics. A kinematic self-similarity vector ξ satisfies the condition

$$\mathcal{L}_\xi u_a = \alpha u_a, \quad (1.10)$$

where α is a constant (i.e., ξ is a continuous kinematic self-similar generator with respect to the flow u_a). Furthermore,

$$\mathcal{L}_\xi h_{ab} = 2\delta h_{ab} \quad (1.11)$$

where δ is a constant. It should be noted that various different cases of self-similarity are included in the definitions (1.10)-(1.11), depending on the relative values of the constants α and δ . The different classes can be summarised as follows:

1. ξ is a Killing Vector: If the two constants α and δ are identically zero then equations (1.10)/(1.11) are equivalent to $\mathcal{L}_\xi g_{ab} = 0$; the Killing equations. The vector ξ is then simply a Killing Vector.
2. ξ is a Homothetic Vector: If the two constants are not zero such that $\alpha = \delta$ the equations (1.10)/(1.11) are equivalent to $\mathcal{L}_\xi g_{ab} = 2g_{ab}$ (after a normalisation of the vector ξ), and the vector is simply a homothetic vector.
3. ξ is a Kinematic Self-Similarity of Infinite type: If $\delta = 0$ and α is non-zero, equations (1.10)/(1.11) become

$$\mathcal{L}_\xi u_a = u_a \quad (1.12)$$

$$\mathcal{L}_\xi h_{ab} = 0 \quad (1.13)$$

In this case the transformation is that of a generalised rigid rotation. Equations (1.12)/(1.13) will now form the definition for a vector ξ to be a kinematic self-similar vector of infinite type. These symmetries will be investigated in Chapter 5.

4. ξ is a proper Kinematic Self-Similarity: When α and δ are not zero (and $\alpha \neq \delta$) a normalisation of the vector ξ results in equations (1.10)/ (1.11) simplifying to

$$\mathcal{L}_\xi u_a = \alpha u_a \quad (1.14)$$

$$\mathcal{L}_\xi h_{ab} = 2h_{ab} \quad (1.15)$$

Equations (1.14)/(1.15) now form the definition for a vector ξ to be a proper KSS. Note that the case of $\alpha = 0$, which will be referred to as KSS of zeroth type, is a special case whose properties will differ from other cases (see below).

Note that the full group of kinematic self-similar vectors defined by (1.10)/(1.11) have as proper subgroups the group of homothetic vectors and the group of killing vectors. Using definitions (1.14)/(1.15), however, the vector has been normalised and the group of Killing vectors are no longer a subgroup. The homothetic vectors, however, remain as a subgroup - characterised by the parameter α having value identically equal to 1.

Carter and Henriksen (1989) then argue that the case $\alpha \neq 1$ ($\alpha = 0$) in equations (1.14)/(1.15) is the natural relativistic counterpart of self-similarity of the more general second kind (zeroth kind). An extensive study of perfect fluid spacetimes that admit a kinematic self-similarity, and the mathematical properties of kinematic self-similarity vectors (including, for example, their Lie algebra structure) was presented in Coley (1997).

The self-similar index α represents the constant relative proportionality factor governing the rates of dilation of spatial length scale and amplification of time scale. Evidently, when $\alpha \neq 1$ (i.e., ξ is not a HV), the relative rescaling of space and time (under ξ) are not the same (and in the zeroth case there is a space dilation without any time amplification).

In the case of spherical symmetry all dimensionless quantities are functions of a single independent variable ξ , which is a dimensionless combination of space coordinates and time. In the absence of any physical dimensional scale this reduces (through the use of c) to $\xi = r/t$ (similarity of the "first" kind). However, in the more general

case ξ can be a more complicated expression (see, for example, equations (1.18) and (1.19) below). Indeed, in the *spherically symmetric* case Carter and Henriksen (1989) have shown that there exist comoving coordinates in which the kinematic self-similar generator is given by

$$\xi^a \frac{\partial}{\partial x^a} = (\alpha t + \beta) \frac{\partial}{\partial t} + r \frac{\partial}{\partial r}, \quad (1.16)$$

and the metric is given by

$$ds^2 = -e^{2\Phi} dt^2 + e^{2\Psi} dr^2 + r^2 S^2 d\Omega^2, \quad (1.17)$$

where $d\Omega^2 \equiv d\theta^2 + \sin^2\theta d\phi^2$ and Φ, Ψ and S depend only on the self-similarity coordinate ξ . In (1.17) the usual metric function $R(t, r)$ is given as $R = rS$. The metric (1.17) is consequently manifestly of the same form as in Cahill and Taub (1971), and the resulting governing differential equations do indeed reduce to a system of ODEs, see Chapter 2.

In the case of self-similarity of the first kind, i.e., the homothetic case, $\alpha = 1$ (and β can be rescaled to zero) and $\xi = r/t$, as usual (Cahill and Taub, 1971).

In the lesser-studied zeroth case, $\alpha = 0$ (and β can be rescaled to unity) and

$$\xi = re^{-t}. \quad (1.18)$$

An example of this case is provided by the solution of Henriksen, Emslie and Wesson (1983) in which a dimensional constant (and hence a fundamental scale) is introduced via the cosmological constant (see also Carter and Henriksen, 1989).

In the general case $\alpha \neq 0, 1$ (β rescaled to zero), corresponding to *self-similarity of the second kind*, the self-similarity coordinate is given by

$$\xi = r(\alpha t)^{-1/\alpha}. \quad (1.19)$$

An important example of the second-kind self-similarities is provided by a class of zero-pressure perfect fluid models (i.e., dust models in which u^a is geodesic; i.e., $\Phi' = 0$ in equation (1.17)) first studied by Lynden-Bell and Lemos (1988) and described in detail by Henriksen (1989) and Carter and Henriksen (1989).

Finally, when considering a perfect fluid, as we are in the present study, equations (1.8) will be satisfied for the energy and pressure if the following conditions are satisfied:

$$\mathcal{L}_{\xi}\mu = a\mu, \quad (1.20)$$

$$\mathcal{L}_{\xi}p = bp, \quad (1.21)$$

where a and b are constants.

1.2 Brief Survey of Techniques in Dynamical Systems

The asymptotic states of various solutions of the EFEs (1.1) are of special importance in the study of cosmology, as these represent possible states of the Universe at *important* times - i.e. at early and late times. Dynamical systems theory is especially suited to determining the possible asymptotic states, especially when the governing equations are a finite system of autonomous ODEs. This section will review some of the results of dynamical systems theory which will be used throughout the thesis in the analysis of the solutions of the EFEs (1.1). The material is primarily taken from two sources: (1) Stephen Wiggins's book *Introduction to Applied Non-linear Systems and Chaos*, and (2) chapter 4 from the text *Dynamical Systems in Cosmology* as written by Reza Tavakol, 1996.

The following are definitions of terms in dynamical systems theory which will be used throughout the thesis:

Definition 1 A *singular point* of a system of autonomous, ordinary differential equations

$$\dot{x} = f(x) \quad (1.22)$$

is a point $\bar{x} \in \mathbb{R}^n$ such that $f(\bar{x}) = 0$.

Definition 2 Let \bar{x} be a singular point of the DE (1.22). The point \bar{x} is called a *hyperbolic singular point* if $Re(\lambda_i) \neq 0$ for all eigenvalues, λ_i , of the Jacobian of the

vector field $f(x)$ evaluated at \bar{x} . Otherwise the point is called *non-hyperbolic*.

Definition 3 Let $x(t) = \phi_a(t)$ be a solution of the DE (1.22) with initial condition $x(0) = a$. The flow $\{g^t\}$ is defined in terms of the solution function $\phi_a(t)$ of the DE by

$$g^t a = \phi_a(t).$$

Definition 4 The orbit through a , denoted by $\gamma(a)$ is defined by

$$\gamma(a) = \{x \in \mathbf{R}^n \mid x = g^t a, \text{ for all } t \in \mathbf{R}\}.$$

Definition 5 Given a DE (1.22) in \mathbf{R}^n , a set $S \subseteq \mathbf{R}^n$ is called an invariant set for the DE if for any point $a \in S$ the orbit through a lies entirely in S , that is $\gamma(a) \subseteq S$.

Definition 6 Given a DE (1.22) in \mathbf{R}^n , with flow $\{g^t\}$, a subset $S \subseteq \mathbf{R}^n$ is said to be a trapping set of the DE if it satisfies:

1. S is a closed and bounded set,
2. $a \in S$ implies that $g^t a \in S$ for all $t \geq 0$.

Qualitative analysis of a system begins with the location of singular points. Once the singular points of a system of ODEs are obtained, it is of interest to consider the dynamics in a local neighbourhood of each of the points. Assuming that the vector field $f(x)$ is of class C^1 the process of determining the local behaviour is based on the linear approximation of the vector field in the local neighbourhood of the singular point \bar{x} . In this neighbourhood we have that:

$$f(x) \approx Df(\bar{x})(x - \bar{x}) \tag{1.23}$$

where $Df(\bar{x})$ is the Jacobian of the vector field at the singular point \bar{x} . The system (1.23) is referred to as the *linearisation of the DE at the singular point*. Each of the singular points can then be classified according to the eigenvalues of the Jacobian of the linearised vector field at the point.

The classification then follows from the fact that if the singular point is hyperbolic in nature the flows of the non-linear system and its linear approximation are

topologically equivalent in a neighbourhood of the singular point. This result is given in the form of the following theorem:

Theorem 1: Hartman-Grobman Theorem Consider a DE: $\dot{x} = f(x)$, where the vector field f is of class C^1 . If \bar{x} is a hyperbolic singular point of the DE then there exists a neighbourhood of \bar{x} on which the flow is topologically equivalent to the flow of the linearisation of the DE at \bar{x} .

Given a linear system of ODEs:

$$\dot{x} = Ax, \quad (1.24)$$

where A is a matrix with constant coefficients, it is a straightforward matter to show that if the eigenvalues of the matrix A are all positive the solutions in the neighbourhood of $\bar{x} = 0$ all diverge from that point. This point is then referred to as a source. Similarly, if the eigenvalues all have negative real parts all solutions converge to the singular point $\bar{x} = 0$, and the point is referred to as a sink. Therefore, it follows from topological equivalence that if all eigenvalues of the Jacobian of the vector field for a non-linear system of ODEs have positive real parts the point is classified as a source (and all orbits diverge from the singular point), and if the eigenvalues all have negative real parts the point is classified as a sink.

In most cases the eigenvalues of the linearised system (1.23) will have eigenvalues with both positive, negative and/or zero real parts. In these cases it is important to identify which orbits are attracted to the singular point, and which are repelled away as the independent variable (usually t) tends to infinity.

For a linear system of ODEs, (1.24), the phase space \mathbf{R}^n is spanned by the eigenvectors of A . These eigenvectors divide the phase space into three distinct subspaces; namely:

$$\text{The stable subspace} \quad E^s = \text{span}(s_1, s_2, \dots, s_{n_s})$$

$$\text{The unstable subspace} \quad E^u = \text{span}(u_1, u_2, \dots, u_{n_u})$$

and

$$\text{The centre subspace} \quad E^c = \text{span}(c_1, c_2, \dots, c_{n_c})$$

where s_i are the eigenvectors whose associated eigenvalues have negative real part, u_i those whose eigenvalues have positive real part, and c_i those whose eigenvalues have zero eigenvalues. Flows (or orbits) in the stable subspace asymptote in the future to the singular point, and those in the unstable subspace asymptote in the past to the singular point.

In the non-linear case, the topological equivalence of flows allows for a similar classification of the singular points. The equivalence only applies in directions where the eigenvalue has non-zero real parts. In these directions, since the flows are topologically equivalent, there is a flow *tangent* to the eigenvectors. The phase space is again divided into stable and unstable subspaces (as well as centre subspaces). The *stable manifold* W^s of a singular point is a differential manifold which is tangent to the stable subspace of the linearised system (E^s). Similarly, the *unstable manifold* is a differential manifold which is tangent to the unstable subspace (E^u) at the singular point. The centre manifold, W^c , is a differential manifold which is tangent to the centre subspace E^c . It is important to note, however, that unlike the case of a linear system, this centre manifold, W^c will contain all those dynamics not classified by linearisation (i.e., the non-hyperbolic directions). In particular, this manifold may contain regions which are stable, unstable or neutral. The classification of the dynamics in this manifold can only be determined by utilising more sophisticated methods, such as centre manifold theorems or the theory of normal forms (see Wiggins, 1990).

Unlike a linear system of ODEs, a non-linear system allows for equilibrium structures which are more complicated than that of the singular points fixed lines or periodic orbits. These structures include, though are not limited to, such things as heteroclinic and/ or homo-clinic orbits, non-linear invariant sub-manifolds, etc (for definitions see Wiggins, 1987). The set of non-isolated singular points will figure into the analysis of solutions in this thesis, and therefore we shall examine its stability more rigorously.

Definition 7: A set of non-isolated singular points is said to be normally hyperbolic if the only eigenvalues with zero real parts are those whose corresponding

eigenvectors are tangent to the set.

Since by definition any point on a set of non-isolated singular points will have at least one eigenvalue which is zero, all points in the set are *non-hyperbolic*. A set which is normally hyperbolic can, however, be completely classified as per its stability by considering the signs of the eigenvalues in the remaining directions (i.e. for a curve, in the remaining $n - 1$ directions) (Aulbach, 1984).

The local dynamics of a singular point may depend on one or more arbitrary parameters. When small continuous changes in the parameter result in dramatic changes in the dynamics, the singular point is said to undergo a bifurcation. The values of the parameter(s) which result in a bifurcation at the singular point can often be located by examining the linearised system. Singular point bifurcations will only occur if one (or more) of the eigenvalues of the linearised systems are a function of the parameter. The bifurcations are located at the parameter values for which the real part of an eigenvalue is zero.

There are several different types of singular point bifurcations, which are classified according to the particular nature of the change in the dynamics. Some of the more common bifurcations are:

- **Saddle-node bifurcation:** A saddle-node bifurcation is characterised by the non-existence of a singular point on one side of the bifurcation value and the existence of two singular points on the other side of the bifurcation value. At the bifurcation value, a singular point in two (or higher) dimensions has a saddle-node structure.
- **Transcritical bifurcation:** A transcritical bifurcation is characterised by the “exchange” of stability. By passing through the bifurcation value the stability of two singular points interchange. Once again, in two-dimensional phase space, the singular point has a saddle-node structure.
- **Poincare-Andronov-Hopf (PAH) bifurcation:** In the preceding examples, the bifurcation occurs when a single eigenvalue is identically zero. In contrast,

a PAH bifurcation occurs when there is a pair of eigenvalues whose real part becomes zero. In this case, the singular point on either side of the bifurcation value is a spiral (either attracting or repelling).

A complete classification of singular point bifurcations can be found in Wiggins (1990).

The future and past asymptotic states of a non-linear system may be represented by any singular or periodic structure. In the case of a plane system (i.e. in two-dimension phase space), the possible asymptotic states can be given explicitly. This result is due to the limited degrees of freedom in the space, and the fact that the flows (or orbits) in any dimensional space cannot cross. The result is given in the form of the following theorem:

Theorem 2: Poincare-Bendixon Theorem: Consider the system of ODEs $\dot{x} = f(x)$ on \mathbf{R}^2 , with $f \in C^2$, and suppose that there are at most a finite number of singular points (i.e. no non-isolated singular points). Then any compact asymptotic set is one of the following:

1. a singular point
2. a periodic orbit
3. the union of singular points and heteroclinic or homo-clinic orbits.

This theorem has a very important consequence in that if the existence of a closed (i.e. periodic, heteroclinic or homo-clinic) orbit can be ruled out it follows that all asymptotic behaviour is located at a singular point.

The existence of a closed orbit can be ruled out by many methods, the most common is to use a consequence of Green's Theorem, as follows:

Theorem 3: Dulac's Criterion: If $D \subseteq \mathbf{R}^2$ is a simply connected open set and $\nabla(Bf) = \frac{\partial}{\partial x_1}(Bf_1) + \frac{\partial}{\partial x_2}(Bf_2) > 0$, or (< 0) for all $x \in D$ where B is a C^1 function, then the DE $\dot{x} = f(x)$ where $f \in C^1$ has no periodic (or closed) orbit which is contained in D .

A fundamental criteria of the Poincare-Bendixon theorem is that the phase space is two-dimensional. When the phase space is of a higher dimension the requirement that orbits cannot cross does not result in such a decisive conclusion. The behaviour in such higher-dimensional spaces is known to be highly complicated, with the possibility of including such phenomena as recurrence and strange attractors (see, for example, Guckenheimer and Holmes, 1983). For that reason, the analysis of non-linear systems in spaces of three or more dimensions cannot in general progress much further than the local analysis of the singular points (or non-isolated singular sets). The one tool which does allow for some progress in the analysis of higher dimensional systems is the possible existence of monotonic functions. Since in this thesis there will be the need to analyse three-dimensional phase spaces the tools for higher dimensional spaces will now be outlined.

Theorem 4: LaSalle Invariance Principle: Consider a DE $\dot{x} = f(x)$ on \mathbf{R}^n . Let S be a closed, bounded and positively invariant set of the flow, and let Z be a C^1 monotonic function. Then for all $x_0 \in S$,

$$w(x_0) \subset \{x \in S | \dot{Z} = 0\}$$

where $w(x_0)$ is the forward asymptotic states for the orbit with initial value x_0 ; i.e. a w -limit set (Tavakol, 1997).

This principle has been generalised to the following result:

Theorem 5: Monotonicity Principle (see LeBlanc et. al., 1995). Let ϕ_t be a flow on \mathbf{R}^n with S an invariant set. Let $Z : S \rightarrow \mathbf{R}$ be a C^1 function whose range is the interval (a, b) , where $a \in \mathbf{R} \cup \{-\infty\}$, $b \in \mathbf{R} \cup \{\infty\}$ and $a < b$. If Z is decreasing on orbits in S , then for all $X \in S$,

$$\begin{aligned} \omega(x) &\subseteq \{s \in \bar{S} \setminus S | \lim_{y \rightarrow s} Z(y) \neq b\}, \\ \alpha(x) &\subseteq \{s \in \bar{S} \setminus S | \lim_{y \rightarrow s} Z(y) \neq a\}, \end{aligned}$$

where $\omega(x)$ and $\alpha(x)$ are the forward and backward limit set of x , respectively (i.e., the w and α limit sets.)

As a result of the lack of analytical tools available for the investigation of higher dimensional systems, many results concerning the global dynamics must be determined through numerical investigations.

The final important feature of the analysis of non-linear systems of ODEs is the consideration of the dynamics on the infinite boundary if the phase space is not compact.

In order to consider the dynamics at infinity, it is necessary to compactify the phase space so that the infinite dynamics are now located at finite values. While there are many different transformations which will transform \mathbf{R}^n to a compact set, the method primarily used throughout this work is that of a Poincare transformation. The Poincare transformation compactifies a \mathbf{R}^n space to the closed sphere S^{n-1} . The dynamics which was located at infinity is now located on the surface of this sphere.

The Poincare transformation is defined as follows:

Given an n -dimensional space with coordinates x_1, \dots, x_n we define the transformation

$$X_i = \frac{x_i}{\sqrt{1 + \sum_1^n x_i^2}}. \quad (1.25)$$

If we define $\Theta = (1 + \sum_1^n x_i^2)^{-1/2}$ the derivatives of the transformed variables, X_i are defined by:

$$\dot{X}_i = \dot{x}_i \Theta - x_i^2 \dot{x}_i \Theta^3. \quad (1.26)$$

At this point a transformation of the time variable is required for all non-linear systems. If the vector field governing the dynamics is of order m then a new time variable τ is defined by

$$dt = \Theta^{m-1} d\tau \quad (1.27)$$

In the case of a quadratic vector field (which will be the case for the systems to be considered here) the transformation of the independent variable results in:

$$X'_i = \dot{x}_i \Theta^2 - x_i^2 \dot{x}_i \Theta^4 \quad (1.28)$$

The system of equations (1.28) then defines the dynamics of the transformed system.

The dynamics on the infinite boundary of the original (non-transformed) system is now located on the boundary of the compactified set; i.e., on the surface of the Poincare sphere. This surface is defined by $\Theta = 0$. Two consequences are important to note:

1. The surface of this sphere, $\Theta = 0$, is an invariant set of the system. Therefore the dynamics of the system at infinity can be determined by considering the system restricted to this set.
2. Locally every point on the surface of a $n - 1$ -dimensional sphere is diffeomorphic to $n - 1$ Euclidean space. In the work of this thesis we will be primarily concerned with the compactification of a three dimensional Euclidean phase space. The infinite boundary, after the application of the Poincare transformation will, therefore, be located on the surface of a 2-sphere. In particular, the analysis of the local dynamics at a singular point on this surface is exactly the same as that of singular points in a plane. Further, if the a two-dimensional sphere can be divided into two-invariant hemispheres then the dynamics in each hemisphere can be determined using all the results for planar dynamical systems (e.g., Poincare Bendixson Theorem, Dulac's Criteria, etc.).

1.3 Outline of Work

The thesis will now proceed as follows:

1. In chapter 2 the EFEs are simplified using the assumption of a KSS solution. A closed system of ODEs results. The conditions under which solutions in this class admit a Homothetic vector are considered.
2. In chapter 3 all solutions of spherical symmetry found in chapter 2 are examined in the case that the KSS is in fact a "physical" KSS. The results in this chapter have appeared in the journal *Classical and Quantum Gravity*, 15, 2397.

3. In chapter 4 the complete dynamics of the governing system of equations is investigated. The exact solutions for the asymptotic states are determined, and the energy conditions are discussed.
4. In chapter 5 the case of "infinite" KSS (excluded from the systems studied in chapter 4) are examined in a similar manner to that of the finite case. The work of this chapter is based on collaborative work between the author and Alicia Sintés.
5. In chapter 6 the work, which in the previous chapters was restricted to a perfect fluid source, is extended to a preliminary examination of KSS in anisotropic fluids exhibiting spherical symmetry. The work in this chapter will appear in a future issue of the Journal of Mathematical Physics.
6. Finally, Chapter 7 contains a discussion of the results determined in the preceding chapters, with an indication of possible areas for future work.

Chapter 2

Einstein's Field Equations with Kinematic Self-Similarity

As described in the Introduction and in Carter and Henriksen (1989) self-similarity implies that the metric functions in (1.13) can be written as

$$S = S(\xi), \quad \Phi = \Phi(\xi), \quad \Psi = \Psi(\xi), \quad (2.1)$$

where ξ is the independent variable found by Carter and Henriksen (1989), given by equation (1.19) when $\alpha \neq 0$ and (1.18) when $\alpha = 0$. From this point forward we shall consider the change of coordinates $z = \ln(\xi)$, such that all functions now depend on the independent variable z and ordinary differentiation will be defined as $\dot{f} = \frac{df}{dz}$ where $f = f(z)$. To simplify the expressions a change of variables $y = \dot{S}/S$ is also made.

In the simplification of the EFEs we shall assume (i) without loss of generality α can be taken to be positive (or zero) quantity, and (ii) the vector ξ is not homothetic, i.e. α is not equal to one.

Consider the spherically symmetric metric given by equation (1.17). The EFEs given in equation (1.1) will be evaluated where T_{ab} is the energy momentum tensor for the perfect fluid given by equation (1.2) with the metric (1.17). We further assume that the fluid is comoving with the inertial observers. This final condition

will guarantee that the Einstein tensor is diagonal in nature. With these assumptions the EFEs give:

$$\mu = r^{-2}W_1(z) + t^{-2}W_2(z), \quad (2.2)$$

$$p = r^{-2}P_1(z) + t^{-2}P_2(z), \quad (2.3)$$

$$p = r^{-2}\bar{P}_1(z) + t^{-2}\bar{P}_2(z). \quad (2.4)$$

where

$$W_1(z) = e^{-2\Psi}[e^{2\Psi}S^{-2} - (1+y)^2 - 2y\dot{\Phi}], \quad (2.5)$$

$$W_2(z) = e^{-2\Phi}\alpha^{-2}[y^2 + 2y\dot{\Psi}], \quad (2.6)$$

$$P_1(z) = e^{-2\Psi}[-e^{2\Psi}S^{-2} + (1+y)^2 + 2y\dot{\Phi} + 2\dot{\Phi}], \quad (2.7)$$

$$P_2(z) = -e^{-2\Phi}\alpha^{-2}[y^2 + 2y\dot{\Psi} + 2\dot{\Psi} - 2y + 2\alpha y], \quad (2.8)$$

$$\bar{P}_1(z) = e^{-2\Psi}[\ddot{\Phi} + \dot{\Phi}^2 + 2y\dot{\Phi} - \dot{\Phi}\dot{\Psi}], \quad (2.9)$$

$$\bar{P}_2(z) = -e^{-2\Phi}\alpha^{-2}[\ddot{\Psi} + \dot{\Psi}^2 + 2y\dot{\Psi} - \dot{\Psi}\dot{\Phi} + \alpha\dot{\Psi} + \dot{\Psi} - y]. \quad (2.10)$$

By equating the two expressions for the pressure (equations (2.3)-(2.4)) we see that:

$$t^2(P_1(z) - \bar{P}_1(z)) = r^2(P_2(z) - \bar{P}_2(z)). \quad (2.11)$$

If $P_2(z) - \bar{P}_2(z) \neq 0$ it immediately follows from equation (2.11) that

$$(\alpha t)^{2(\alpha-1)/\alpha} = \text{a function of } z. \quad (2.12)$$

Differentiating equation (2.12) with respect to r it follows that the only consistent solution is found when $\alpha = 1$, which contradicts the original assumption that ξ is not homothetic. It follows, therefore, that

$$P_2(z) = \bar{P}_2(z), \quad (2.13)$$

and as an immediate consequence

$$P_1(z) = \bar{P}_1(z). \quad (2.14)$$

Substituting the definitions (2.7)-(2.10) into the two equations (2.13)-(2.14) results in the differential equations:

$$\ddot{\Psi} = (\alpha - 1)y + y^2 - (\alpha - 1)\dot{\Psi} - \dot{\Psi}^2 + \dot{\Phi}\dot{\Psi}, \quad (2.15)$$

$$\ddot{\Phi} = -\frac{e^{2\Psi}}{S^2} + (1 + y)^2 + \dot{\Phi}\dot{\Psi} + 2\dot{\Phi} - \dot{\Phi}^2. \quad (2.16)$$

The third and final equation results from the assumption that the fluid is comoving. From this assumption we can set all off-diagonal terms of the Einstein tensor identically to zero. This assignment results in the equation:

$$\dot{y} = y\dot{\Phi} + (1 + y)(\dot{\Psi} - y). \quad (2.17)$$

Equations (2.15)-(2.17) then form a closed system of three *ordinary* differential equations which govern the metric functions.

Through an exactly analogous analysis, a system of ordinary differential equations for the metric functions can be determined in the case of *zereth* order kinematic self similarity. In this case the metric functions depend on the independent variable $\xi = re^{-t}$, or $z = \ln(\xi)$. The EFEs then result in a set of definitions for the matter density and pressure which are defined as:

$$\mu = W_1(z) + r^{-2}W_2(z), \quad (2.18)$$

$$p = P_1(z) + r^{-2}P_2(z), \quad (2.19)$$

$$\bar{p} = \bar{P}_1(z) + r^{-2}\bar{P}_2(z). \quad (2.20)$$

where

$$W_1(z) = \frac{1}{S^2} - e^{-2\Psi}[(1 + y)^2 + 2\dot{\Phi}y], \quad (2.21)$$

$$W_2(z) = ye^{-2\Phi}(y + 2\dot{\Psi}), \quad (2.22)$$

$$P_1(z) = \frac{-1}{S^2} + e^{-2\Psi}(1 + y)[1 + y + 2\dot{\Phi}], \quad (2.23)$$

$$P_2(z) = -e^{-2\Phi}(3y^2 + 2\dot{y} - 2y\dot{\Phi}), \quad (2.24)$$

$$\bar{P}_1(z) = e^{-2\Psi}[\ddot{\Phi} + \dot{\Phi}^2 + 2y\dot{\Phi} - \dot{\Phi}\dot{\Psi}], \quad (2.25)$$

$$\bar{P}_2(z) = -e^{-2\Phi}[\ddot{\Psi} + \dot{\Psi}^2 + 2y\dot{\Psi} - \dot{\Psi}\dot{\Phi} + \dot{\Psi} - y]. \quad (2.26)$$

Once again it is an straightforward calculation to show that equations (2.19) and (2.20) along with (2.23)-(2.26) imply two differential equations, with a third resulting from the condition of a comoving fluid. The form of the equations which result from the the condition (2.19)=(2.20) are identical to those in the non-zero case when α is set identically to zero. The third equation calculated from the non-diagonal terms of the Einstein tensor is also the same as the $\alpha \neq 0$ case.

While the differential equations governing the metric functions are identical in each of these cases, it is important to note that the zeroth order case results in matter functions of a different form that that of the second order KSS.

2.1 Comparison to Cahill and Taub's Derivations

In their detailed analysis of perfect fluid, spherically symmetric solutions which admit a *homothetic* vector Cahill and Taub (1971) simplified the EFEs to the following system of partial differential equations:¹:

$$m_r = \mu R^2 R_r, \quad (2.27)$$

$$m_t = -p R^2 R_t, \quad (2.28)$$

$$m = R(1 + e^{-2\Phi} R_t^2 - e^{-2\Psi} R_r^2), \quad (2.29)$$

$$\Phi_r = -\frac{p_r}{\mu + p}, \quad (2.30)$$

$$\Psi_t = -\frac{\mu_t}{\mu + p} - \frac{2R_t}{R}, \quad (2.31)$$

$$0 = R_{rt} - R_t \Phi_t - R_r \Psi_t, \quad (2.32)$$

where the mass function m is defined through the “first integral” of the EFEs and the function R is equivalent the metric function rS in equation (1.17). Each of the metric functions R , Φ , and Ψ as well as the matter functions μ , p and m are functions of both t and r . By assuming the existence of self-similarity (kinematic self-similarity of the *first* kind) the metric functions are then assumed to be functions of the similarity

¹see equations (3.4)-(3.6), (1.6), (1.8)-(1.9) in Cahill and Taub (1971).

variable $\xi = r/t$. In this case two ordinary differential equations result. In order to close the system a further assumption regarding the functional relationship between the density and pressure must be assumed.

Using the equations (2.27)-(2.32) we can follow Cahill and Taub's derivation by substituting the similarity variable of equation (1.19) where they used $\xi = r/t$. In this case the result is the following set of equations:

$$M_1 + \dot{M}_1 = W_1 S^2 (S + \dot{S}), \quad (2.33)$$

$$3M_2 + \dot{M}_2 = W_2 S^2 (S + \dot{S}), \quad (2.34)$$

$$\dot{M}_1 = -P_1 S^2 \dot{S}, \quad (2.35)$$

$$2\alpha M_2 + \dot{M}_2 = -P_2 S^2 \dot{S}, \quad (2.36)$$

$$M_1 = S(1 - e^{-2\Psi}(S + \dot{S})^2), \quad (2.37)$$

$$\alpha^2 M_2 = S \dot{S}^2 e^{-2\Phi}, \quad (2.38)$$

$$(P_1 + W_1)\dot{\Phi} = 2P_1 - \dot{P}_1, \quad (2.39)$$

$$(P_2 + W_2)\dot{\Phi} = -\dot{P}_2, \quad (2.40)$$

$$\dot{W}_1 S = -(P_1 + W_1)(\dot{\Psi} S + 2\dot{S}), \quad (2.41)$$

$$(2\alpha W_2 + \dot{W}_2)S = -(P_2 + W_2)(\dot{\Psi} S + 2\dot{S}), \quad (2.42)$$

and

$$\dot{S} + \ddot{S} = \dot{S}\dot{\Phi} + (S + \dot{S})\dot{\Psi}. \quad (2.43)$$

where

$$m = rM_1(z) + r^3 t^{-2} M_2(z), \quad (2.44)$$

is the mass function defined by the first integral of the EFEs and P_i , W_i are defined by the density and pressure as given in equations (2.2) and (2.3). The system of

equations (2.33)-(2.43) then reduces to equations (2.15)-(2.17) with definitions (2.5)-(2.8).

We note that strictly speaking the subcase $S + \dot{S} = 0$ has been factored out of this derivation. However, it can be shown that this restriction will not generate any perfect fluid solutions for the spherically symmetric metric, and hence no solutions to the system of equations (2.33)-(2.43). The restriction does not, therefore, require any further consideration. The analysis in the $\alpha = 0$ case is analogous, and results in the system considered previously.

It is important to note that while we consider the idea of *Kinematic* self-similarity (i.e. self-similarity of the second kind) more general than that of self-similarity (i.e. homothety), the number of governing DEs has increased (over that in the homothetic case). Therefore, although we shall use the terminology that the general case refers to $\alpha \neq 1$, this is not meant to imply that the resulting solution set is necessarily larger (than that of the homothetic case). In fact the subset of solutions to equations (2.15)-(2.17) which admit a homothetic vector are only those which satisfy equations (2.13) and (2.14). This is not necessarily the case for **all** self similar solutions since the form of the similarity variable (of the *first kind*) $\xi = \tau/t$ is consistent with equation (2.11) without demanding (2.13) and (2.14) be satisfied.

2.2 Plane and Hyperbolic Symmetry

In all of the previous analysis it was first assumed that the metric possessed spherical symmetry. We can, however, also consider the results of the kinematic self similarity assumption when the metrics have either plane or hyperbolic symmetry. In these cases the metric given by equation (1.17) is replaced by:

$$ds^2 = -e^{2\Phi(t,r)} dt^2 + e^{2\Psi(t,r)} dr^2 + S^2(t, r)(d\theta^2 + \Sigma(\theta, k)^2 d\phi^2) \quad (2.45)$$

where

$$\Sigma(\theta, k) = \begin{cases} \sin \theta & k = +1 \\ \theta & k = 0 \\ \sinh \theta & k = -1. \end{cases} \quad (2.46)$$

The parameter k indicates the type of symmetry, i.e. $k = 1$: spherical symmetry, $k = 0$: plane symmetry, and $k = -1$: hyperbolic symmetry.

The EFEs then yield the matter functions of density and pressure. In the case of plane symmetry the functions are once again of the form (2.2)-(2.3), with

$$W_1(z) = e^{-2\Psi}[-(1+y)^2 - 2y\dot{\Phi}], \quad (2.47)$$

$$W_2(z) = e^{-2\Phi}\alpha^{-2}[y^2 + 2y\dot{\Psi}], \quad (2.48)$$

$$P_1(z) = e^{-2\Psi}[(1+y)^2 + 2y\dot{\Phi} + 2\dot{\Phi}], \quad (2.49)$$

$$P_2(z) = -e^{-2\Phi}\alpha^{-2}[y^2 + 2y\dot{\Psi} + 2\dot{\Psi} - 2y + 2\alpha y], \quad (2.50)$$

$$\bar{P}_1(z) = e^{-2\Psi}[\ddot{\Phi} + \dot{\Phi}^2 + 2y\dot{\Phi} - \dot{\Phi}\dot{\Psi}], \quad (2.51)$$

$$\bar{P}_2(z) = -e^{-2\Phi}\alpha^{-2}[\ddot{\Psi} + \dot{\Psi}^2 + 2y\dot{\Psi} - \dot{\Psi}\dot{\Phi} + \alpha\dot{\Psi} + \dot{\Psi} - y]. \quad (2.52)$$

In the case of hyperbolic symmetry the functions are once again of the form (2.2)-(2.3), with

$$W_1(z) = e^{-2\Psi}[-e^{2\Psi}S^{-2} - (1+y)^2 - 2y\dot{\Phi}], \quad (2.53)$$

$$W_2(z) = e^{-2\Phi}\alpha^{-2}[y^2 + 2y\dot{\Psi}], \quad (2.54)$$

$$P_1(z) = e^{-2\Psi}[e^{2\Psi}S^{-2} + (1+y)^2 + 2y\dot{\Phi} + 2\dot{\Phi}], \quad (2.55)$$

$$P_2(z) = -e^{-2\Phi}\alpha^{-2}[y^2 + 2y\dot{\Psi} + 2\dot{\Psi} - 2y + 2\alpha y], \quad (2.56)$$

$$\bar{P}_1(z) = e^{-2\Psi}[\ddot{\Phi} + \dot{\Phi}^2 + 2y\dot{\Phi} - \dot{\Phi}\dot{\Psi}], \quad (2.57)$$

$$\bar{P}_2(z) = -e^{-2\Phi}\alpha^{-2}[\ddot{\Psi} + \dot{\Psi}^2 + 2y\dot{\Psi} - \dot{\Psi}\dot{\Phi} + \alpha\dot{\Psi} + \dot{\Psi} - y]. \quad (2.58)$$

If we define

$$w = -ke^{2\Psi}S^{-2} \quad (2.59)$$

the systems (2.47)-(2.52), (2.53)-(2.58) and (2.5)-(2.10) are identical when k is defined as for the metric (2.45). Therefore we can write the system (2.15)-(2.17) in a form

which is valid for all three types of symmetry, namely:

$$\ddot{\Psi} = (\alpha - 1)y + y^2 - (\alpha - 1)\dot{\Psi} - \dot{\Psi}^2 + \dot{\Phi}\dot{\Psi}, \quad (2.60)$$

$$\ddot{\Phi} = w + (1 + y)^2 + \dot{\Phi}\dot{\Psi} + 2\dot{\Phi} - \dot{\Phi}^2. \quad (2.61)$$

$$\dot{w} = 2w(\dot{\Psi} - y) \quad (2.62)$$

$$\dot{y} = y\dot{\Phi} + (1 + y)(\dot{\Psi} - y), \quad (2.63)$$

with the physical properties of density and pressure now given by:

$$\mu = e^{-2\Phi}\alpha^{-2}[y^2 + 2y\dot{\Psi}]t^{-2} + e^{-2\Psi}[-w - (1 + y)^2 - 2y\dot{\Phi}]r^{-2} \quad (2.64)$$

$$p = -e^{-2\Phi}\alpha^{-2}[y^2 + 2y\dot{\Psi} + 2\dot{\Psi} - 2y + 2\alpha y]t^2 \\ + e^{-2\Psi}[e^{2\Psi}S^{-2} + (1 + y)^2 + 2y\dot{\Phi} + 2\dot{\Phi}]r^{-2}. \quad (2.65)$$

2.3 Algebraic Structure

We can investigate the algebraic structure of the space of kinematic self-similar vectors and their relationship to the spaces of Killing vectors (KV) and Homothetic vectors (HV). This will become important as we study the nature of various solutions which arise in subsequent chapters.

The group of kinematic self-similarities can be subdivided into those which are (1) Killing vectors, (2) Homothetic vectors and (3) (*purely*) Kinematic self similar vectors. The covariant definitions for each of these cases is as follows:

$$\begin{aligned} (1) \quad & \textit{Killing vector} & \mathcal{L}_\xi h_{ab} &= 0 & \mathcal{L}_\xi u^a &= 0 \\ (2) \quad & \textit{homothetic vector} & \mathcal{L}_\xi h_{ab} &= 2h_{ab} & \mathcal{L}_\xi u^a &= -u^a \\ (3) \quad & \textit{kinematic vector} & \mathcal{L}_\xi h_{ab} &= 2h_{ab} & \mathcal{L}_\xi u^a &= -\alpha u^a \end{aligned}$$

As a result it is straightforward to see that a basis for this group of kinematic self similarities will be composed of those vectors which are killing vectors and those which are purely kinematic self similar vectors. We will use that fact to determine the conditions required for the a kinematic self similar solutions to the EFEs to also admit a homothetic vector.

If we assume the existence of a proper KSS vector field, ξ , (i.e, not a Homothetic or Killing vector) then from the Jacobi identities and the property that the Lie bracket of a proper KSS and a KV is a KSS, it is straightforward to show that:

$$\xi = (\xi^0(t, r), \xi^1(t, r), 0, 0) \quad (2.66)$$

The condition $\mathcal{L}_\xi u^a = u^a$ then immediately results in $\xi^0(t, r) = \xi^0(t)$. Further, the condition $\mathcal{L}_\xi g_{ab} = g_{ab}$ yields $\xi^1(t, r) = \xi^1(r)$. In other words:

$$\xi = (\xi^0(t), \xi^1(r), 0, 0) \quad (2.67)$$

Solving, then, the homothetic equations (1.3) for the metric which is defined as solutions to the system (2.60)-(2.63) yields the conditions:

$$1 = \dot{\Phi}\xi^0 + \dot{\Phi}\xi^1 + \xi^0_{,0} \quad (2.68)$$

$$1 = \dot{\Psi}\xi^0 + \dot{\Psi}\xi^1 + \xi^1_{,1} \quad (2.69)$$

$$1 = \frac{\dot{S}}{S}\xi^0 + \frac{\dot{S}}{S}\xi^1 + \xi^1/r \quad (2.70)$$

We shall refer to these conditions in the investigation of various exact solutions found throughout chapters 3 and 4.

Chapter 3

Physical Self-Similarity for Spherically Symmetric Metrics

In general equations of the form (1.8) for μ and p are not automatically satisfied. We can, however, determine the criteria which guarantees that equations (1.8) are satisfied for the matter functions of density and pressure. In each case the solutions would then be, in addition to *geometrically* self-similar, *physically* self-similar. There are three special sub cases in which equations of the form (1.8) are satisfied for the pressure and density. In each case the forms of equations (2.15)-(2.17) simplify, the number of governing ODEs reduce, and exact solutions are easier to find.

1. $\alpha = 1$ (homothetic case). In this sub case $\xi = r/t$ and equations (2.4)-(2.6) reduce to $\mu = W(\xi)r^{-2}$, $p = P(\xi)r^{-2}$, and $m = M(\xi)r$ (Cahill and Taub, 1971).
2. $M_1 = 0$, and hence $W_1 = P_1 = 0$. This sub case contains the exact solutions of Lynden-Bell and Lemos (1988) and Carter and Henriksen (1989) and will be analysed completely in subsection 3.1.
3. $M_2 = 0$, and hence S is constant. This subcase, which also includes the static subcase, will also be dealt with separately in subsection 3.2.

These cases are in fact the only cases in which the physical quantities μ and p satisfy equations of the form (1.8). In the general case $\alpha \neq 1$, μ and p do not “individually” and “totally” satisfy equations of the form (1.8). However, if we write μ and p in (2.64) and (2.65) in the form

$$\mu = \mu_1 + \mu_2, \quad (3.1)$$

$$p = p_1 + p_2; \quad (3.2)$$

that is, the source of the gravitational field is interpreted as the sum of two separate comoving perfect fluids with densities and pressures μ_1, p_1 and μ_2, p_2 , respectively (i.e., the model is a two fluid model - Coley and Tupper, 1986), where

$$\mu_1 = W_1 r^{-2}, \quad p_1 = P_1 r^{-2}, \quad (3.3)$$

$$\mu_2 = W_2 t^{-2}, \quad p_2 = P_2 t^{-2}, \quad (3.4)$$

then

$$\mathcal{L}_\xi \mu_1 = -2\mu_1, \quad \mathcal{L}_\xi p_1 = -2p_1, \quad (3.5)$$

and

$$\mathcal{L}_\xi \mu_2 = -2\alpha\mu_2, \quad \mathcal{L}_\xi p_2 = -2\alpha p_2. \quad (3.6)$$

Therefore, the two fluids each separately satisfy equations of the form (1.8).

We will now consider each of the non-homothetic (i.e. $\alpha \neq 1$), cases which exhibit physical self-similarity for the energy pressure and density.

3.1 Special Subcase: $M_1 = 0$

We first consider the subcase $M_1 = 0$. From this condition it automatically follows from equation (2.37) that $e^{2\psi} = S^2(1+y)^2$. The system given by equations (2.60)-(2.63) and the definitions for the matter functions then yield the following:

$$ds^2 = -dt^2 + S^2(1+y)^2 dr^2 + r^2 S^2 d\Omega^2, \quad (3.7)$$

and

$$m = \frac{r^3 S^3 y^2}{\alpha^2} t^{-2}, \quad (3.8)$$

$$p = p_0 t^{-2}, \quad (3.9)$$

$$\mu = \frac{y[(3 - 2\alpha)y - \alpha^2 p_0]}{\alpha^2(1 + y)} t^{-2}, \quad (3.10)$$

where the evolution of the arbitrary function $y = \dot{S}/S$ is given by

$$2y + 3y^2 + 2\alpha y + \alpha^2 p_0 = 0. \quad (3.11)$$

Since $\dot{\Phi} = 0$, we note that this solution corresponds to the geodesic case studied in Coley (1997). We note that in the solution above there is a dimensional constant, p_0 , appearing (in the pressure), a property that is characteristic of self-similarity of the second kind (Barenblatt and Zel'dovich, 1972).

We can consider the cases in which the solution (3.7) admits a homothetic vector (HV) by recalling the conditions derived in Chapter 2 (see equations (2.81)-(2.83)). In the case of (3.7) the conditions simplify to

$$\xi_0^0 = 1 \quad \rightarrow \quad \xi^0 = t + c \quad (3.12)$$

and

$$\dot{\Psi}(1 - \xi^1/r) = y(1 - \xi_1^1), \quad \text{if } y\dot{\Psi} \neq 0 \quad (3.13)$$

$$\xi^1 = r \quad \text{if } y\dot{\Psi} = 0. \quad (3.14)$$

Differentiating equation (3.13) with respect to t and substituting into the governing equation for y (equation (3.11)) it is straightforward to show that the only consistent solutions occur when y is a constant or $\dot{\Psi}$ is a constant, each of which corresponds to a singular point of the governing differential equation (3.11). The solution in this case is then given by

$$ds^2 = -dt^2 + s_0^2(dr^2 + r^2 d\Omega^2) \quad (3.15)$$

$$p = p_0 t^{-2}, \quad \mu = \mu_0 t^{-2}, \quad (3.16)$$

the flat FRW model, which is known to admit a HV, $\xi = (t, r, 0, 0)$. In all other cases there is no model in this class of solutions which admits a HV.

In the case $p_0 = 0$ we can integrate equation (3.11) completely to obtain

$$S = s_0(1 + s_1\xi^{-\alpha})^{2/3}, \quad (3.17)$$

where s_0 and s_1 are constants. This is the dust solution of the Tolman family described in Carter and Henriksen (1989) in which $M_2 \propto \xi^{-2\alpha}$, $m \propto r(r/t)^2[rt^{-1/\alpha}]^{-2\alpha} = r^{3-2\alpha}$.

In the case $p_0 \neq 0$, we can employ qualitative techniques to consider the asymptotic properties of the solution. Equation (3.11) is an autonomous ODE for y . The singular points are given by

$$y = -y_{\pm}; \quad y_{\pm} = \frac{\alpha}{3}(1 \pm \sqrt{1 - 3p_0}). \quad (3.18)$$

Therefore, asymptotically we obtain the solutions

$$S = S_{\pm}\xi^{-y_{\pm}}, \quad (3.19)$$

where S_{\pm} are constants. That is, solutions of equation (3.11) are asymptotic to the exact power law solutions given by

$$S = S_+\xi^{-y_+} \quad (\xi \ll 1), \quad (3.20)$$

$$S = S_-\xi^{-y_-} \quad (\xi \gg 1). \quad (3.21)$$

These exact solutions represent flat, power-law FRW models, which are known to admit a homothetic vector (Carr and Coley, 1997).

Indeed, assuming that $p_0 < \frac{1}{3}$, so that $y^2 + \frac{2\alpha}{3}y + \frac{\alpha^2 p_0}{3}$ has two real roots, we can integrate equation (3.11) to obtain

$$\ln \left| \frac{y + y_-}{y + y_+} \right| = \frac{-2\alpha}{3} \sqrt{1 - 3p_0} \ln \xi + c, \quad (3.22)$$

or

$$y = \kappa \frac{1 + c\xi^{-2\kappa}}{1 - c\xi^{-2\kappa}} - \alpha/3 \equiv F(\xi), \quad (3.23)$$

where $\kappa = \frac{\alpha}{3}\sqrt{1-3p_0}$. S is then obtained from

$$S = S_0 \exp \int F(\xi) \xi^{-1} d\xi. \quad (3.24)$$

From these equations the asymptotic solutions (3.20) and (3.21) are apparent. In terms of y , M_2 and W_2 are given by

$$M_2 = \frac{S^3 y^2}{\alpha^2}, \quad W_2 = \left[\frac{3-2\alpha}{\alpha^2} y - p_0 \right] y (1+y)^{-1}. \quad (3.25)$$

Thus, asymptotically $M_2 \propto S^3$, and $W_2 = \text{constant}$.

In the more interesting range $0 \leq p_0 < 1/3$, there are certainly values of the arbitrary constants appearing in the solutions for which the asymptotic solutions (for both $\xi \ll 1$ and $\xi \gg 1$) are physically well behaved (e.g., the weak and dominant energy conditions are satisfied). Equation (3.11) can also be solved in the cases $p_0 = 1/3$ ($e^y \propto \xi^{(2/3)}$) and $p_0 > 1/3$ ($y = \text{const.} + \tan[\ln(c\xi^{-3/2})]$).

In the special case of dust ($p_0 = 0$) we obtain from either (3.18) or (3.20) and (3.21) that

$$S \sim S_+ \xi^{-2\alpha/3} \quad (\xi \ll 1), \quad (3.26)$$

$$S \sim S_- \quad (\xi \gg 1). \quad (3.27)$$

For $\xi \ll 1$, the properties of the non-zero pressure models (from continuity for small p_0) are qualitatively similar to those of the dust models. When $p_0 = 0$, if $\alpha = 6n/(3+4n)$ (for n a positive integer) then the solution will be analytic at the centre [$n = 1, \alpha = 6/7$ corresponds to the Penstone solution (Penstone, 1969)]. A central cusp singularity can develop, either before or after an "apparent horizon" is reached at $2Mr^{-1} = 1$, that may or may not be hidden by a "true horizon" (see Lynden-Bell and Lemos, 1988, and Carter and Henriksen, 1989, for more details). However, in the case of dust, for $\xi \gg 1$ the solution is asymptotically static (Lynden-Bell and Lemos, 1988); for $1 < \alpha < 3/2$ the metric is asymptotically flat in the sense that $2Mr^{-1} \rightarrow 0$ as $r \rightarrow \infty$ (Carter and Henriksen, 1989).

3.1.1 Zeroth Order geodesic solutions

When $\alpha = 0$, the equation equivalent to equation (2.37) gives $e^{2\Psi} = S^2(1 + y)^2$. The solution in this subcase is then given by

$$ds^2 = -dt^2 + S^2(1 + y)^2 dr^2 + r^2 S^2 d\Omega^2, \quad (3.28)$$

and

$$m = r^2 S^3 y^2, \quad (3.29)$$

$$\mu = \frac{y(3y - p_0)}{1 + y}, \quad (3.30)$$

$$p = p_0, \quad (3.31)$$

where the evolution of the function $y(z)$ is governed by the differential equation

$$2\dot{y} + 3y^2 + p_0 = 0. \quad (3.32)$$

Once again we notice that a dimensional constant, p_0 , appears in this solution. The equations are analogous to those examined in subsection 2.3 in the case $\alpha \neq 0$.

In the case $p_0 = 0$ we can integrate this equation completely to obtain

$$S = s_0(s_1 + 3z)^{2/3}, \quad (3.33)$$

where s_0 and s_1 are constants. In this case we can see that $m \propto r^3$, which is equivalent to the result found in the $\alpha \neq 0$ case (see previous discussion)

In the case $p_0 \neq 0$, we can again employ qualitative techniques to consider the asymptotic properties of the solution. As in the case with $\alpha \neq 0$, equation (3.32) is an autonomous ODE for y . If we assume a positive pressure, then the ODE has no singular points at finite values. The singular points at infinity are equivalent to the solutions with zero pressure described above. (Note, these solutions are also equivalent to the singular points at infinity for equation (2.31) in the $\alpha \neq 0$ case). Actually, equation (3.32) can be explicitly integrated to give

$$S(x) = \begin{cases} s_0(s_1 e^{3/2x} - e^{-3/2x})^{2/3} \sqrt{\frac{2p_0}{3}}; & p_0 < 0. \\ s_0 \sec^2(s_1 + \sqrt{\frac{2p_0}{12}} x); & p_0 > 0. \end{cases}$$

Allowing for the possibility of a negative pressure, we see that equation (3.32) has singular points at the finite values

$$y_{\pm} = \pm(-\frac{p_0}{3})^{1/2}, \quad (3.34)$$

each of which represents a flat FRW model (as in the $\alpha \neq 0$ case). We can show that for $y < y_+$ this model is not physically valid (i.e., the weak energy condition, WEC, is violated since $\mu \leq 0$). Therefore, the only region of physical interest is $y \geq y_+$, which satisfies $\mu \geq 0$ and $\mu + p \geq 0$. For $y \geq y_+$ we find that all solutions asymptote in the past to the solution represented by the singular point at infinity (the case described above). To the future, all solutions will asymptote to $y = y_+$. This model is characterised by $S \propto \xi^{-y_+}$ which has been shown to represent a flat FRW model.

3.2 Special Subcase: $M_2 = 0$

When $M_2 = 0$, we find from equation (2.38) that $y = 0$. We note that this special subcase will include the static models as a subcase when $\dot{\Phi} = k$, where k is a constant. Substituting $y = 0$ into equations (2.60)-(2.63), we find that the metric can be written as

$$ds^2 = -e^{2\Phi} dt^2 + a^2 dr^2 + r^2 s_0^2 d\Omega^2, \quad (3.35)$$

where $e^{\Psi} = a$ and $S = s_0$; a, s_0 constants. It follows that $W_2 = P_2 = 0$, $W_1 = \mu_0$, $M_1 = s_0^3 \mu_0$, and consequently the matter functions are given by

$$\mu = \mu_0 r^{-2}, \quad p = (2\dot{\Phi} a^{-2} - \mu_0) r^{-2}, \quad (3.36)$$

where $\mu_0 = s_0^{-2} - a^{-2}$. From equation (3.36) we note that $\dot{\Phi}$ must be bounded for physically acceptable solutions (recall that in the static models $\dot{\Phi} = k$). The arbitrary function $\Phi(z)$ is governed by the differential equation

$$\ddot{\Phi} = -a^2 \mu_0 + 2\dot{\Phi} - \dot{\Phi}^2. \quad (3.37)$$

This differential equation has three different solutions, depending on the relationship between μ_0 and a^2 . The solutions are given by:

$$e^{2\Phi} = \begin{cases} (i) & \mu_0 < a^{-2}; \quad [c_1 e^{(1+n)z} + c_2 e^{(1-n)z}]^2, \\ (ii) & \mu_0 = a^{-2}; \quad e^{2z}(c_1 + c_2 z)^2, \\ (iii) & \mu_0 > a^{-2}; \quad e^{2z}(c_1 \cos(nz) + c_2 \sin(nz))^2, \end{cases}$$

where c_1 and c_2 are arbitrary constants and $n \equiv \sqrt{|1 - a^2 \mu_0|}$. Notice that the metric function $e^{2\Phi}$ can become zero at a single value of x in the first case, does become zero at a single point in the second case and becomes zero an infinite number of times in the third case, where the corresponding metric is therefore singular. When $e^{2\Phi} \rightarrow 0$, $\dot{\Phi} \rightarrow \pm\infty$ and hence from (2.23) we have that $p/\mu \rightarrow \pm\infty$! Clearly case (iii) is unphysical, while the first two exact solutions may be physical for an appropriate range of values of z (e.g., for large z). Notice that in the first two cases as $z \rightarrow \pm\infty$, $\dot{\Phi} \rightarrow \text{constant}$ and $\ddot{\Phi} \rightarrow 0$ (see below).

It can be shown from the homothetic criteria derived in Chapter 2 (i.e. equations (2.68)-(2.70)) that the metric (3.35) admits a homothetic vector *if and only if* $\ddot{\Phi} = 0$. In this case, the metric function $e^{2\Phi}$ has a power law dependence on $\xi = r(\alpha t)^{-1/\alpha}$ and a coordinate redefinition can be applied to absorb all of the time dependence so that the metric can be put into an explicitly static form. Therefore the static metrics in this subclass of models necessarily admit a homothetic vector. It is also important to note that the static solution is the only subcase in which this solution can have an equation of state of the form $p = p(\mu)$, since this condition implies (from equations (3.36)) that $\ddot{\Phi} = 0$. Static spherically symmetric spacetimes admitting a homothetic vector were studied by Ibanez and Sanz (1982) (see also Carot and Sintès, 1994).

3.2.1 Static Models

Consider the general static spherically symmetric metric in the following (comoving) coordinates:

$$ds^2 = -e^{2A(R)}dT^2 + e^{2B(R)}dR^2 + R^2d\Omega^2. \quad (3.38)$$

This metric will admit a kinematic self-similarity of the form

$$\xi^a = (\xi^0(T, R), \xi^1(T, R), 0, 0), \quad (3.39)$$

when equations (1.10) and (1.11) are satisfied. From equation (3.38) it follows that (in these coordinates) $\mu = \mu(R)$ and $p = p(R)$ and hence the models necessarily admit an equation of state of the form $p = p(\mu)$.

Equation (1.10) implies that $\xi^0 = f(T)$ and that

$$A_{,1} \xi^1 + \xi^0_{,0} = \alpha. \quad (3.40)$$

Equation (1.11) is solved as follows. The (1,0) term implies that $\xi^1 = g(R)$, whence the (2,2) and (3,3) terms imply that $\xi^i = R$. Hence $\xi^0 = a_1 T + a_2$, where a_1 and a_2 are arbitrary constants. The (1,1) term then implies that

$$B_{,1} \xi^1 + \xi^1_{,1} = 1. \quad (3.41)$$

Hence equations (3.40) and (3.41) imply that

$$B_{,1} = 0, \quad A_{,1} = \frac{\alpha - a_1}{R}. \quad (3.42)$$

Therefore, metric (3.38) admits a kinematic self-similarity when it is of the form

$$ds^2 = -a^2 R^{2k} dT^2 + b^2 dR^2 + R^2 d\Omega^2, \quad (3.43)$$

where a, b and $k = \alpha - a_1$ are arbitrary constants. The kinematic self-similarity admitted by (3.43) is of the form

$$\xi = (a_1 T + a_2) \frac{\partial}{\partial T} + R \frac{\partial}{\partial R}. \quad (3.44)$$

Hence, any particular metric of the form (3.43) (i.e., with a particular value for k) admits kinematic self-similarities of all types, since we can choose a_1 in (3.44) to give any value of α according to $a_1 = \alpha - k$. In particular, each metric of the form (3.43) necessarily admits a homothetic vector ($\alpha = 1$). Note that since $a_2 \frac{\partial}{\partial T}$ is a Killing vector for the static metric (3.38), the constant a_2 can be set to zero in this case without loss of generality.

We can compare these results to those obtained in terms of the conventional coordinates in which ξ is given by equation (1.16) and the metric is written as (1.17).

By applying the coordinate transformation

$$T = \frac{(\alpha t)^{a_1/\alpha}}{a_1}, \quad (3.45)$$

$$R = r, \quad (3.46)$$

assuming $a_1 \neq 0$, $\alpha \neq 0$, the metric (3.43) becomes

$$ds^2 = -c_0^2(\tau(\alpha t)^{-1/\alpha})^{2k} dt^2 + b^2 dr^2 + r^2 d\Omega^2, \quad (3.47)$$

where c_0 is a constant and ξ is given by equation (1.16). Therefore, all static metrics which admit a kinematic self-similarity can be written in the form (3.47). Note that $\dot{S} = \dot{\Psi} = \ddot{\Phi} = 0$ in metric (3.47). Therefore, since in this case $\dot{S} = \dot{\Psi} = 0$, all kinematic self-similar static metrics are contained within the $M_2 = 0$ subcase. Finally, since $\ddot{\Phi} = 0$, we have that all static, kinematic self-similar spacetimes necessarily admit a homothetic vector.

We note that this analysis is independent of the field equations and hence is valid for any matter content and not only for the perfect fluid case examined in this chapter. However, in the perfect fluid case the exponent k in (3.47) is not arbitrary but must satisfy

$$k^2 - 2k + b^2 - 1 = 0; \quad (3.48)$$

i.e., $k = 1 \pm \sqrt{2 - b^2}$.

Therefore all static solutions which admit a kinematic self-similarity are necessarily contained within the $M_2 = 0$ subcase, and all such metrics necessarily admit a homothetic vector. However, the static solutions correspond to finite equilibrium points of the autonomous system of ODEs given by equations (2.60)-(2.62) and will feature in the analysis of Chapter 4, and hence we shall explicitly exhibit these solutions here as follows:

$$ds^2 = -c^2(\tau t^{-1/\alpha})^{2k} dt^2 + a^2 dr^2 + r^2 s_0^2 d\Omega^2, \quad (3.49)$$

and

$$\mu = \mu_0 r^{-2}, \quad p = (2ka^{-2} - \mu_0) r^{-2}, \quad (3.50)$$

where $\dot{\Phi} = k$ is one of the roots of equation (2.24) when $\ddot{\Phi} = 0$ [i.e., $k = 1 \pm \sqrt{2 - a^2 s_0^{-2}}$] and c, a and s_0 are constants. This metric is the same as that given by (3.47). The constants c and s_0 can be rescaled to unity. We note that there are no solutions in this set when $\mu_0 > a^{-2}$. Metric (3.47) can be put into explicitly static form by a simple redefinition of the time coordinate.

3.2.2 Zeroth Type static solutions

We note that in the subcase $M_2 = 0$ (in which $\dot{S} = 0$) the resulting metrics and matter functions are identical to those found in subsection 3.2 with α set identically to zero, and the self-similarity coordinate appropriately changed to $\xi = r e^{-t}$.

Chapter 4

Qualitative Behaviour of Governing Equations

As the equations for the $\alpha = 0$ case have been shown to simply be a subcase of those in the $\alpha \neq 0$ case we need only consider the one set of equations to analyse the dynamics of the models in both cases.

Applying the definitions $x_1 = \dot{S}/S$, $x_2 = \dot{\Psi} - y$, $x_3 = \dot{\Phi}$, and $x_4 = w$, we find that the governing equations (2.60)-(2.63) become

$$\dot{x}_1 = x_1 x_3 + (1 + x_1)x_2, \quad (4.1)$$

$$\dot{x}_2 = -x_2(3x_1 + x_2 - x_3 + \alpha), \quad (4.2)$$

$$\dot{x}_3 = x_4 + (1 + x_1)^2 + x_1 x_3 + x_2 x_3 + 2x_3 - x_3^2, \quad (4.3)$$

$$\dot{x}_4 = 2x_4 x_2, \quad (4.4)$$

a four-dimensional autonomous system of ODEs. The qualitative behaviour of the solutions to this system can now be examined.

It is straightforward to see that the hyperplanes $x_2 = 0$ and $x_4 = 0$ are each invariant sets. These hyperplanes then divide the space into four invariant sets in which the derivative of the function x_4 is monotonic, namely:

$$I_1 = \{(x_1, x_2, x_3, x_4) | x_2 > 0, x_4 > 0\}: \quad \dot{x}_4 > 0$$

$$I_2 = \{(x_1, x_2, x_3, x_4) | x_2 < 0, x_4 > 0\}: \quad \dot{x}_4 < 0$$

$$I_3 = \{(x_1, x_2, x_3, x_4) | x_2 < 0, x_4 < 0\}: \quad \dot{x}_4 > 0$$

$$I_4 = \{(x_1, x_2, x_3, x_4) | x_2 > 0, x_4 < 0\}: \quad \dot{x}_4 < 0$$

It follows, therefore, from the monotonicity principle (see the Introduction) that there are no periodic orbits or closed invariant surfaces in any of these invariant sets; $I_i, i = 1..4$. As a consequence any asymptotic behaviour (past or future) must be located on one of the invariant sets $x_2 = 0$ or $x_4 = 0$ (or at $x_4 = \pm\infty$). Each of these cases will be considered separately.

In all cases we will begin by considering the singular points. There are two different types of singular points which must be considered, finite and infinite. The finite singular points are located at the values of (x_1, x_2, x_3, x_4) where the vector field for the system (4.1)-(4.4) vanishes. They are listed in Table 4.1. The local analysis for each of these points will be given in the appropriate invariant set analysis.

In order to complete the analysis in each of the cases $x_2 = 0$ or $x_4 = 0$ (or at $x_4 = \pm\infty$), it will be necessary to consider the singular points located at infinity. These will be considered by compactifying the phase space using a standard Poincare transformation as described in Chapter 1. In the case of equations (4.1)-(4.4) the transformation takes on the form:

$$X = x_1\Theta, \quad X_2 = x_2\Theta, \quad X_3 = x_3\Theta, \quad X_4 = x_4\Theta$$

$$\Theta = (1 + x_1^2 + x_2^2 + v^2 + w^2)^{-1/2}.$$

The equations (4.1)-(4.4) become

$$X'_1 = X_1(X_1 + X_3 - K) - X_1(X_2^2 + X_3X_4)\Theta \quad (4.5)$$

$$X'_2 = X_2(X_3 - X_2 - 3X_1 - K) - X_2(X_2^2 + X_3X_4 - X_2)\Theta \quad (4.6)$$

$$X'_3 = X_1^2 + X_3(X_1 + X_2 - X_3 - K) - X_3(X_2^2 + X_3X_4 - X_4)\Theta \quad (4.7)$$

$$X'_4 = X_4(2X_2 - K) - X_4(X_2^2 + X_3X_4)\Theta \quad (4.8)$$

Table 4.1: **Finite Singular Points** for equations (4.1)-(4.4). The local analysis for each singular point will be discussed in subsequent sections, according to their classification. **Q** and **R_±** are isolated singular points and **S** and **T** are curves of non-isolated singular points (i.e. one- dimension equilibrium sets). Note that the point **Q** intersects **T** when $\alpha = 3$, and the curves **S** and **T** intersect at the point $(0, 0, 0, 0)$

	(x_1, x_2, x_3, x_4)	Eigenvalues	Exact Solution
Q	$(-1, 3 - \alpha, 0, 0)$	$\lambda_1 = -\lambda_2 = 3 - \alpha$ $\lambda_4 = 6 - 2\alpha, \lambda_3 = -\alpha$	Metric: eqn. (4.37) Geodesic (plane symmetric) solutions
R_±	$\left(\frac{(-5\alpha-3\pm\Delta)}{8}, \frac{(7\alpha^2+18\alpha+23\mp(3\alpha+5)\Delta)}{16(\alpha+1)}, \frac{-(7\alpha^2+14\alpha-5\mp(3\alpha+1)\Delta)}{16(\alpha+1)}, 0 \right)$ $\Delta=9\alpha^2-2\alpha+25$	see subsection 4.2	Metric: eqn. (4.39)
S	$(0, 0, c_1, c_1^2 + 2c_1 - 1)$	$\lambda_1, \lambda_2, \lambda_3$: see table 4.3 $\lambda_4 = c_1 - \alpha$	Metric: eqn (4.41) Static solution
T	$(c_2, 0, 0, -c_2^2 - 2c_2 - 1)$	$\lambda_1, \lambda_2, \lambda_3$: see table 4.3 $\lambda_4 = -(3c_2 + \alpha)$	Metric: eqn (4.43) Geodesic (spherically symmetric) solution Static fluid

where

$$K = X_1^2 X_2 + 2X_1^2 X_3 - 3X_1 X_2^2 + X_1 X_3^2 - X_2^3 + X_2^2 X_3 + X_2 X_3^2 - X_3^3 + 2X_2 X_4. \quad (4.9)$$

The singular points located on the invariant boundary $\Theta = 0$ [which is now the location of the infinite singular points for equations (4.1)-(4.4)] are given in table 4.2, with the associated eigenvalue/eigenvector pairs for the Jacobian of the system (4.5)-(4.8). Each of the points will be considered in the appropriate invariant sets. It is important to note that the only case in which the variable $x_4 \rightarrow \pm\infty$ is when the remaining three variables vanish; i.e. as $x_4 \rightarrow \pm\infty$, x_2 necessarily tends to zero. As a result this asymptotic behaviour will be considered as a subset of the $x_2 = 0$ invariant set.

Table 4.2: **Classification of the Infinite Singular Points** of the system of equations (4.5)-(4.8) [the Poincare transformation of the system (4.1)-(4.4)]. The exact solutions for each of these points are described in subsection 4.4.2.

	(X_1, X_2, X_3, X_4)	Eigenvalue - Eigenvector Pairs		Classification
A_±	$(0, \pm 1, 0, 0)$	± 2	$(1, 0, 0, 0)$	A₊ : Source
		± 2	$(0, 1, 0, 0)$	
		± 2	$(0, 0, 1, 0)$	A₋ : Sink
		± 3	$(0, 0, 0, 1)$	
B_±	$(0, 0, \pm 1, 0)$	± 2	$(1, 0, 0, 0)$	B₊ : Source
		± 2	$(0, 1, 0, 0)$	
		± 2	$(0, 0, 1, 0)$	B₋ : Sink
		± 1	$(0, 0, 0, 1)$	
C_±	$(0, 0, 0, \pm 1)$	0	$(1, 0, 0, 0)$	Saddle-Node <i>see section 4.3</i>
		0	$(0, 1, 0, 0)$	
		0	$(0, 0, 1, 0)$	
		0	$(0, 0, 0, 1)$	
D_±	$\frac{\sqrt{2}}{2}(\pm 1, 0, \pm 1, 0)$	$\mp\sqrt{2}$	$(1, 0, 1, 0)$	D₊ : Sink
		$\mp\frac{\sqrt{2}}{2}$	$(0, 0, 0, 1)$	
		$\mp\frac{3\sqrt{2}}{2}$	$(-1, 0, 1, 0)$	D₋ : Source
		$\mp\frac{3\sqrt{2}}{2}$	$(0, 1, 0, 0)$	
E_±	$\frac{\sqrt{5}}{5}(\mp 2, 0, \pm 1, 0)$	$\pm\frac{6\sqrt{5}}{5}$	$(0, 1, 0, 0)$	Saddle
		$\mp\frac{6\sqrt{5}}{5}$	$(1, 0, 2, 0)$	
		$\mp\frac{\sqrt{5}}{5}$	$(0, 0, 0, 1)$	
		$\mp\frac{2\sqrt{5}}{5}$	$(-2, 0, 1, 0)$	
F_±	$\frac{\sqrt{2}}{2}(0, \pm 1, \pm 1, 0)$	$\mp\sqrt{2}$	$(0, -1, 1, 0)$	Saddle
		$\pm\sqrt{2}$	$(2, -1, 1, 0)$	
		$\pm\sqrt{2}$	$(0, 0, 0, 1)$	
		0	$(0, 1, 1, 0)$	
G_±	$\frac{\sqrt{14}}{14}(\mp 2, \pm 3, \pm 1, 0)$	$\pm\frac{\sqrt{14}}{7}$	$(0, 0, 0, 1)$	Saddle
		$\mp\frac{4\sqrt{14}}{7}$	$(2, -3, -1, 0)$	
		$\mp\frac{3\sqrt{14}}{7}$	$(1, 0, 2, 0)$	
		$\mp\frac{3\sqrt{14}}{7}$	$(0, 1, -3, 0)$	
H_±	$\frac{\sqrt{17}}{17}(\pm 1, \mp 3/2, \pm 1, 0)$	$\mp\frac{27\sqrt{17}}{136}$	$(134, -201, 257, 0)$	Saddle
		$\mp\frac{\sqrt{17}}{34}$	$(2, -3, 2, 0)$	
		$\pm\frac{21\sqrt{17}}{136}$	$(63, 118, 63, 0)$	
		$\mp\frac{23\sqrt{17}}{136}$	$(0, 0, 0, 1)$	

4.1 Shear-Free Solutions: $x_2 = 0$

The invariant set $x_2 = 0$ was shown to represent possible asymptotic behaviour of the system (4.1)-(4.4). Note when the kinematic quantities are calculated for the spherically symmetric metric given by (1.17) the non-zero shear terms are:

$$\begin{aligned}\sigma_{11} &= 2x_4x_2S^2(3\alpha te^\phi)^{-1} \\ \sigma_{22} &= r^2x_2S^2(3\alpha te^\phi)^{-1} \\ \sigma_{33} &= r^2\sin^2(\theta)x_2S^2(3\alpha te^\phi)^{-1}.\end{aligned}\tag{4.10}$$

Therefore this invariant set corresponds to solutions which have the physical property of zero shear.

In the case $x_2 = 0$ the governing equations (4.1)-(4.4) reduce to a one parameter family of two-dimensional systems:

$$\dot{x}_1 = x_1x_3 \tag{4.11}$$

$$\dot{x}_3 = w_0 + (1 + x_1)^2 + x_1x_3 + 2x_3 - x_3^2 \tag{4.12}$$

$$x_4 = w_0 \tag{4.13}$$

Therefore, the dynamics can be represented in the (x_1, x_3) plane with the parameter w_0 (in the direction of x_4 there is no motion). All analysis will thus be considered in the directions x_1 and x_3 .

Analysis of the system then begins by locating and characterising each of the finite singular points. The finite singular points are those given in 4.1 which have the condition $x_2 = 0$, namely **S** and **T**. In the three dimensions of (x_1, x_3, x_4) the corresponding eigenvalue-eigenvector pairs which will be used to determine the local stability are given in Table 4.3.

Each of these classes of singular points represents a (neutral) curve of non-isolated singular points parameterised by the constants c_1 or c_2 . In the direction tangent to

Table 4.3: **Finite Singular Points** for equations (4.11)-(4.12). Each of the points **S** and **T** will intersect the (x_1, x_3) plane of consideration at either 2, 1, or no points, depending on the value of the parameter w_0 (see equations 4.15). **T** will exist only in the case of spherical symmetry, and **S** exists iff $w_0 \geq -2$.

	(x_1, x_3, x_4)	Eigenvalue - Eigenvector Pairs	
S	$(0, c_1, c_1^2 + 2c_1 - 1)$	c_1 $-2(c_1 + 1)$ 0	$(3c_1 + 2, 2 + c_1, 0)$ $(0, 1, 0)$ $(0, 1, 2c_1 + 2)$
T	$(c_2, 0, -c_2^2 - 2c_2 - 1)$	$\frac{1}{2}(-1 + c_2 + \sqrt{4 + 4c_2 + 9c_2^2})$ $\frac{1}{2}(-1 + c_2 - \sqrt{4 + 4c_2 + 9c_2^2})$ 0	$(2c_2, -2 + c_2 + \sqrt{4 + 4c_2 + 9c_2^2}, 0)$ $(2c_2, -2 + c_2 - \sqrt{4 + 4c_2 + 9c_2^2}, 0)$ $(1, 0, -2c_2 - 2)$

the curve the eigenvalue is zero, as expected. In all other directions the eigenvalues are generally non-zero, changing sign at the various bifurcation values, thus the equilibrium set is said to be normally hyperbolic. It should be noted that in each of the two-dimensional planes which partition the three-dimensional space these neutral curves intersect at 2, 1 or no points, depending on the values of the parameters c_1 and c_2 . The intersection of the curve with the two-dimensional plane will be label by \pm . The constants c_1 and c_2 are related to the parameter w_0 in the following manner:

$$w_0 = c_1^2 + 2c_1 - 1 \quad \text{and} \quad w_0 = -c_2^2 - 2c_2 - 1, \quad (4.14)$$

i.e.

$$c_1 = -1 \pm \sqrt{2 + w_0} \quad c_2 = -1 \pm \sqrt{-w_0} \quad (4.15)$$

Both the singular points and their associated eigenvalues show a dependence on the parameter w_0 , indicating that the dynamics will depend on the value of w_0 ; the bifurcation values are $w_0 = -2, 1$, and 0 .

Using these bifurcation values we find that the qualitative nature of the system (4.11)-(4.12) can be determined by considering the seven cases:

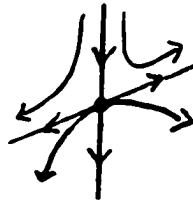
Case I:	$w_0 < -2$
Case II:	$w_0 = -2$
Case III:	$-2 < w_0 < -1$
Case IV:	$w_0 = -1$
Case V:	$-1 < w_0 < 0$
Case VI:	$w_0 = 0$
Case VII:	$w_0 > 0$

For each of these seven cases the sign of the eigenvalues can be determined from Table 4.3. When the parameter w_0 is not equal to one of the bifurcation values (i.e. -2 , -1 , or 0) the singular points are hyperbolic and can be classified using the Hartman-Grobman theorem. In cases II, IV, and VI, however, the points are non-hyperbolic. Note that Cases I-V represent the possible behaviours resulting in the spherically symmetric case, Case VI represents the plane symmetric case and Case VII represents the hyperbolically symmetric case.

In case II (i.e. $c_1 = -1$, $c_2 = -1 \pm \sqrt{2}$) we see that the points S_- and S_+ coincide. There is one positive eigenvalue and one zero eigenvalue. The eigenvector associated with the zero eigenvalue at this point is $(0,1)$. Therefore the exact dynamics can be determined by simply examining the dynamics on the invariant line $x_1 = 0$ (a simple application of *Centre Manifold Theory*, Wiggins, 1990). On this line we then have:

$$\dot{x}_3 = -(1 - x_3)^2 \leq 0. \quad (4.16)$$

Since the derivative of x_3 is always negative it follows that the point $S_+(\equiv S_-)$ is a saddle-node; i.e.



In case IV (i.e. $c_1 = 0$, -2 , $c_2 = 0$, -2) we see that the points S_- and T_+ coincide.

Table 4.4: **Classification of Local dynamics** for finite singular points of (4.11)-(4.12), the two-dimensional system with parameter w_0 . Note that "DNE" indicates that the point does not exist in that particular case.

	S_+	S_-	T_+	T_-
$w_0 > 0$	saddle	saddle	DNE	DNE
$w_0 = 0$	saddle	saddle	saddle-node	($\equiv T_+$)
$-1 < w_0 < 0$	saddle	saddle	source	saddle
$w_0 = -1$	saddle	saddle-node	($\equiv S_-$)	saddle
$-2 < w_0 < -1$	saddle	source	saddle	saddle
$w_0 = -2$	saddle-node	($\equiv S_+$)	saddle	saddle
$w_0 < -2$	DNE	DNE	saddle	saddle

There is one positive eigenvalue and one zero eigenvalue. The eigenvector associated with the zero eigenvalue at this point is $(1,-1)$. In the direction of the eigenvector and near the singular point we have:

$$\dot{x}_1 = x_1 x_3 \quad (4.17)$$

where the right-hand side is always negative. Therefore it follows that the point $T_+(\equiv S_-)$ is a saddle-node.

In case VI (i.e. $c_1 = -1 \pm \sqrt{2}$, $c_2 = 0$) we see that the points T_+ and T_- coincide. There is one positive eigenvalue and one zero eigenvalue. The eigenvector associated with the zero eigenvalue at this point is $(1,0)$. In the direction of the eigenvector and near the singular point we have:

$$\dot{x}_3 = (1 + x_1)^2 \quad (4.18)$$

where the right hand side is always positive. Therefore it follows that the point $T_+(\equiv T_-)$ is a saddle-node.

Having completed the classification of the non-hyperbolic singular points, a summary of the classification of each of the finite singular points restricted to the case $x_2 = 0$ is given in Table 4.4

The analysis of this case is completed by considering the infinite singular points and their local behaviour. The transformed system is given by (4.5) - (4.8). When restricted to the case $x_2 = X_2 = 0$, only the points B_{\pm} , C_{\pm} , D_{\pm} and E_{\pm} come into consideration. The points C_{\pm} corresponds to a value of $x_4 = w_0 = \pm\infty$ and will therefore be considered separately below. The other three pairs of infinite singular points are then classified as *source-sink* pairs according to the eigenvalues contained within the two-dimensional planes.

A summary of the dynamics in each of these invariant two-dimensional planes, with their relationship to the parameter w_0 , can be seen in Figures 4.1 - 4.3 (separated according to the symmetry of the metric; i.e. spherical, plane or hyperbolic.)

4.1.1 Curvature Dominated Solutions: $x_4 \rightarrow \pm\infty$

The solutions characterised by $x_4 \rightarrow \pm\infty$ correspond to the points C_{\pm} as listed in table 4.2, found by compactifying the phase space using a Poincare transformation. This point is 'non-hyperbolic' in all four directions. To determine the exact nature of the local behaviour of these points we consider the dynamics in the direction of the eigenvectors by noting that the sets $x_1 = x_2 = x_4 = 0$, $x_1 = x_3 = x_4 = 0$ and $x_1 = x_2 = x_3 = 0$ are invariant for the system (4.5)-(4.8).

The invariant set $x_1 = x_2 = x_4 = 0$ corresponds exactly to the eigenvector $(0, 0, 1, 0)$. In this case we have that $\dot{x}_3 = x_3^2(x_3^2 - 1)$ which is negative near the value $x_3 = 0$ (i.e. near the points C_{\pm}). Likewise, the invariant set $x_1 = x_3 = x_4 = 0$ corresponds to the eigenvector $(0, 1, 0, 0)$. In this direction we have that $\dot{x}_2 = x_2^2(x_2^2 - 1)$ which is negative near the value $x_2 = 0$ (i.e. near the points C_{\pm}). Therefore in these two directions the point acts as a saddle-node. In the third invariant set $x_1 = x_2 = x_3 = 0$ we have that $\dot{x}_4 \equiv 0$ always, and no dynamics are present in that direction.

The fourth and final direction to be considered is $(1, 0, 0, 0)$. This direction does not correspond to the tangent of any obvious invariant sets. To complete this analysis we will consider examining the singular points $x_4 = \pm\infty$ through a different change

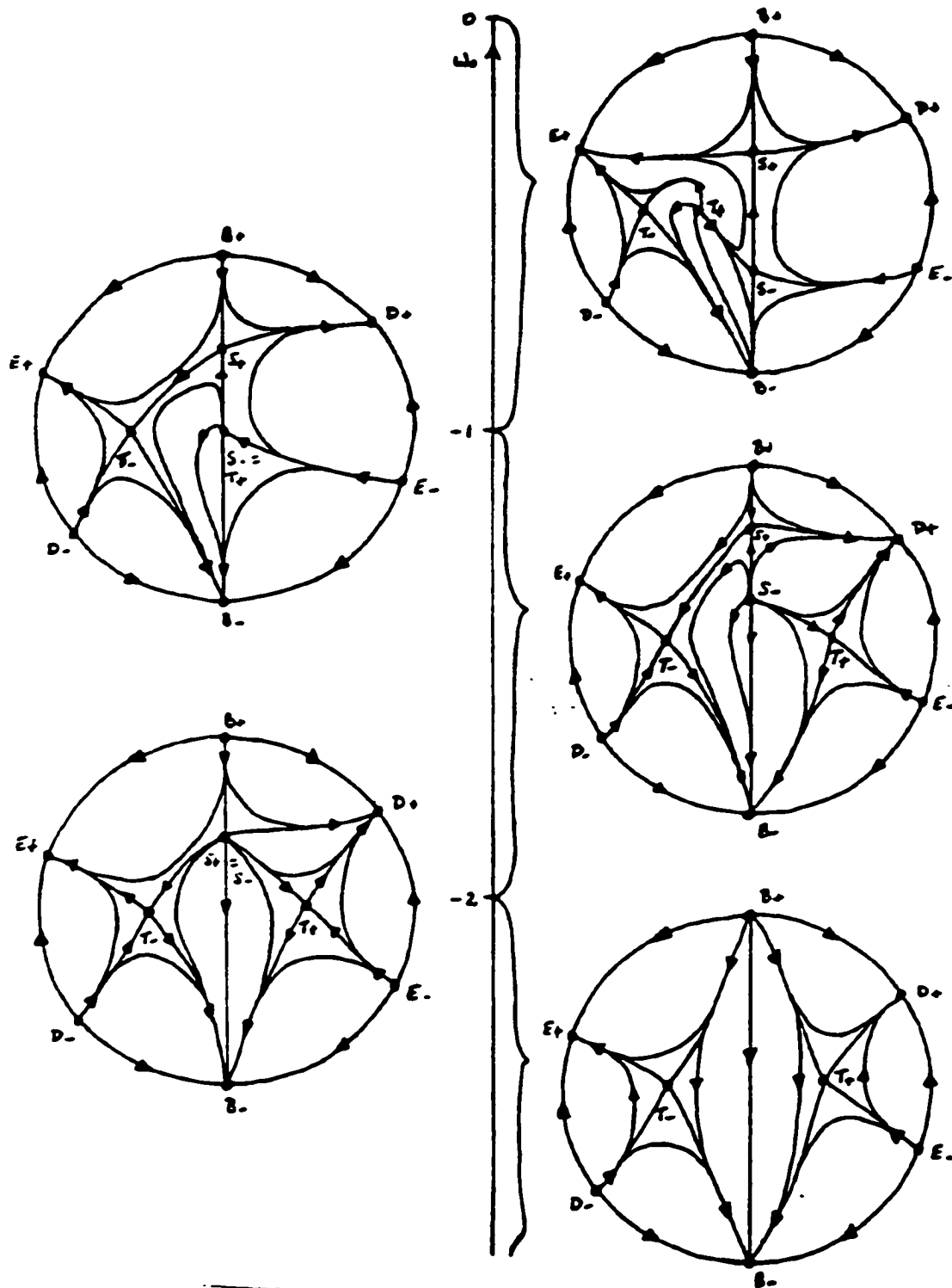


Figure 4.1: Phase portrait of spherically symmetric solutions with zero shear: *Each plot is of the compactified space (X_1, X_3) .*

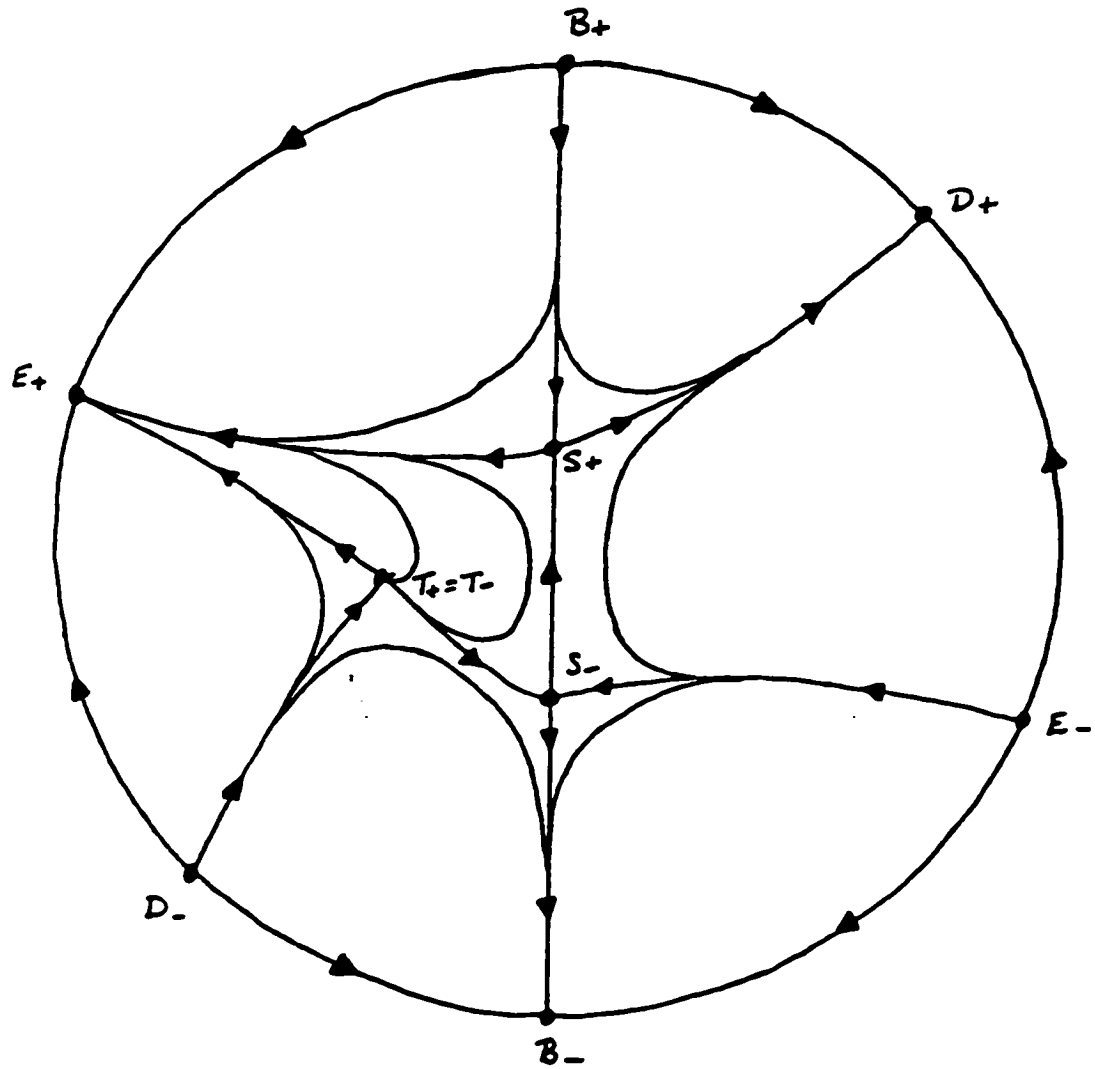


Figure 4.2: Phase portrait of plane symmetric solutions with zero shear: *Each plot is of the compactified space (X_1, X_3) .*

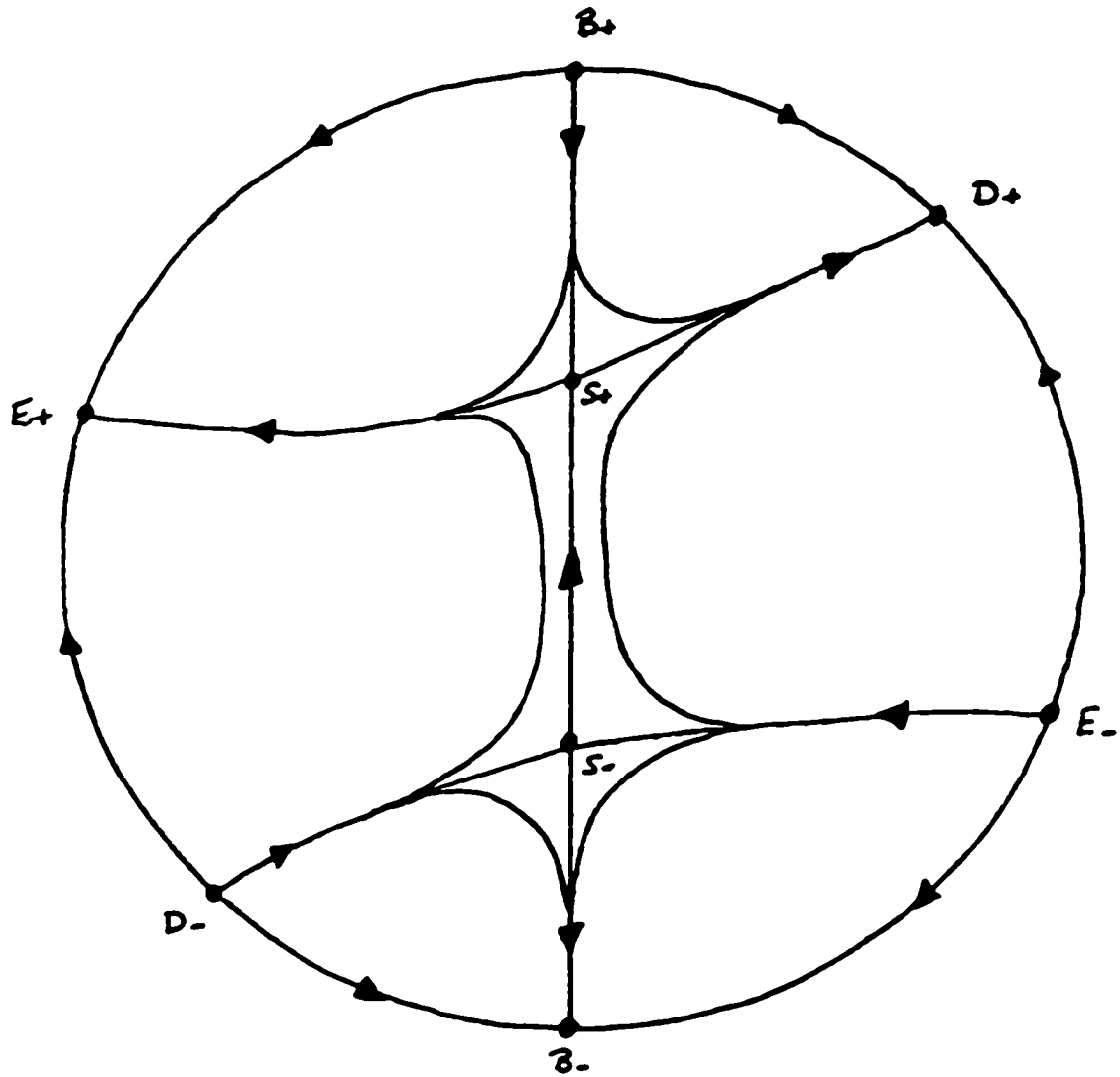


Figure 4.3: Phase portrait of hyperbolically symmetric solutions with zero shear: Each plot is of the compactified space (X_1, X_3) .

of variables, one which will move the points C_{\pm} to the origin. Consider:

$$A = \frac{x_1}{x_4}, \quad B = \frac{x_2}{x_4}, \quad C = \frac{x_3}{x_4}, \quad \text{and} \quad D = \frac{1}{x_4}, \quad (4.19)$$

and a "time" variable that is defined by $f' = D\dot{f}$. The system (4.1)-(4.4) then becomes:

$$A' = AC + AB + BD - 2AB \quad (4.20)$$

$$B' = -3AB - B^2 + BC - \alpha BD - 2BD \quad (4.21)$$

$$C' = D + D^2 + 2AD + A^2 + 2CD - C^2 + AC + BC \quad (4.22)$$

$$D' = -2CD. \quad (4.23)$$

The singular points of interest (namely C_{\pm}) are now located at $(0, 0, 0, 0)$. The three invariant sets $A = C = D = 0$, $A = B = D = 0$ and $A = B = C = 0$ are equivalent to those found when using the previous Poincare transformation. The dynamics in the fourth direction can then be determined by considering the two-dimensional set $B = D = 0$, i.e.:

$$A' = AC \quad (4.24)$$

$$C' = A^2 - C^2 + AC. \quad (4.25)$$

In this case $A = C$ and $A = -2C$ are invariant sets. On each of these sets the derivatives are strictly positive or strictly negative, indicating that this point is a saddle-node.

Therefore in three of the four directions (of the full phase space) through the singular points C_{\pm} the derivative does not change sign, and in the fourth direction there is no motion (as this direction is normal to the sheets of invariant planes described in the previous section). This point is, therefore, a higher dimensional saddle-node.

4.1.2 Shear-free solutions in the full four-dimensional space

For each of the points S_{\pm} , T_{\pm} the dynamics in the fourth direction must then be determined. Relative to the system (4.1) - (4.4) there is a fourth eigenvalue (see Table 4.1).

$$\mathbf{S}_{\pm} \quad \text{eigenvalue: } c_1 - \alpha$$

$$\mathbf{T}_{\pm} \quad \text{eigenvalue: } -(3c_2 + \alpha)$$

The bifurcations for the points \mathbf{S}_{\pm} are $c_1 = \alpha$ (i.e. $w_0 = (\alpha + 1)^2 - 2$). For $w_0 < (\alpha + 1)^2 - 2$ the vector field is attracting towards the line \mathbf{S} in the 3-dimensional set $x_2 = 0$ (or towards the points \mathbf{S}_+ and \mathbf{S}_- in the two-dimensional cross sections given in Figures 4.1-4.3. Likewise, for $w_0 > (\alpha + 1)^2 - 2$ the vector field is repelling.

The bifurcations for the points \mathbf{T}_{\pm} are $c_2 = -\alpha/3$ (i.e. $w_0 = -(3 - \alpha)^2/9$). For $w_0 < -(3 - \alpha)^2/9$ the vector field is attracting towards the line \mathbf{T} in the 3-dimensional set $x_2 = 0$ (or towards the points \mathbf{T}_+ and \mathbf{T}_- in the two-dimensional cross sections given in Figures 4.1-4.3. Likewise, for $w_0 > -(3 - \alpha)^2/9$ the vector field is repelling.

4.2 Plane Symmetric Solutions: $x_4 = 0$

The invariant set $x_4 = 0$ is shown to represent possible asymptotic behaviour of the system (4.1)-(4.4). Note that in Chapter 2 the variable x_4 was defined in terms of the curvature of the metric (see equation (2.61)), such that the case $x_4 = 0$ corresponds to a plane symmetric metric. Therefore this invariant set corresponds to all possible solutions with plane symmetry.

In the case $x_4 = 0$ the governing system of equations (4.1)-(4.4) reduces to

$$\dot{x}_1 = x_1 x_3 + (1 + x_1) x_2, \quad (4.26)$$

$$\dot{x}_2 = -x_2(3x_1 + x_2 - x_3 + \alpha), \quad (4.27)$$

$$\dot{x}_3 = (1 + x_1)^2 + x_1 x_3 + x_2 x_3 + 2x_3 - x_3^2, \quad (4.28)$$

In this case the dynamics are contained in a three-dimensional space, making the analysis more complicated. We will proceed by examining the local dynamics near finite and infinite singular points, and then use numerics to determine the global behaviour of the system.

The finite singular points in this invariant set are \mathbf{Q} , \mathbf{R}_{\pm} as given in Table 4.1 and \mathbf{S}_{\pm} and \mathbf{T}_0 (the intersection of the curves \mathbf{S} and \mathbf{T} with the hyperplane $x_4 = 0$).

The points \mathbf{S}_\pm and \mathbf{T}_0 have been completely analysed in the previous section (see special case $w_0 = 0$), therefore only the remaining two points need to be considered to complete the local analysis. The classification will be determined from the sign of the eigenvalues. In cases in which the real part of the eigenvalue is non-zero the Hartman Grobman theorem is invoked. In all other cases a more detailed derivation of the local dynamics is given.

Point Q: $(-1, 3 - \alpha, 0, 0)$

The eigenvalues for this point are

$$3 - \alpha, \quad \alpha - 3, \quad \text{and} \quad -\alpha \quad (4.29)$$

(see Table 4.1). The different values of the parameter α determine the exact nature of the local dynamics about this point. The bifurcation values are $\alpha = 0$ and 3 . When $\alpha \neq 0, 3$ this point is a saddle, with a 2-dimensional stable manifold and a 1-dimensional unstable manifold. At the bifurcation value of $\alpha = 0$ one of the four eigenvalues vanish. The eigenvector-eigenvalue pairs are then

$$\begin{array}{ll} 0 & (1, 0, 3) \\ 3 & (2, -3, 0) \\ -3 & (0, 1, 0) \end{array}$$

Small perturbations in the direction of the eigenvector $(1, 0, 3)$ show that the function x_1 is monotonic. Therefore in this direction there are both attracting and repelling regions. In the directions of each of the remaining eigenvectors the point is a saddle with one stable and one unstable manifold.

At the bifurcation value of $\alpha = 3$ two of the three eigenvalues vanish. The eigenvector-eigenvalue pairs are then

$$\begin{array}{ll} 0 & (1, 0, 0) \quad (0, 1, 0) \\ -3 & (1, 0, 3) \end{array}$$

This point now coincides with the point \mathbf{T}_0 as seen in the case $w_0 = 0, x_2 = 0$ in the previous section. The local dynamics in the various regions of α are sketched in Figure 4.4.

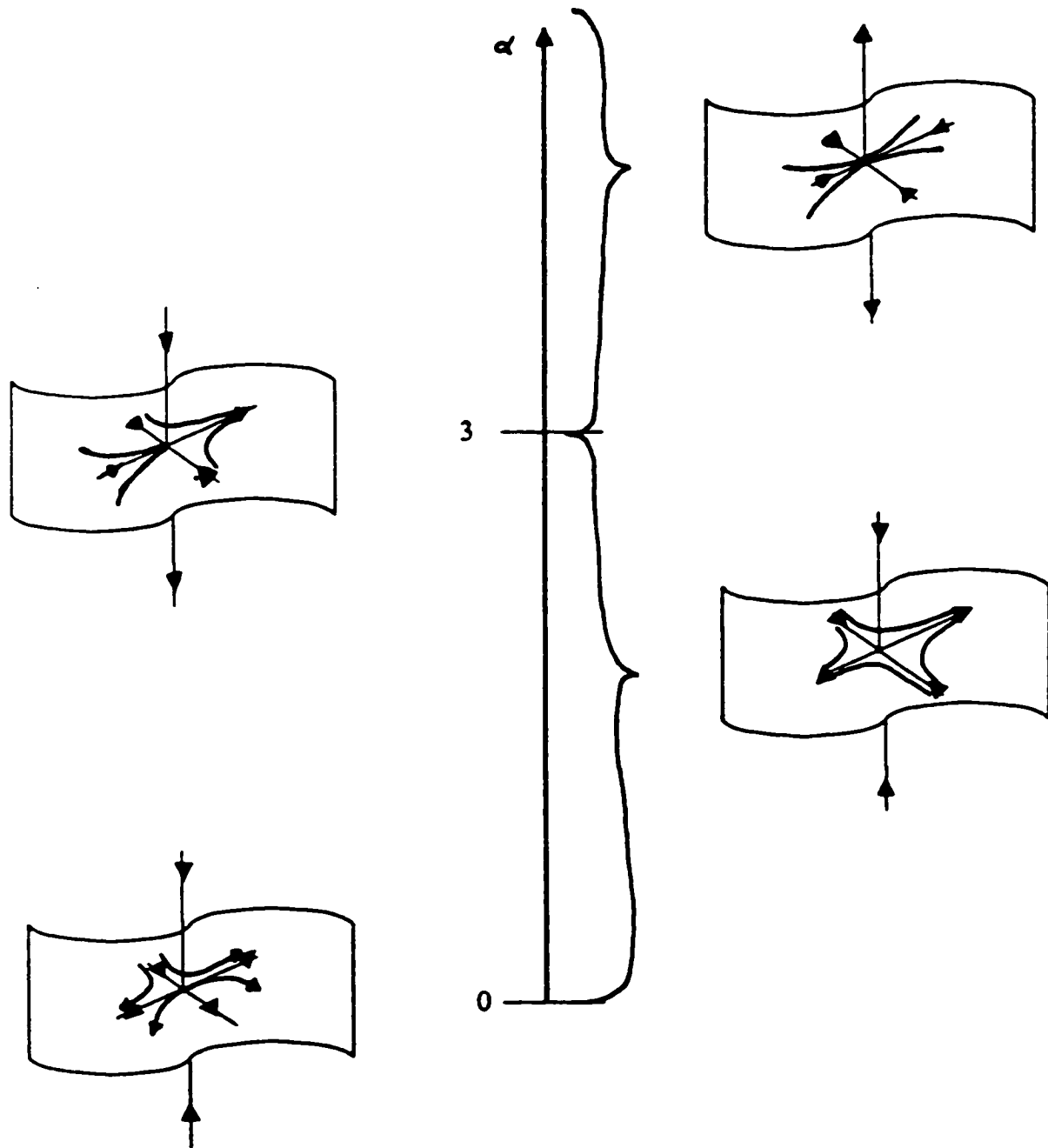


Figure 4.4: Local Dynamics of the singular point Q : *in the case of plane symmetry. Bifurcations occur at $\alpha = 0$ and 3 .*

$$\text{Point } \mathbf{R}_{\pm}: \left(\frac{-5\alpha-3\pm\Delta}{8}, \frac{(7\alpha^2+18\alpha+23\mp(3\alpha+5)\Delta)}{16(\alpha+1)}, \frac{-(7\alpha^2+14\alpha-5\mp(3\alpha+1)\Delta)}{16(\alpha+1)} \right)$$

where $\Delta^2 \equiv 9\alpha^2 - 2\alpha + 25$. In the full four-dimensional phase space the eigenvalues of these points are given by the solutions to the quartic characteristic equation:

$$a(\alpha)\lambda^4 + b(\alpha)\lambda^3 + c(\alpha)\lambda^2 + d(\alpha)\lambda + e(\alpha) = 0 \quad (4.30)$$

where

$$a(\alpha) = 256 + 768\alpha + 768\alpha^2 + 256\alpha^3 \quad (4.31)$$

$$b(\alpha) = -416 - 1152\alpha - 1344\alpha^2 - 896\alpha^3 - 288\alpha^4 \\ \pm (224 + 608\alpha + 544\alpha^2 + 160\alpha^3)\sqrt{25 - 2\alpha + 9\alpha^2} \quad (4.32)$$

$$c(\alpha) = -2648\alpha - 2736\alpha^2 - 2864\alpha^3 - 1944\alpha^4 - 632\alpha^5 \\ \pm (168 + 368\alpha + 640\alpha^2 + 656\alpha^3 + 216\alpha^4)\sqrt{25 - 2\alpha + 9\alpha^2} \quad (4.33)$$

$$d(\alpha) = 6714 + 13380\alpha + 24630\alpha^2 + 24824\alpha^3 + 16326\alpha^4 + 8196\alpha^5 + 2186\alpha^6 \\ \pm (1422 + 2634\alpha + 4476\alpha^2 + 4814\alpha^3 + 722\alpha^5 + 2838\alpha^4)\sqrt{25 - 2\alpha + 9\alpha^2} \quad (4.34)$$

$$e(\alpha) = -25 - 6823\alpha - 17113\alpha^2 - 19295\alpha^3 - 14419\alpha^4 - 7933\alpha^5 - 3259\alpha^6 - 765\alpha^7 \\ \pm (-5 + 1400\alpha + 3491\alpha^2 + 3640\alpha^3 + 2401\alpha^4 + 1104\alpha^5 + 257\alpha^6) \\ \sqrt{25 - 2\alpha + 9\alpha^2} \quad (4.35)$$

Each of the eigenvalues, λ_i , is a function of the parameter α . We can determine the relative signs of these eigenvalues without actually algebraically solving for the roots of the characteristic equation. The details are given in Appendix A. Plots of the three eigenvalues [in the $x_4 = 0$ plane] as functions of the parameter α are given in Figures 4.5 (for R_+) and 4.7 (for R_-).

Bifurcations occur when the real part of one (or more) eigenvalues vanishes. The complete list of the bifurcation values for the points \mathbf{R}_{\pm} is

$$\mathbf{R}_+ \quad \alpha = \sqrt{2} - 1, \quad 3, \quad \text{and} \quad \tau_1 \approx 1.067836956; \\ \mathbf{R}_- \quad \alpha = 0$$

For all other values of α the points \mathbf{R}_{\pm} are hyperbolic and can be characterised by the

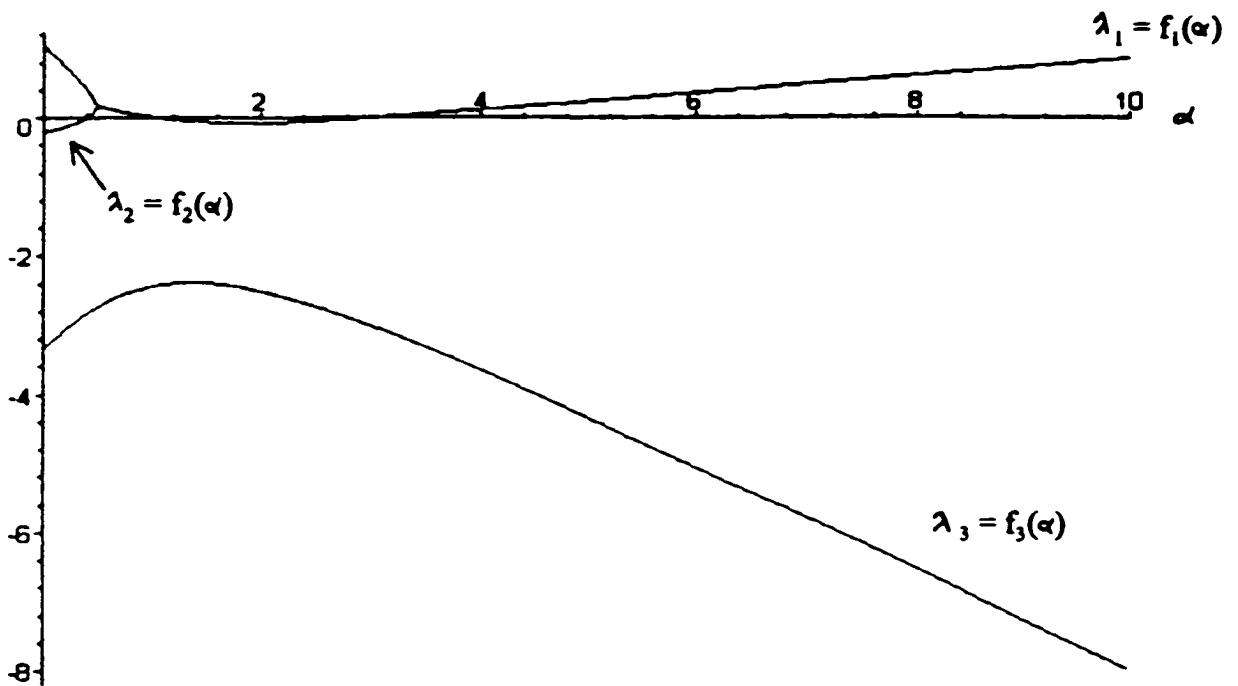


Figure 4.5: Eigenvalues for the singular point R_+ : in the case of plane symmetry; i.e. in the set $x_4 = 0$. Note that λ_1 and λ_2 are conjugate pairs.

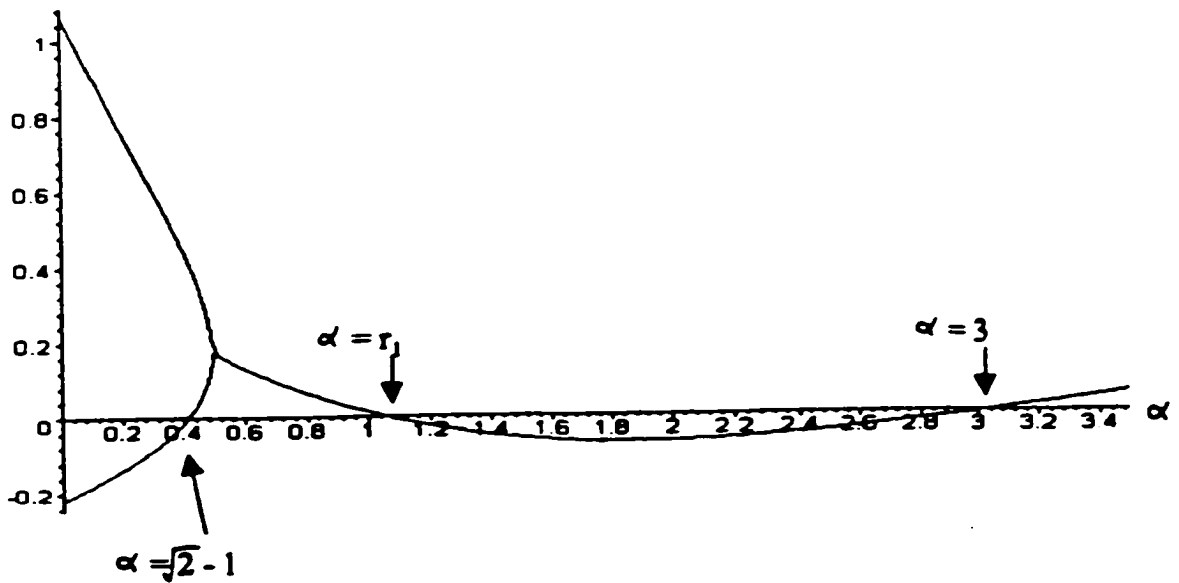


Figure 4.6: Eigenvalues for the singular point R_+ : zoomed on in the range $0 \leq \alpha \leq 3.5$.

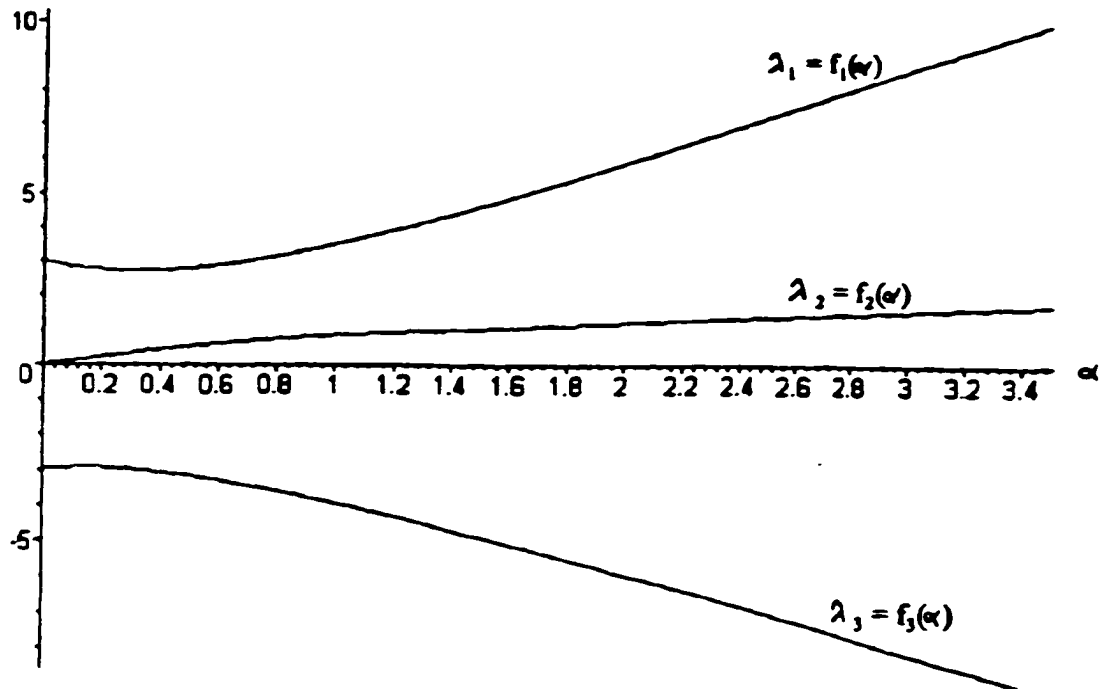


Figure 4.7: Eigenvalues for the singular point \mathbf{R}_- : in the case of plane symmetry; i.e. in the set $x_4 = 0$.

sign of the eigenvalues (see appendix A). Therefore in the range $\alpha \in [0, r_1) \cup (3, \infty)$ the point \mathbf{R}_+ is a **saddle**. In the range $\alpha \in (r_1, 3)$ it is a **sink**.

At the bifurcation point $\alpha = \sqrt{2} - 1$ two eigenvalues vanish. One of the remaining eigenvalues is positive and one negative. The zero eigenvalues have eigenvectors $(1, 1 - \sqrt{2}, 0, 2 - 3\sqrt{2})$ and $(0, 0, 1, 2\sqrt{2})$. At the bifurcation value of $\alpha = 3$ this point coincides with \mathbf{Q} . Finally, at the bifurcation value of r_1 there is a conjugate pair of purely imaginary eigenvalues plus one positive and one negative eigenvalue. A summary of the local dynamics of the point \mathbf{R}_+ is sketched in Figure 4.8.

For the point \mathbf{R}_- in the range $\alpha \in (0, \infty)$ the point \mathbf{R}_- is a **saddle**. This is true both in the full phase space and in the invariant set $x_4 = 0$. At the bifurcation value of $\alpha = 0$ the point \mathbf{R}_- coincides with \mathbf{Q} . A summary of the local dynamics of the point \mathbf{R}_- is given in Figure 4.9.

At infinity we can consider the singular points by considering the phase space compactified by the Poincaré transformation. The singular points are then those listed in Table 4.2 with the property $X_4 = 0$, namely all points except C_{\pm} . The

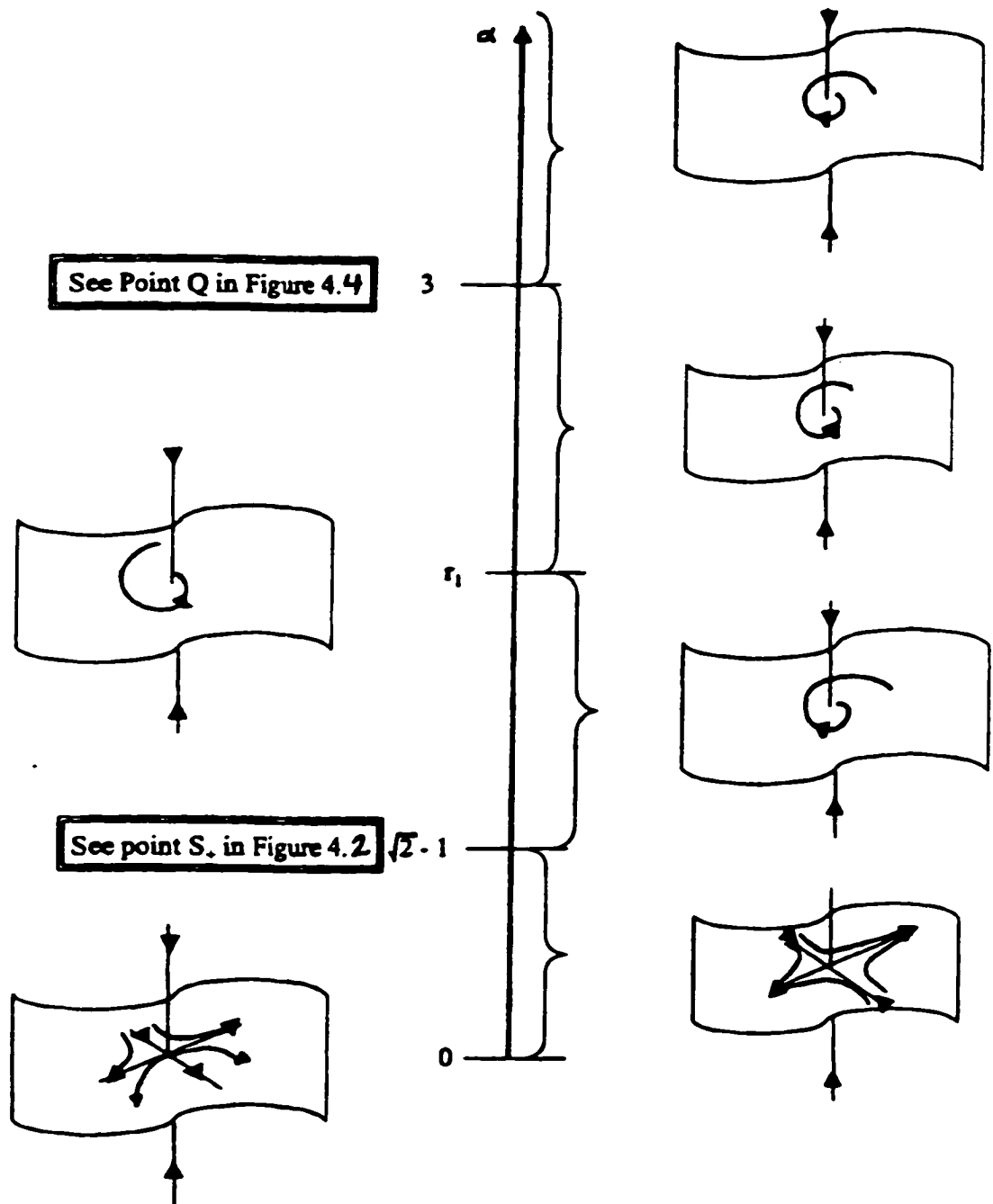


Figure 4.8: Local dynamics of the singular point R_+ : in the case of plane symmetry; i.e. in the set $x_4 = 0$. Bifurcations occur at $\alpha = 0, \sqrt{2}-1, r_1$, and 3. At $\alpha = \sqrt{2}-1$ $R_+ = S_+$, and at $\alpha = 3$, $R_+ \equiv Q$

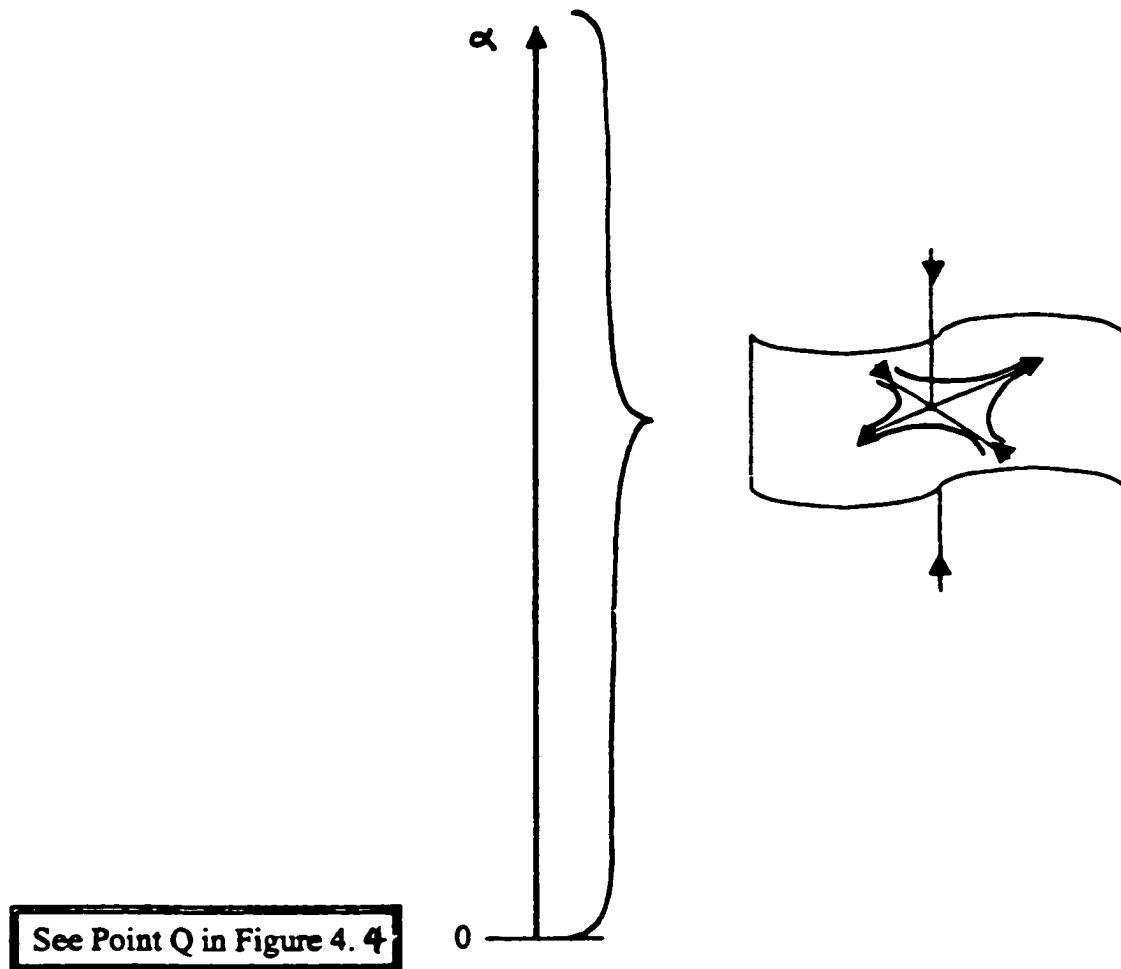


Figure 4.9: Local dynamics of the singular point R_- : *in the case of plane symmetry; i.e. in the set $x_4 = 0$. Bifurcations occur at $\alpha = 0$. At $\alpha = 0$, $R_- \equiv Q$*

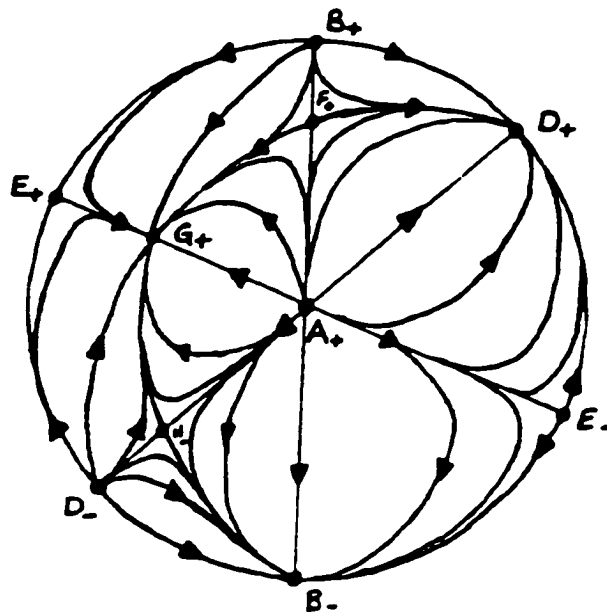


Figure 4.10: Dynamics on the infinite boundary for the plane symmetric solutions: for the compactified phase space. Top hemisphere; i.e. $X_2 > 0$

classification is once again determined by applying the Hartman-Grobman theorem. We note that the infinite boundary ($\Theta = 0$) is now the surface of a unit sphere; i.e. a two-dimensional surface. This surface possesses several invariant *circles*, in particular $X_2 = 0$, $X_1 = 0$, $X_1 = X_3$ and $X_1 + 2X_3 = 0$. These invariant circles then divide the sphere into several invariant regions. If we consider the invariant circle $X_2 = 0$ we see that the surface of the sphere is divided into two invariant parts, $X_2 \geq 0$ and $X_2 \leq 0$. Each of these invariant surfaces is then globally homeomorphic to the plane, and the complete dynamics on the surface can be determined using the properties of planar dynamical systems. The dynamics of each of these invariant surfaces, $X_2 \geq 0$ and $X_2 \leq 0$, are given in Figures 4.10 and 4.11.

The final step of the determination of possible asymptotic states is to consider the global dynamics, and in particular rule out the possibility of closed surfaces or closed (periodic) orbits away from the finite (or infinite) singular points discussed

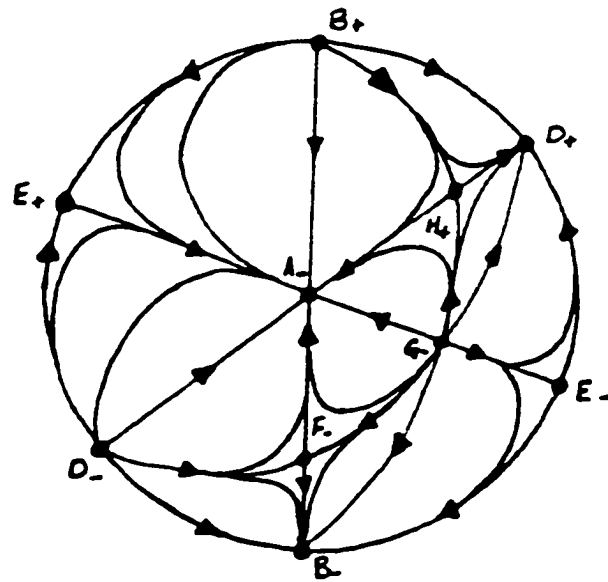


Figure 4.11: Dynamics on the infinite boundary for the plane symmetric solutions: for the compactified phase space. Bottom hemisphere; i.e. $X_2 < 0$

previously. As was stated in the Introduction, the determination of global dynamics in a three-dimensional phase space is very complicated, and can not always be determined analytically. The major tool - the monotonicity principle - will be used extensively in the discussion which follows. Regions for which a monotonic function has not been found have been considered numerically. The global dynamics was then determined by piecing together the analytical and numerical results. Throughout the discussion of the determination of the global dynamics the reader will be referred to Figures 4.13 through 4.16 which give a visual summary.

The numerical calculations were performed using the software `dstools`, version *tk*. Integration was performed using fifth order Runge-Kutta techniques with a tolerance of 10^{-4} . Figures 4.13 and 4.16 provide samples of the numerically calculated orbits in the regions for which the monotonicity principle cannot be applied. While only sample orbits have been illustrated, extensive numerical experimentation has shown no evidence for the existence of closed orbits. In fact, in the regions "away" from the finite singular points, the dynamics are very simple.

We begin the discussion of the global dynamics by considering the behaviour at large finite values for one (or more) of the variables. We shall consider various regions of the space separately.

1. $x_2 \gg 1, x_1, x_3 \approx 1$: In this case we have that the derivative of x_2 is strictly negative.
2. $x_1 \gg 1, x_2, x_3 \approx 1$: In this case we have that the derivative of x_3 is strictly positive.
3. $x_3 \gg 1, x_1, x_2 \approx 1$: In this case we have that the derivative of the function x_3 is strictly negative.
4. In all other combinations of *large* values the monotonicity of the coordinate directions can be determined if the surfaces which are the isoclines do not come into play. We can see from Figure 4.12 that the isocline surfaces are located at

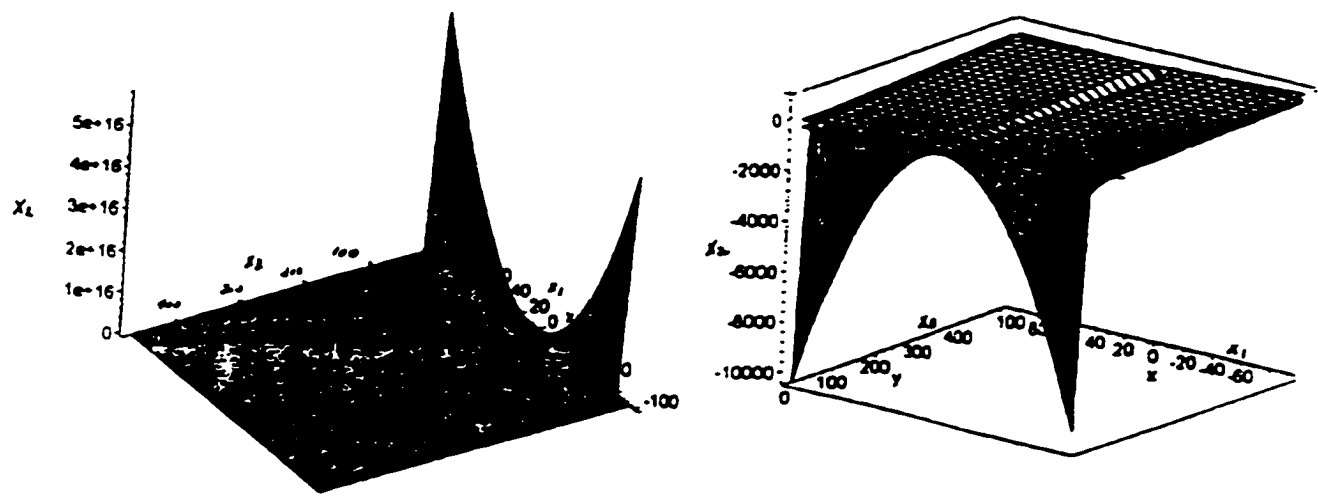


Figure 4.12: Plot of isocline surfaces for the system (4.26)-(4.28): *three surfaces representing the surfaces of zero change for each of the dependent variables x_1 , x_2 and x_3 are shown. Note that "away" from the coordinate planes each of these surfaces is asymptotically a plane.*

(relatively) small values of the coordinates x_1, x_2 , and x_3 , and do not effect the rate of change in coordinate directions at large values

Having determined that the behaviour at large values is simple (i.e. devoid of closed surfaces or periodic orbits), we consider the remainder of the three-dimensional space. The full space will be divided for convenience as follows:

$$R^3 = \Sigma_1^{13} U_i$$

$U_1 \dots U_6$ represent positive shear, i.e. $x_2 > 0$

$U_7 \dots U_{12}$ represent negative shear, i.e. $x_2 < 0$

U_{13} is all solutions with $x_2 = 0$ as seen in Figure 4.2

Positive shear solutions¹

- $U_1 = \{(x_1, x_2, x_3) | x_1, x_2, x_3 > 0\}$ Since all orbits which intersect $x_3 = 0$ and $x_1 = 0$ necessarily enter U_1 and the boundary $x_2 = 0$ is invariant (thus can not be crossed) this set is a positive trapping set. In this case it is clear that for all points in U_1 all orbits increase monotonically in the direction of x_1 . There are, therefore, no periodic orbits or closed surfaces in this set. Therefore all orbits must asymptote towards the set $x_2 = 0$.
- $U_2 = \{(x_1, x_2, x_3) | x_1, x_2 > 0, x_3 < 0\}$ In this case the set is not a trapping set. Orbits intersecting the $x_1 = 0$ plane enter the set, and those on the $x_3 = 0$ plane exit the set. It is clear, however, that if the orbits intersect the $x_3 = 0$ plane and leave the set, they necessarily enter the set U_1 and are governed by the dynamics above. For all other orbits the asymptotic behaviour is clear from the fact that for all points in the set all orbits decrease monotonically in the direction of x_2 . There are, therefore, no periodic orbits, and all asymptotic behaviour is located on $x_2 = 0$.
- $U_3 = \{(x_1, x_2, x_3) | -1 < x_1 < 0, x_2 > 0, x_3 < 0\}$ Once again this set is not a trapping set. Solutions which intersect the $x_1 = 0$ plane will be forced into the set U_2 and their asymptotic behaviour is then governed by the above. If the orbits intersect the plane $x_3 = 0$ they move into the set U_6 to be described below. In all cases, solutions will necessarily intersect one of these planes or asymptote to the plane $x_2 = 0$ since the flow is monotonically increasing in the direction of x_1 everywhere in this set.
- $U_4 = \{(x_1, x_2, x_3) | x_1 < -1, x_2 > 0, x_3 < 0\}$ We know immediately that all solutions stay in the set in *backward* time. The dynamics of orbits within this set, however, are complicated by the presence of the finite singular point R_- . This point is located in U_4 in all cases except $\alpha = 0$ in which case it is equal to

¹The discussion in this section considers the forward trajectories of each initial point. The backward trajectories can be deduced in an analogous fashion.

the point Q and found on the edge of the set. There is no (obvious) direction in which the rate of change is monotonic. Numerical investigations show no evidence of periodic orbits or closed surfaces. A summary of the numerically calculated orbits in this region are given in Figures 4.8a. While the presence of the singular point complicates the study of the direction fields, the numerics indicate that with the exception of the two isolated orbits which comprise the stable manifold of the singular point R_- , all other orbits (*in forward time*) leave the region.

- $U_5 = \{(x_1, x_2, x_3) | x_1 < -1, x_2 > 0, x_3 > 0\}$ Since all orbits which intersect $x_3 = 0$ and $x_1 = -1$ necessarily enter U_5 and the boundary $x_2 = 0$ is invariant (thus can not be crossed) this set is a trapping set. In this case it is clear that for all points in U_5 all orbits decrease monotonically in the direction of x_1 . There are, therefore, no periodic orbits or closed surfaces in this set, and all orbits must asymptote to the set $x_2 = 0$.
- $U_6 = \{(x_1, x_2, x_3) | -1 < x_1 < 0, x_2 > 0, x_3 > 0\}$ In this final set, the dynamics is also (as in U_4) complicated by the singular point Q lying on one edge of the set and the singular point R_+ which is in this set when $\sqrt{2} - 1 < \alpha < 3$. In the range $r_1 < \alpha < 3$ the point R_+ is in fact a sink, with an open set of orbits attracted to it. Numerical investigations once again do not indicate any behaviour other than orbits tending out of this set when R_+ is not present in the set. When R_+ is in this set orbits away from the singular point R_+ have the generic behaviour of leaving the set for U_5 or U_1 .

The previous discussion is shown schematically with direction fields in Figure 4.13. For the regions in which no monotonic function was found, samples of numerically calculated results are shown in Figure 4.14 and 4.15.

Negative shear solutions

- $U_7 = \{(x_1, x_2, x_3) | x_1, x_3 > 0, x_2 < 0\}$ The direction field for the boundary of this set is easily determined. On $x_1 = 0$ all orbits exit the set, and on $x_3 = 0$ all

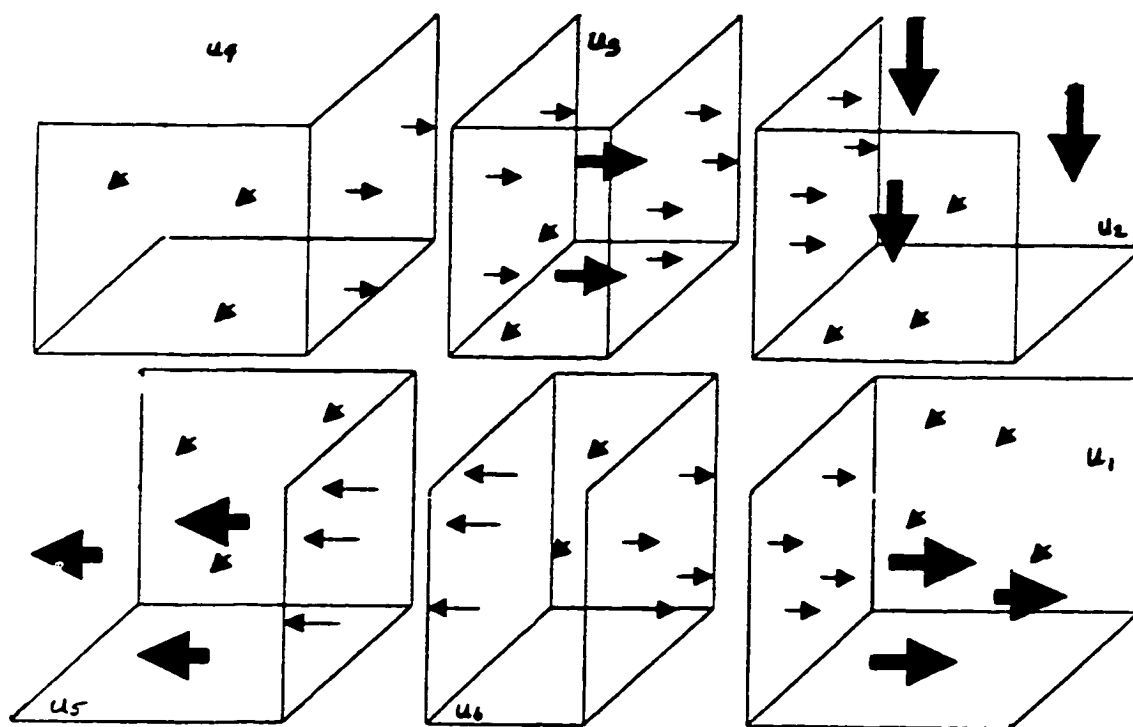


Figure 4.13: Direction fields for plane symmetric solutions with positive shear: *The three dimensional diagrams show the stratification of the positive shear phase space as described in the text (i.e., regions $U_1 - U_6$) The monotonic function is denoted with a bold arrow when it exists. The direction on the boundary is indicated for each region. In those regions in which no monotonic function was located details of the orbits are given in the summary of numerical results: Figures 4.14-4.15*

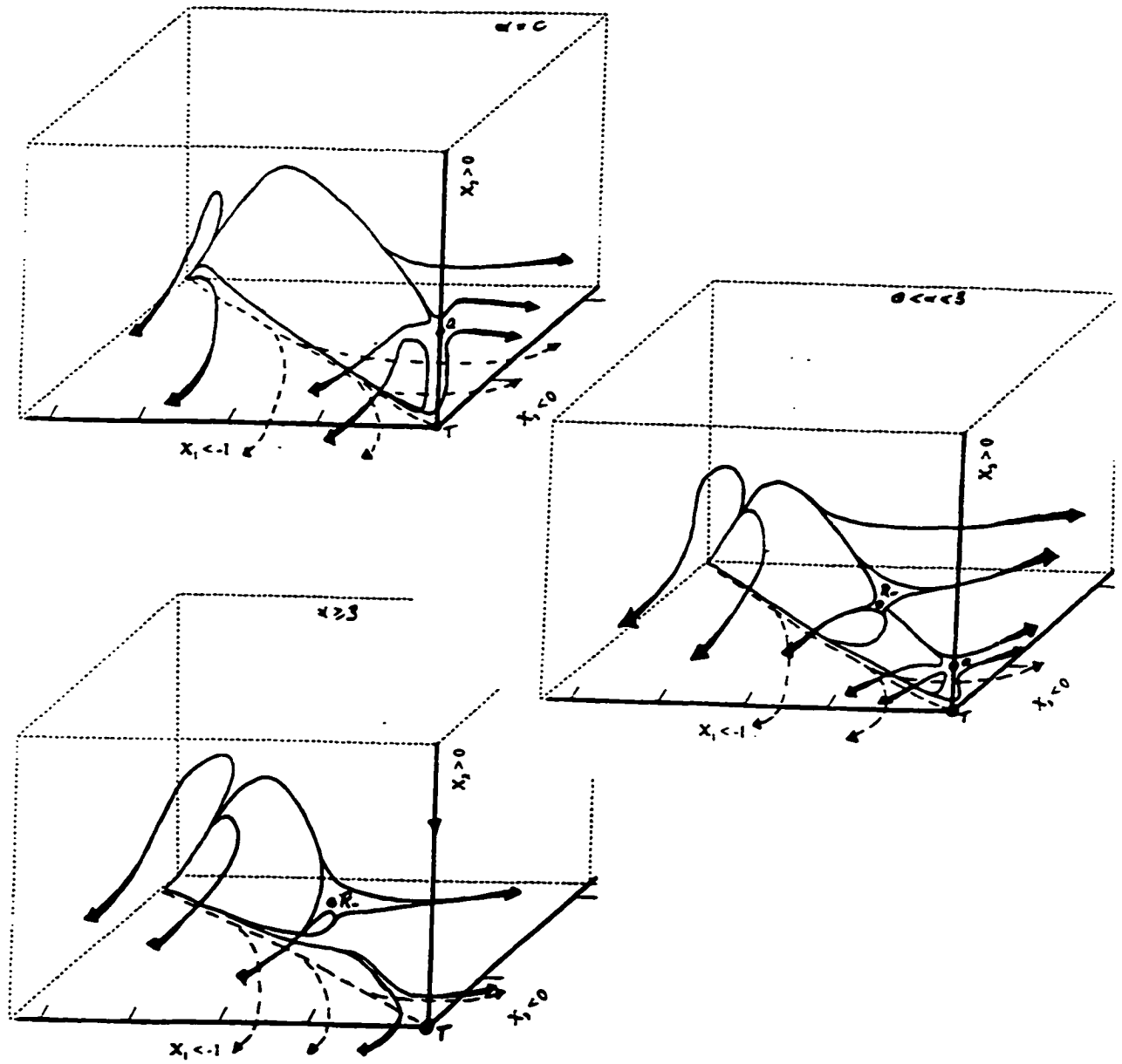


Figure 4.14: Numerically generated orbits for the region U_4 : Each diagram represents a different region of the parameter space $\alpha \geq 0$

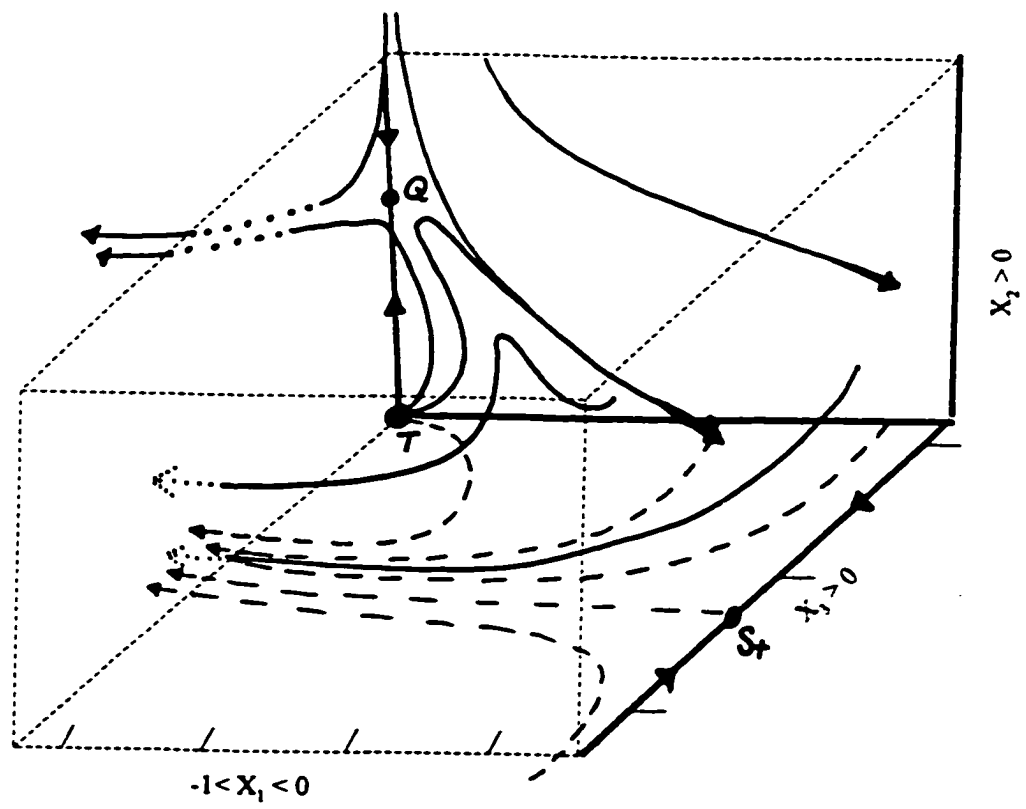


Figure 4.15: Numerically generated orbits for the region U_6

orbits exit the set. In general, no monotonic function can be found, however, numerical results indicate that there are no closed orbits or closed surfaces.

- $U_8 = \{(x_1, x_2, x_3) | x_1 > 0, x_3 < 0, x_2 < 0\}$ All orbits which intersect with the boundary of this set necessarily leave the set (moving into U_7 or U_9). For all other orbits the asymptotic behaviour is clear from the fact that for all points in the set all orbits decrease monotonically in the direction of x_1 . The only possibility of a closed surface (or orbit) would then, necessarily, exit the set. Since no orbit enter this set in forward time, however, this is not possible.
- $U_9 = \{(x_1, x_2, x_3) | -1 < x_1 < 0, x_2 < 0, x_3 < 0\}$ Once again this set is not a trapping set. Solutions which intersect the $x_1 = 0$ and $x_1 = -1$ planes will be forced into the set, those intersecting the plane $x_3 = 0$ move into the set U_{12} to be described below. In general, no monotonic function can be found, however, numerical results indicate that there are no closed orbits or closed surfaces.
- $U_{10} = \{(x_1, x_2, x_3) | x_1 < -1, x_2 < 0, x_3 < 0\}$ We know immediately that all solutions stay in the set in *backward* time. For all orbits within the set the function x_1 increases monotonically, precluding the possibility of closed structures. All orbits necessarily tend to $x_2 = 0$ or move into the sets U_9 (described above) or U_{10} to be discussed below.
- $U_{11} = \{(x_1, x_2, x_3) | x_1 < -1, x_2 < 0, x_3 > 0\}$ Since all orbits which intersect $x_3 = 0$ and $x_1 = -1$ necessarily enter U_{11} and the boundary $x_2 = 0$ is invariant (thus can not be crossed) this set is a trapping set. In general, no monotonic function can be determined for all values of α . In the case $\alpha \leq 3$, however, the function $3x_1 + x_2$ decreases monotonically and all asymptotic behaviour is necessarily located at $x_2 = 0$. In the case $\alpha > 3$ the singular point R_+ is located in this set. However the numerical results indicate that the asymptotic behaviour is the same, as seen in Figure 4.19.
- $U_{12} = \{(x_1, x_2, x_3) | -1 < x_1 < 0, x_2 < 0, x_3 > 0\}$ While this set is not a trapping

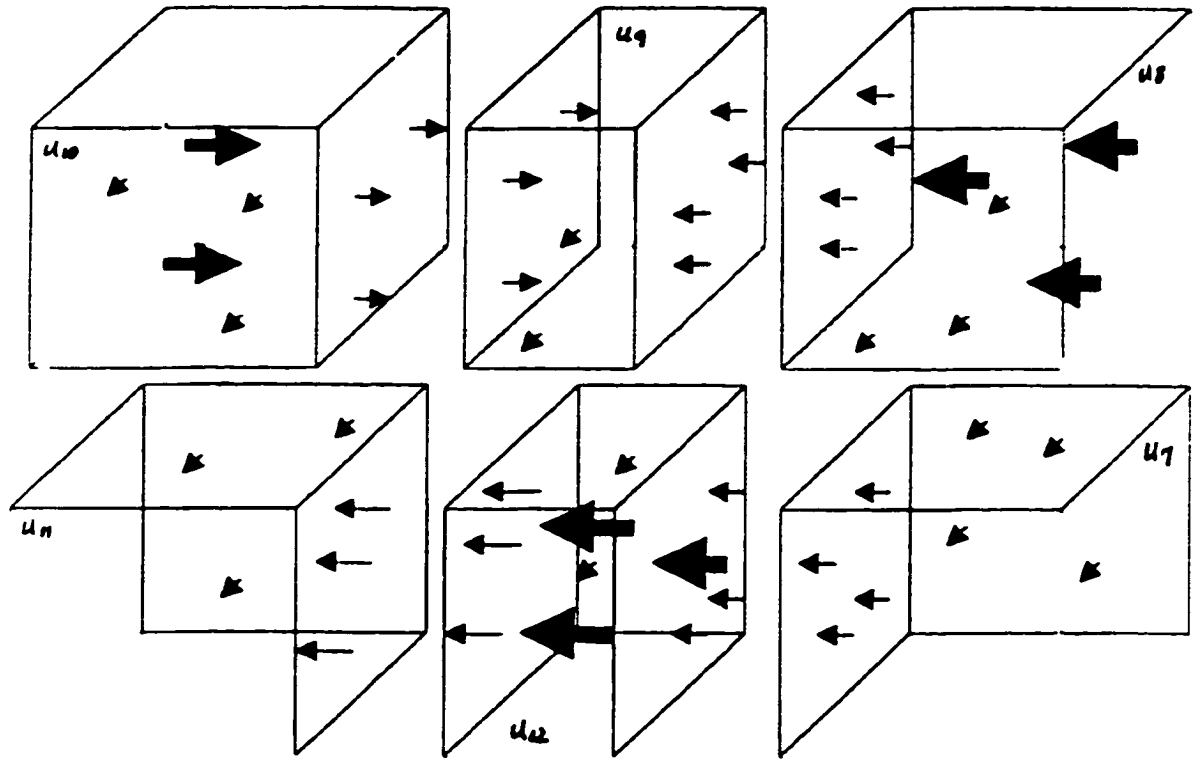


Figure 4.16: Direction fields for plane symmetric solutions with negative shear: *The three dimensional diagrams show the stratification of the positive shear phase space as described in the text (i.e., regions U_7 - U_{12}) The monotonic function is denoted with a bold arrow when it exists. The direction on the boundary is indicated for each region. In those regions in which no monotonic function was located details of the orbits are given in the summary of numerical results: Figures 4.17-4.19*

set, it is clear that x_1 decreases in a strictly monotonic fashion. All solutions necessarily leave this set and end up in U_{11} or in $x_2 = 0$.

The previous discussion is shown schematically in Figure 4.16. For the regions in which no monotonic function was found, numerical results are shown in Figure 4.17 - 4.19.

While the numerical results can not be demonstrated rigorously in all cases there is one class of solutions of the EFEs for which these results can indeed be shown analytically.

Consider the class of solutions which satisfy the weak energy conditions (WEC)

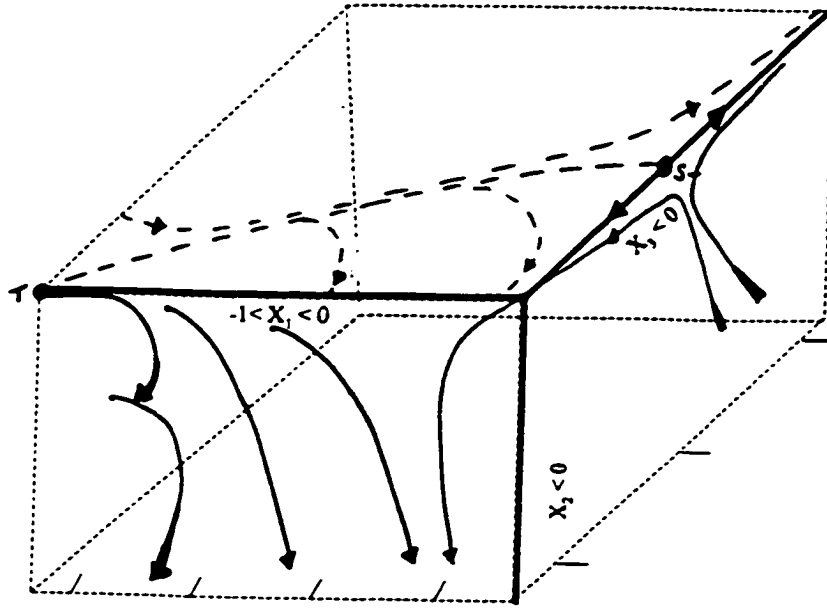


Figure 4.17: Numerically generated orbits for the region U_q for all values of α

for all values of the original variables r and t . Referring to the definitions for the energy density and pressure given in chapter 2, (2.18)-(2.19), we see that the WECs

$$\begin{aligned}\mu &\geq 0 \\ \mu + p &\geq 0;\end{aligned}$$

immediately imply:

$$x_3 \geq 0 \quad \text{and} \quad \alpha x_1 + x_2 \leq 0, \quad (4.36)$$

which then implies that

$$x_1 \leq 0 \quad (3x_1 + 2x_2) \leq 0 \quad \text{and} \quad (1 + x_1)^2 + 2x_1x_3 \leq 0. \quad (4.37)$$

We can consider the regions of interest as follows:

1. $\mathbf{R}_1 = \{(x_1, x_2, x_3) | x_1 \leq 0, x_2 < 0, x_3 \geq 0, \alpha \leq 3/2\} = U_{11} \oplus U_{12}, \alpha \leq 3/2,$
2. $\mathbf{R}_2 = \{(x_1, x_2, x_3) | x_1 \leq 0, x_2 = 0, x_3 \geq 0\} \subset U_{13}.$

For the case \mathbf{R}_1 the dynamics were completely determined analytically since monotonic functions were found when $\alpha \leq 3$. The asymptotic behaviour is completely

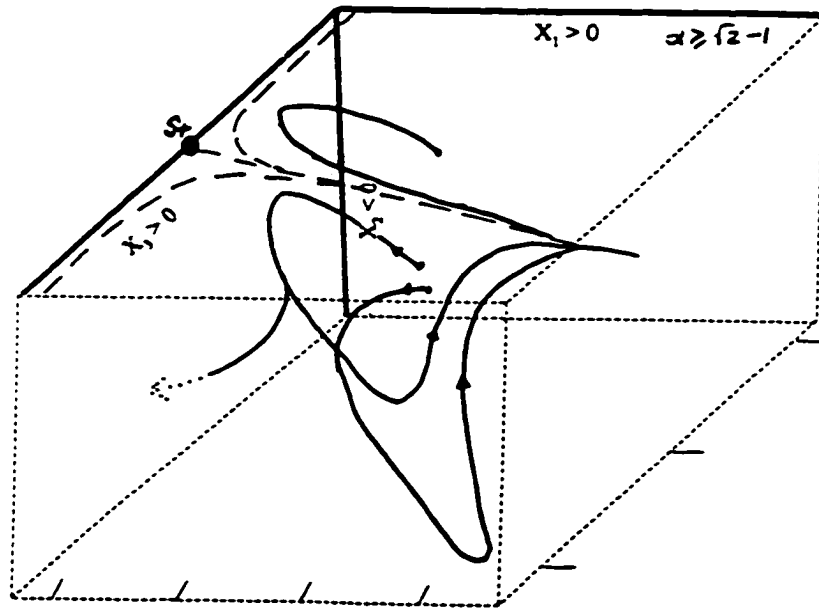
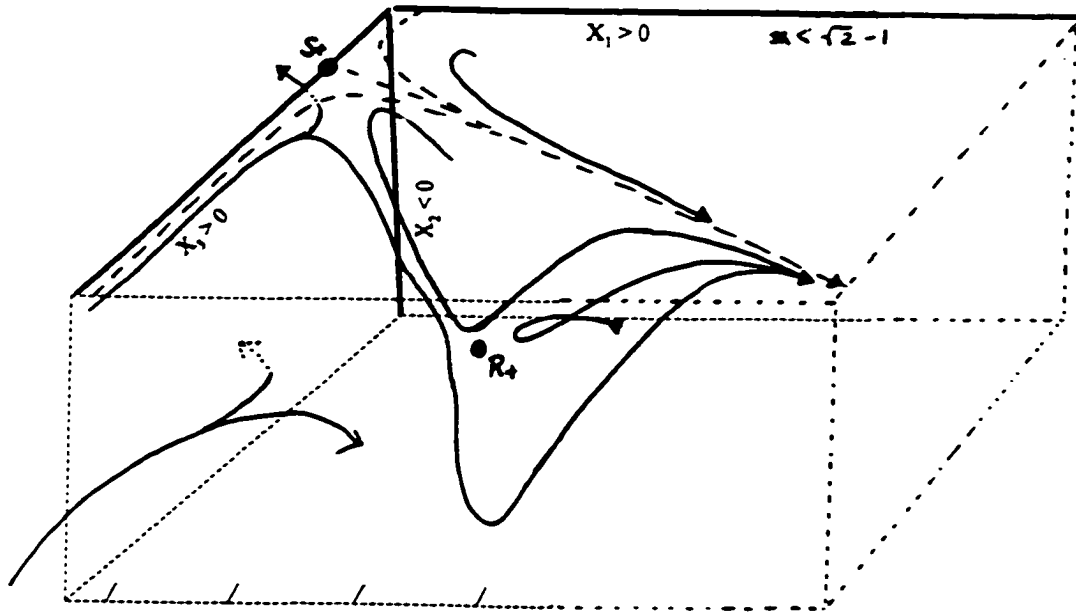


Figure 4.18: Numerically generated orbits for the region U_7 : Each diagram represents a different region of the parameter space $\alpha \geq 0$.

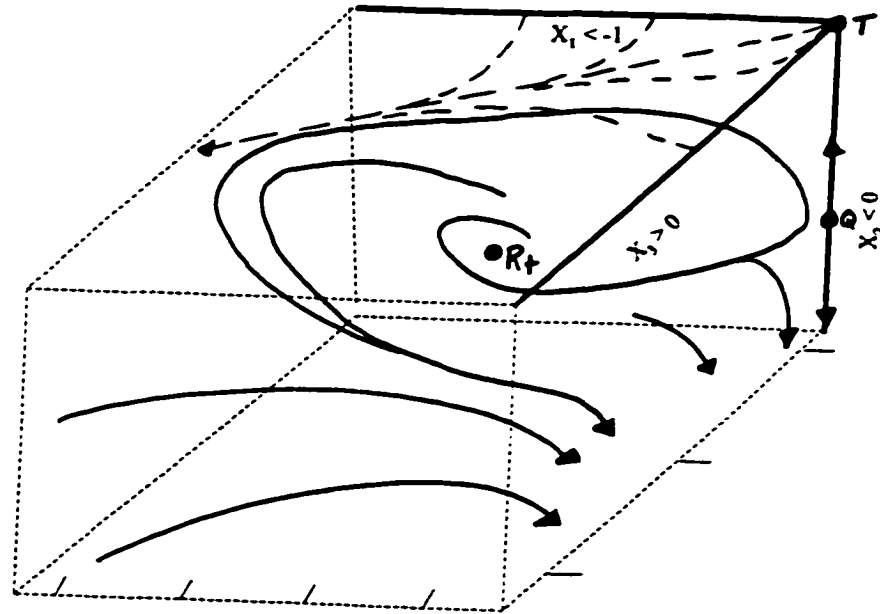


Figure 4.19: Numerically generated orbits for the region U_{11} : For the cases $\alpha \leq 3$ the dynamics are determined through the use of monotonic functions (see the accompanying text).

determined, as summarised by the direction field plots in Figure 4.13. Generically, the forward asymptotic solution is the solution represented by the singular point A_- , and the backward asymptotic behaviour is the solution represented by the singular point B_+ . The singular point E_+ is an intermediate solution (i.e., a saddle). The dynamics have been completely determined in the invariant set U_{13} , as shown in figure 4.2. As can be seen, the solutions which are in \mathbf{R}_2 for all *time* necessarily start at the singular point B_+ , ending at E_+ with an intermediate solution of S_+ or they start at the point T and end at E_+ with no defined intermediate behaviour.

Therefore, while we must rely on numerics to make conclusions about the dynamics in some regions of space, we have shown that at least for solutions of particular physical interest the asymptotic behaviour is determined by singular points at either finite or infinite singular points.

4.3 Physical Nature of Asymptotic Solutions

Now that the asymptotic behaviour has been determined, it is necessary to examine the nature of the exact solutions corresponding to the singular points. In each case the singular points which represent the asymptotic behaviour will impose a relationship between the metric functions Φ, Ψ and S . These relationships were used with the algebraic package *GRTensor* in the *Maple* environment to determine the exact form of the metric. Throughout the discussion we shall pay particular attention to those solutions which satisfy the weak energy conditions (WEC), namely:

$$\begin{aligned}\mu &\geq 0 \\ \mu + p &\geq 0.\end{aligned}$$

4.3.1 Finite Singular Points

Case 1: $\mathbf{Q} = (-1, 3 - \alpha, 0, 0)$

In this case the metric necessarily exhibits plane symmetry. The metric and the physical properties of energy density and pressure are given by

$$ds^2 = -a^2 dt^2 + b^2 \left[\frac{r}{t^{1/\alpha}} \right]^{2(2-\alpha)} dr^2 + r^2 s_0^2 \frac{t^{2/\alpha}}{r^2} (d\theta^2 + \theta^2 d\phi^2) \quad (4.38)$$

$$\mu = a^2 \alpha^{-2} (\alpha - 3) t^{-2} \quad \text{and} \quad p = a^2 \alpha^{-2} (2\alpha - 3) t^{-2}. \quad (4.39)$$

The WEC are then satisfied *iff* $\alpha \geq 3$. Solutions with $\alpha < 3$ necessarily violate the WECs at the point \mathbf{Q} , as do all solutions which asymptote to this singular point.

Case 2: $\mathbf{R}_{\pm} = (c_1, c_2, c_3, 0)$

The values of the constants c_1, c_2 , and c_3 are given in Table 4.1. In this case the metric is once again necessarily plane symmetric. The metric and the physical properties of energy density and pressure are given by

$$ds^2 = -a^2 (\xi)^{2c_3} dt^2 + b^2 (\xi)^{2c_2} dr^2 + r^2 s_0^2 (\xi)^{2c_1} (d\theta^2 + \theta^2 d\phi^2) \quad (4.40)$$

$$\begin{aligned}\mu &= -[(1 + c_1)^2 + 2c_1 c_3] \xi^{-2c_2} r^{-2} + \alpha^{-2} [c_1^2 + 2c_1 c_2] \xi^{-2c_3} t^{-2} \\ p &= [(1 + c_1)^2 + 2c_1 c_3 + 2c_3] \xi^{-2c_2} r^{-2} \\ &\quad + \alpha^{-2} [c_1^2 + 2c_1 c_2 + 2c_2 + 2(\alpha - 1)c_1] \xi^{-2c_3} t^{-2}\end{aligned} \quad (4.41)$$

The WEC are satisfied if one of the following cases is true:

1. $\alpha \in (\sqrt{2} - 1, 3)$ (i.e. $c_3 > 0$) and $\frac{c_2 + (\alpha - 1)c_1}{c_3} \leq \frac{a^2 t^2}{b^2 r^2} \xi^{2(c_3 - c_2)}$.
2. $\alpha \in (3, \infty)$ (i.e. $c_3 < 0$) and $\frac{c_2 + (\alpha - 1)c_1}{c_3} \geq \frac{a^2 t^2}{b^2 r^2} \xi^{2(c_3 - c_2)}$.

Note that neither of these conditions is satisfied for **all** values of the coordinates t and r ; however, it is possible that solutions which asymptote towards this point will always satisfy the WECs.

Case 3: $\mathbf{S} = (0, 0, c, c^2 + 2c - 1)$

In this case the metric may be hyperbolically, plane, or spherically symmetric. The metric and the energy density and pressure are given by

$$ds^2 = -a^2 \xi^{2c} dt^2 + b^2 dr^2 + r^2 s_0^2 d\Omega^2 \quad (4.42)$$

$$\mu = b^{-2} \alpha^{-2} (c^2 + 2c - 2) r^{-2} \quad \text{and} \quad p = b^{-2} \alpha^{-2} (2 - c^2) r^{-2}. \quad (4.43)$$

Note: This metric is static since by a redefinition of the variable t all metric functions (as well as all physical definitions) are independent of time.

The WEC require that the parameter c be greater than (or equal to) $\sqrt{3} - 1$. In this case it necessarily follows that x_4 is strictly positive. Thus the only cases in which (4.42) satisfies the WEC is in the case of hyperbolic symmetry. When the WEC is violated for this singular point they are also violated for all solutions which asymptote towards this point.

Case 4: $\mathbf{T} = (c, 0, 0, -(c + 1)^2)$

This case is equivalent to the singular points located in the study of the geodesic solutions (see section 3.1). The solutions are necessarily spherically symmetric. The metric and the physical properties of energy density and pressure are given by

$$ds^2 = -a^2 dt^2 + \xi^{2c} [b^2 dr^2 + r^2 s_0^2 (d\theta^2 + \sin\theta d\phi^2)] \quad (4.44)$$

$$\mu = 3c^2 a^{-2} \alpha^{-2} t^{-2} \quad \text{and} \quad p = -3c^2 a^{-2} \alpha^{-2} t^{-2}. \quad (4.45)$$

These energy conditions are valid for all values of the parameters c and α . A detailed discussion is given in section 3.1.

4.3.2 Infinite Singular points

In addition to those singular points at finite values, it has been shown that solutions may asymptote (to the past or future) to values on the infinite boundary of the phase space - in fact this is the generic behaviour.

Case 1: $\mathbf{A}_\pm : x_1 = x_3 = x_4 = 0$

Solutions at this point are necessarily plane symmetric. The metric and the physical properties of energy density and pressure are given by

$$ds^2 = -a^2 dt^2 + e^{2\Psi} dr^2 + r^2 s_0^2 (d\theta^2 + \theta d\phi^2) \quad (4.46)$$

where

$$\ddot{\Psi} = -\dot{\Psi}(\dot{\Psi} + \alpha) \quad (4.47)$$

and

$$\mu = -e^{-2\Psi} r^{-2}, \quad p = e^{-2\Psi} r^{-2}. \quad (4.48)$$

This metric is static, and the solutions belong to the geodesic class (and therefore are physically self-similar). In this case the energy density (μ) is strictly negative. Thus the energy conditions are not satisfied for the singular point or for any solutions which asymptote to this singular point.

Case 2: $\mathbf{B}_\pm : x_1 = x_2 = x_4 = 0$

Solutions at this point are necessarily plane symmetric. The metric and the physical properties of energy density and pressure are given by

$$ds^2 = -e^{2\Phi} dt^2 + b^2 dr^2 + r^2 s_0^2 (d\theta^2 + \theta d\phi^2) \quad (4.49)$$

where $\ddot{\Phi} \approx -\dot{\Phi}^2$ and

$$\mu = -b^{-2} r^{-2}, \quad p = b^{-2} (1 + 2\dot{\Phi}) r^{-2}. \quad (4.50)$$

The metric is static (therefore solutions are physically self-similar) and the fluid has zero shear. In this case the energy conditions are not satisfied (as the density is strictly negative) for the singular point or for any solutions which asymptote to this singular point.

Case 3: $C_{\pm} : x_1 = x_2 = x_3 = 0$

Solutions at the point C_+ are spherically symmetric and those at C_- exhibit hyperbolic symmetry. The metric and the physical properties of energy density and pressure are given by

$$ds^2 = -dt^2 + dr^2 + r^2 d\Omega^2 \quad (4.51)$$

where $k = +1$ for C_+ , $k = -1$ for C_- and

$$\mu = (x_4 - 1)b^{-2}r^{-2}, \quad p = (1 - x_4)b^{-2}r^{-2}. \quad (4.52)$$

The metric is static, and the solutions are in the geodesic class (therefore are physically self-similar). In addition, the fluid has zero shear. In this case the energy conditions are satisfied at C_+ . At C_- , however, the energy conditions are not satisfied at the singular point or for any solutions which asymptote to this singular point.

Case 4: $D_{\pm} : x_1 = x_3 \quad x_2 = x_4 = 0$

Solutions at this point are necessarily plane symmetric. The metric and the physical properties of energy density and pressure are given by

$$ds^2 = e^{2\Phi}[-dt^2 + b^2 dr^2 + r^2 s_0^2 (d\theta^2 + \theta d\phi^2)] \quad (4.53)$$

$\ddot{\Phi} \approx \dot{\Phi}^2$ and

$$\begin{aligned} \mu &= e^{-2\Phi} [b^{-2}(-(1+x_1)^2 - 2x_1^2)r^{-2} + 3x_1^2 \alpha^{-2} t^{-2}], \\ p &= e^{-2\Phi} [b^{-2}(3x_1^2 + 4x_1 + 1)r^{-2} - (3x_1^2 + 2\alpha x_1)\alpha^{-2} t^{-2}]. \end{aligned} \quad (4.54)$$

The fluid in this case has zero shear. These solutions are not physically self-similar. In this case the energy conditions are not satisfied in general for the singular point or for any solutions which asymptote to this singular point.

Case 5: $E_{\pm} : x_1 = -2x_3 \quad x_2 = x_4 = 0$

Solutions at this point are necessarily plane symmetric. The metric and the physical properties of energy density and pressure are given by

$$ds^2 = -e^{2\Phi} dt^2 + e^{-4\Phi} [b^2 dr^2 + r^2 s_0^2 (d\theta^2 + \theta d\phi^2)] \quad (4.55)$$

$\ddot{\Phi} \approx -\dot{\Phi}^2$ and

$$\begin{aligned}\mu &= e^{4\dot{\Phi}} b^{-2} (-1 - 2x_1) r^{-2} + 3x_1^2 \alpha^{-2} e^{-2\dot{\Phi}} t^{-2}, \\ p &= e^{4\dot{\Phi}} b^{-2} r^{-2} - (3x_1^2 + 2\alpha x_1) \alpha^{-2} e^{-2\dot{\Phi}} t^{-2}.\end{aligned}\quad (4.56)$$

The fluid in this case has zero shear. These solutions are not physically self-similar. In this case the energy conditions are satisfied at \mathbf{E}_+ . At \mathbf{E}_- , however, the energy conditions are not satisfied at the singular point or for any solutions which asymptote towards this singular point.

Case 6: $\mathbf{F}_\pm : x_2 = x_3 \quad x_1 = x_4 = 0$

Solutions at this point are necessarily plane symmetric. The metric and the physical properties of energy density and pressure are given by

$$ds^2 = e^{2\dot{\Phi}} [-dt^2 + b^2 dr^2] + r^2 s_0^2 (d\theta^2 + \theta d\phi^2) \quad (4.57)$$

$\ddot{\Phi} \approx 2\dot{\Phi}$ and

$$\mu = -e^{-2\dot{\Phi}} b^{-2} r^{-2}, \quad p = e^{-2\dot{\Phi}} (1 + \dot{\Phi}) b^{-2} r^{-2}. \quad (4.58)$$

The metric is static, and therefore the solutions are physically self-similar. In this case the energy conditions are not satisfied since $\mu < 0$ for the singular point or for any solutions which asymptote to this singular point.

Case 7: $\mathbf{G}_\pm : x_1 = -2x_3 \quad x_2 = 3x_3 \quad x_4 = 0$

Solutions at this point are necessarily plane symmetric. The metric and the physical properties of energy density and pressure are given by

$$ds^2 = -e^{2\dot{\Phi}} dt^2 + b^2 e^{-6\dot{\Phi}} dr^2 + r^2 s_0^2 e^{-4\dot{\Phi}} (d\theta^2 + \theta d\phi^2) \quad (4.59)$$

$\ddot{\Phi} \approx \dot{\Phi}^2$ and

$$\mu = (4\dot{\Phi} - 1) e^{-2\dot{\Phi}} b^{-2} r^{-2} - 8\dot{\Phi}^2 \alpha^2 e^{-2\dot{\Phi}} t^{-2}, \quad (4.60)$$

$$p = (1 - 2\dot{\Phi}) e^{-2\dot{\Phi}} b^{-2} r^{-2} + (8\dot{\Phi}^2 - 10\dot{\Phi} - 4\alpha\dot{\Phi}) \alpha^2 e^{-2\dot{\Phi}} t^{-2}. \quad (4.61)$$

In this case the WECs are satisfied for the point \mathbf{G}_+ when $\alpha \geq 5/2$, otherwise both points violate the WECs. General solutions which asymptote towards these points, however, will not violate the WEC in the following cases:

1. Solutions asymptoting to G_+ : If $t^2 + (2\alpha - 5)b^2e^{4\Phi}r^2 \geq 0$
2. Solutions asymptoting to G_- : If $t^2 + (2\alpha - 5)b^2e^{4\Phi}r^2 \leq 0$

In all other cases solutions which asymptote to this singular point will violate the WECs.

Case 8: H_\pm : $x_1 = x_3$ $x_2 = -3/2x_3$ $x_4 = 0$

Solutions at this point are necessarily plane symmetric. The metric and the physical properties of energy density and pressure are given by

$$ds^2 = -e^{2\Phi}dt^2 + b^2e^{-3\Phi}dr^2 + r^2s_0^2e^{2\Phi}(d\theta^2 + \theta d\phi^2) \quad (4.62)$$

$\ddot{\Phi} \approx -1/2\dot{\Phi}^2$ and

$$\mu = -((1 + \dot{\Phi})^2 + 2\dot{\Phi}^2)e^{-2\Phi}b^{-2}r^{-2} - 2\dot{\Phi}^2\alpha^2e^{-2\Phi}t^{-2}, \quad (4.63)$$

$$p = ((1 + \dot{\Phi})^2 + 2\dot{\Phi}^2 + 2\dot{\Phi})e^{-2\Phi}b^{-2}r^{-2} + (2\dot{\Phi}^2 + (2\alpha - 5)\dot{\Phi})\alpha^2e^{-2\Phi}t^{-2}. \quad (4.64)$$

In this case the WECs are violated at the singular points. In addition, all solutions which asymptote to these singular points will also violate the WECs

4.4 Summary of the Dynamics

At this point a summary of the complete dynamics will be given. Recall that $x_4 = 0$ and $x_2 = 0$ are invariant sets, and specifically $x_4 = 0$ divides the full phase space into three distinct (and invariant) sets. Each of these sets corresponds exactly to the three different forms of metric to be considered, namely:

- $x_4 < 0$: Spherically symmetric solutions
- $x_4 = 0$: Plane symmetric solutions
- $x_4 > 0$: Hyperbolically symmetric solutions

We have shown that all solutions asymptote in the past or to the future to the set $x_2 = 0$ or to the set $x_4 = 0$. For that reason special attention has been paid to solutions in these classes. In addition, most physically interesting and important applications lie in the spherically symmetric class of solutions, so the dynamics in this set will be given special focus. Because of the natural split of the solutions, we shall consider the dynamics according to the symmetry of the metric.

Case I Plane Symmetric Solutions [$x_4 = 0$]

The dynamics of the solutions in this class occur in a three-dimensional set. There are six finite singular points. Three of these points lie in the invariant set $x_2 = 0$. The set $x_2 = 0$ divides the phase space, and the complete dynamics in this case are outlined in Figure 4.2. Through a combination of analytic methods and numerical results it was determined that the only stable asymptotic behaviour (not in $x_2 = 0$) was located either at finite or infinite singular points (namely A_{\pm} , B_{\pm} , D_{\pm} and G_{\pm} as well as R_+ in the parameter region $r_1 < \alpha < 3$). The infinite points have been classified and are given in Table 4.2, with the dynamics on the infinite boundary (which are independent of the parameter α) sketched in Figures 4.10 and 4.11. In this case the global sinks are located at A_- , B_- , D_+ and G_+ , whereas the global sources are located at A_+ , B_+ , D_- and G_- . There are various values of the parameter α for which the stability of the finite singular points changed. We therefore summarise the dynamics of the singular points not located on the plane $x_2 = 0$ according to the values of the parameter α in Table 4.5.

The only sink or source located at finite values is found at the point R_+ in the parameter range $\alpha \in (r_1, 3)$. Schematics of the local behaviour of each of these points was given in Figures 4.4 - 4.9. The global behaviour can be summarised through a schematic of the path of the orbits showing initial, intermediate and final asymptotic regions. The schematics are given in Figures 4.20 and 4.21. These figures, coupled with Figures 4.13 and 4.16, act as a summary of the possible dynamics in this case. As can be seen, the singular points located on the infinite boundary are of special

Table 4.5: Summary of finite singular points for plane symmetric solutions with non-zero shear.

α	Q	R_+	R_-
0	saddle-node	saddle	$\equiv Q$
$(0, \sqrt{2} - 1)$	saddle	saddle	saddle
$\sqrt{2} - 1$	saddle	$\equiv S_+$ (see Figure 4.2)	saddle
$(\sqrt{2} - 1, r_1)$	saddle	saddle	saddle
r_1	saddle	saddle	saddle
$(r_1, 3)$	saddle	sink	saddle
3	$\equiv T$ (see Figure 4.2)	$\equiv Q$	saddle
$(3, \infty)$	saddle	saddle	saddle

importance as they are initial or final states. Some finite singular points represent intermediate behaviour. It is important to note that the WEC conditions are always violated for solutions which asymptote to the point R_+ in the case that it is a sink (i.e., when $\alpha \in (r_1, 3)$). The sinks and sources located on the infinite boundary violate the WEC in all cases except G_{\pm} , which are valid in specific cases as illustrated in Case 8 of section 4.3.

Case II Spherically Symmetric Solutions [$x_4 < 0$]

Most interesting and important physical examples are located in this set of solutions. For this reason, we focus on the dynamics in this set. The solutions which exhibit the so-called "physical self-similarity" for a single fluid model were examined in Chapter 3 in some detail. These solutions are contained as subsets here. In particular the geodesic (i.e., $x_3 = 0$) solutions are located in the two-dimensional invariant set $x_4 = -(1 + x_1)^2, x_3 = 0$, and the solutions with $M_2 = 0$ (i.e., the class containing all static solutions) are located in the invariant set $x_1 = 0, x_4 = (x_3 + 1)^2 - 2$. In each case the analysis given in chapter 3 is simplified to the study of a one-dimensional system (rather than the two-dimension invariant sets as listed here) as a result of the intrinsic relationship between the variable x_1, x_2 and x_4 .

As a result of the fact that x_4 is a monotonic function for all solutions in this class, we know that solutions are asymptotic to either (1) a shear-free fluid solution, i.e., $x_2 = 0$ (as described in 4.1), (2) a solution with zero-curvature (i.e., $x_4 = 0$ as given

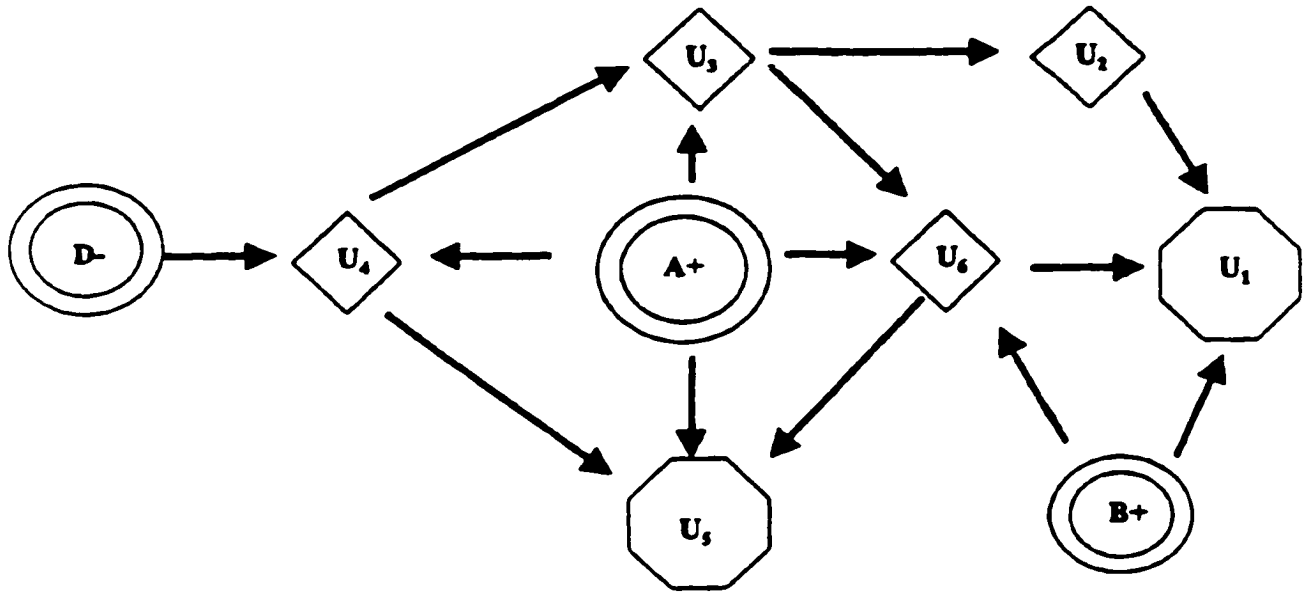


Figure 4.20: Schematic of the path of generic orbits for plane symmetric solutions with positive shear: \bullet denotes a source points, \diamond an intermediate region and \circ a terminal region (arrows represent the passage of positive "time").

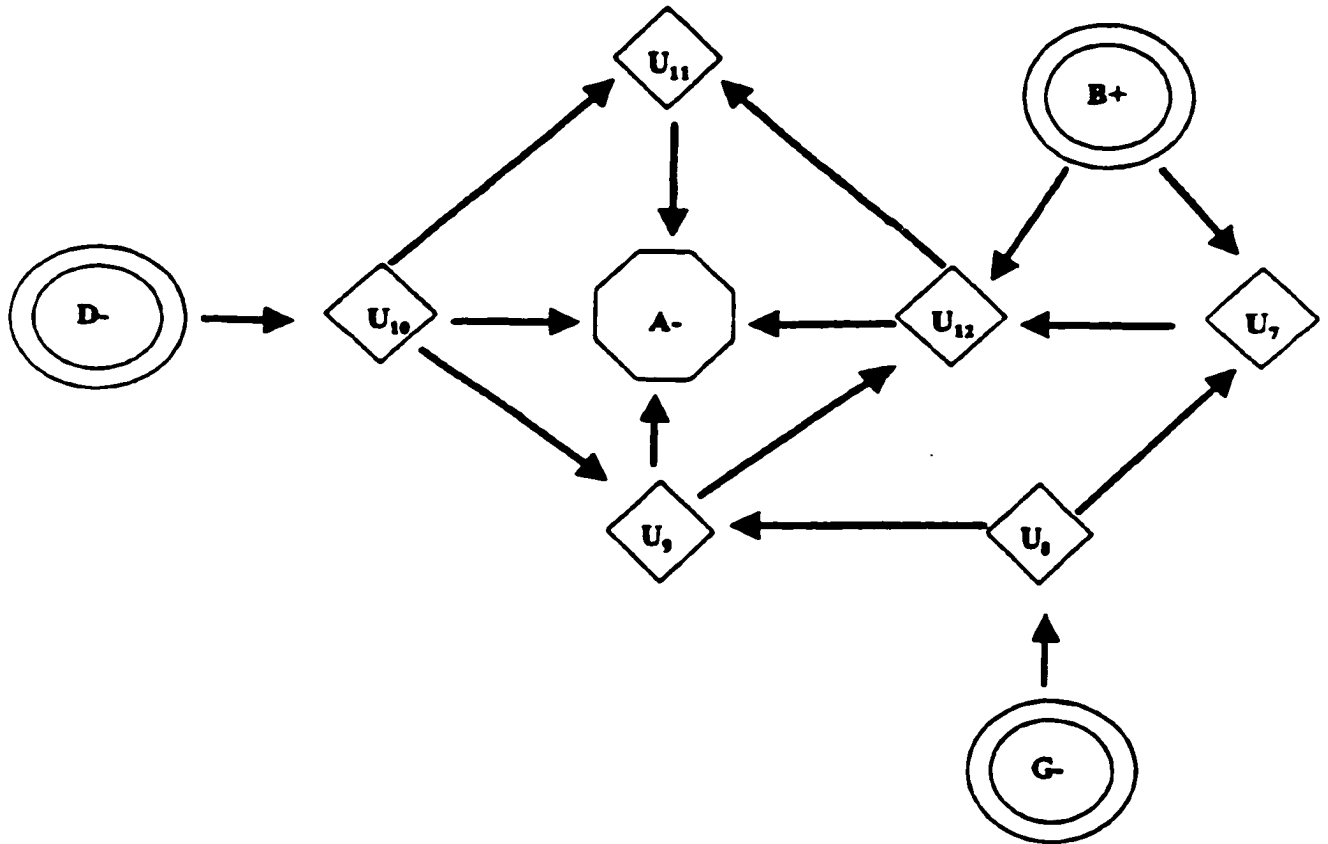


Figure 4.21: Schematic of the path of generic orbits for plane symmetric solutions with negative shear: \odot denotes a source points, \diamond an intermediate region and \ominus a terminal region (arrows represent the passage of positive "time").

in 4.2 and summarised above), (3) a solution with infinite curvature as described in section 4.3, or (4) a solution represented by the finite singular points of **S** or **T**. These singular points **S** and **T** are necessarily "physically self-similar" in the single fluid model and we have shown in chapter 3 that they admit a homothetic vector. More details of the physical nature of each of the asymptotic solutions will be given in the next section.

Case III: Hyperbolically Symmetric Metrics [$x_4 > 0$]

The general analysis in this case is similar to that of the spherically symmetric case. All asymptotic behaviour is either located on the invariant sets $x_2 = 0$, $x_4 = 0$ or infinity, or at one of the finite singular points. The only finite singular points in this class consist of the points along the one-dimensional equilibrium set **S**, which corresponds to the shear-free fluids. Their complete dynamics are given in section 4.1 and are summarised in figure 4.3.

Chapter 5

Infinite Kinematic Self Similarity

In the preceding chapters the class of solutions exhibiting a finite KSS were considered, and their qualitative behaviour determined. There is a further type of kinematic self-similarity which we shall refer to as kinematic self-similarity of ‘infinite’ type, or simply infinite KSS, corresponding to a generalisation of rigid transformations, which will now be considered. Once again emphasis is placed on those models which can be interpreted as perfect fluid solutions of Einstein’s field equations (EFE). The governing system of differential equations once again reduces to a system of autonomous ordinary differential equations and the qualitative behaviour of the models will be examined in a manner similar to that of Chapter 4.

5.1 Reduction of the EFEs in full

When considering infinite KSS three different cases arise, depending on the orientation of the fluid flow u relative to the KSS vector field, i.e., fluid flow parallel to ξ , fluid flow orthogonal to ξ , and the most general ‘tilted’ case in which the fluid flow is neither parallel nor orthogonal to ξ . It can easily be shown that in the cases of parallel and orthogonal fluid flow there are no perfect fluid solutions, therefore the general tilted case will be the focus of this chapter.

The general ‘tilted’ case occurs when the four-velocity is neither parallel nor orthogonal to the self-similar vector field. In this case one can choose coordinates so that the KSS takes the form:

$$\xi = t\partial_t + r\partial_r \quad (5.1)$$

In such coordinates, and solving the self-similar equations [see equations (1.10)-(1.11)], it is easy to show that the metric can be given by

$$ds^2 = -e^{2\Phi} dt^2 + \frac{e^{2\Psi}}{r^2} dr^2 + S^2(d\theta^2 + \Sigma(\theta, k)^2 d\phi^2) \quad (5.2)$$

where Φ, Ψ and S are functions depending only on the self-similar coordinate

$$\xi = \frac{t}{r} \quad (5.3)$$

The field equations for a perfect fluid source are

$$0 = S''t + S'r - \Phi'S't - \Psi'S't \quad (5.4)$$

$$0 = t^2\Sigma_1(\xi) + \Sigma_2(\xi) , \quad (5.5)$$

where a dash denotes derivative with respect to ξ and

$$\Sigma_1 \equiv -(S')^2 + \frac{r}{t}S^2\Phi' - S^2\Phi'\Psi' + S^2\Phi'' + k\frac{r^2}{t^2}e^{2\Psi} + S^2(\Phi')^2 \quad (5.6)$$

$$\Sigma_2 \equiv e^{2\Psi-2\Phi} \left[-\frac{r}{t}SS' - S^2(\Psi')^2 + S^2\Phi'\Psi' - S^2\Psi'' + (S')^2 \right] . \quad (5.7)$$

The only possibility which will satisfy equation (5.5) is when $\Sigma_1 = \Sigma_2 = 0$.

Note that if we assume a perfect fluid source such that $\mu + p \neq 0$, we have that S' cannot vanish. Then defining $z = \ln(\xi)$, and $\dot{} = d/dz$, we have equations (5.4) and (5.5) as

$$0 = \frac{\ddot{S}}{S} - \dot{\Phi} - \dot{\Psi} \quad (5.8)$$

$$0 = -\left(\frac{\dot{S}}{S}\right)^2 - \dot{\Phi}\dot{\Psi} + k\frac{e^{2\Psi}}{S^2} + \dot{\Phi}^2 \quad (5.9)$$

$$0 = -\frac{\dot{S}}{S} + \left(\frac{\dot{S}}{S}\right)^2 - \dot{\Psi}^2 + \dot{\Phi}\dot{\Psi} - \ddot{\Psi} + \dot{\Psi} . \quad (5.10)$$

Applying now the definitions

$$y \equiv \dot{S}/S, \quad u \equiv \dot{\Psi}, \quad v \equiv \dot{\Phi}, \quad w \equiv -ke^{2\Psi}S^{-2}, \quad (5.11)$$

(as was done in Chapter 2) equations (5.8)-(5.10) reduce to a four-dimensional autonomous system of ODEs

$$\dot{y} = y(u + v - y), \quad (5.12)$$

$$\dot{u} = -y + y^2 - u^2 + u + uv, \quad (5.13)$$

$$\dot{v} = w + y^2 + uv - v^2, \quad (5.14)$$

$$\dot{w} = 2w(u - y). \quad (5.15)$$

The matter quantities are given by

$$\mu = e^{-2\Phi}[2yu + y^2]t^{-2} - e^{-2\Psi}[w + 2yv + y^2], \quad (5.16)$$

$$p = e^{-2\Phi}[-2yu + 2y - y^2]t^{-2} + e^{-2\Psi}[w + 2yv + y^2]. \quad (5.17)$$

At this point we note that equations (5.12)-(5.15) are of a form similar to the governing equations in the case of finite KSS. In fact, the quadratic terms of the vector field for equations (5.12)-(5.15) are identical to those of (2.60)-(2.63). This result is an immediate consequence of the choice of the metric (5.2) (and, necessarily, the choice of the coordinate form of the KSS). The immediate difference between the governing equations of finite and infinite KSS is that the system (5.12)-(5.15) admits many more invariant sets which, as will be seen, greatly simplify the analysis.

Note that the density and pressure can be split as $\mu = \mu_1 + \mu_2$ and $p = p_1 + p_2$ where $\mu_1 = \hat{\mu}_1(\xi)t^{-2}$, $p_1 = \hat{p}_1(\xi)t^{-2}$ and $-p_2 = \mu_2 = \hat{\mu}_2(\xi)$. As was the case for finite KSS each component of the energy and pressure then exhibit self-similarity since $\mathcal{L}_\xi \mu_1 = -2\mu_1$, $\mathcal{L}_\xi p_1 = -2p_1$ and $\mathcal{L}_\xi \mu_2 = \mathcal{L}_\xi p_2 = 0$.

There are some physical consequences which are important to note here.

1. For the particular case $w + 2yv + y^2 = 0$ (i.e., $\mu_2 = p_2 = 0$) the fluid is said to be 'physically' self-similar (Coley, 1996).

2. The vacuum solutions correspond to $y = w = 0$.
3. The perfect fluid (with $\mu + p \neq 0$) will exhibit a barotropic equation of state ($p = p(\mu)$) if and only if

$$w + 2yv + y^2 = c_0 e^{2\psi} \quad \text{and} \quad 2u + y = c_1 \quad (5.18)$$

where c_0 and c_1 are constants.

4. If we are to demand that the solutions satisfy the weak energy conditions (i.e. $\mu + p \geq 0$ and $\mu \geq 0$) over the entire manifold the following inequalities serve as necessary conditions

$$\begin{aligned} y &\geq 0, \\ 2u + y &\geq 0, \\ w + 2yv + y^2 &\leq 0. \end{aligned} \quad (5.19)$$

5.2 Qualitative Analysis

The system given by equations (5.12) - (5.15) is an autonomous system of first order ODEs. As such, the asymptotic solutions of the system can be determined by studying the qualitative dynamics.

The full system of equations, (5.12) - (5.15), describing all possible solutions, exhibits a number of invariant sets, including the planes

$$w = 0, \quad y = u, \quad y = 0, \quad (5.20)$$

as well as the surfaces

$$w + 2yv + y^2 = 0, \quad w - yv - y^2 = 0. \quad (5.21)$$

To allow for the simplification of the analysis we make the following change of variables (as in Chapter 4):

$$x_1 = y; \quad x_2 = u - y, \quad x_3 = v, \quad x_4 = w$$

In these coordinates the equations (5.12) - (5.15) become:

$$\dot{x}_1 = x_1(x_2 + x_3), \quad (5.22)$$

$$\dot{x}_2 = x_2(1 + x_3 - x_2 - 3x_1), \quad (5.23)$$

$$\dot{x}_3 = x_4 + x_1^2 + x_1x_3 + x_2x_3 - x_3^2, \quad (5.24)$$

$$\dot{x}_4 = 2x_4x_2. \quad (5.25)$$

The finite singular points can then be located. They are summarised in Table 5.1 There are three distinct hyperbolic singular points and two sets of non-isolated singular points each of which have zero eigenvalues in the direction tangent to the curve and non-zero eigenvalues in all other directions (i.e., they are normally hyperbolic). The finite singular points can be classified by the eigenvalues of the Jacobian for the vector field. This classification will be given in each of the sections to follow. The singular points for system (5.22)-(5.25) do not depend on a parameter value. The classification will, therefore, not require the bifurcation analysis completed in Chapter 4.

We can also consider the singular points located at infinity. To do this we once again employ the Poincare transformation as described in Section 1.3, using the variables:

$$X = x_1\theta, \quad X_2 = x_2\theta, \quad X_3 = v\theta, \quad X_4 = w\theta \\ \theta = (1 + x_1^2 + x_2^2 + v^2 + w^2)^{-1/2}.$$

In this case the equations (5.22)-(5.25) become

$$X'_1 = X_1(X_1 + X_3 - K) - X_1(X_2^2 + X_3X_4)\theta, \quad (5.26)$$

$$X'_2 = X_2(X_3 - X_2 - 3X_1 - K) - X_2(X_2^2 + X_3X_4 - X_2)\theta, \quad (5.27)$$

$$X'_3 = X_1^2 + X_3(X_1 + X_2 - X_3 - K) - X_3(X_2^2 + X_3X_4 - X_4)\theta, \quad (5.28)$$

$$X'_4 = X_4(2X_2 - K) - X_4(X_2^2 + X_3X_4)\theta, \quad (5.29)$$

Table 5.1: **Finite Singular Points** for equations (5.22)-(5.25). The local analysis for each singular point will be discussed in the subsequent sections, according to their classification. $Q_{1,2,3}$ are isolated singular points and L_1 and L_2 are curves of non-isolated singular points (one-dimension equilibrium sets). Note that the curves L_1 and L_2 intersect at the point $(0, 0, 0, 0)$. β and σ are constants.

(x_1, x_2, x_3, x_4)	Eigenvalue - Eigenvector Pairs		Classification	Notes
Q_1 (0, 1, 0, 0)	1 1 -1 2	(0, 1, 2, 0) (1, 0, 3, 0) (0, 1, 0, 0) (0, 1, 3, 3)	Saddle	Metric: eqn. (5.52) Geodesic, vacuum solution Plane symmetric Phys. self-sim.
Q_2 (1, -1, 1, 0)	-3 -2 $1 + \sqrt{2}$ $1 - \sqrt{2}$	(5, -6, -9, 0) (-4, 5, 3, 7) (1, $\sqrt{2}$, 1, 0) (1, $-\sqrt{2}$, 1, 0)	Saddle	Violates WECs
Q_3 ($\frac{1}{4}, \frac{1}{8}, \frac{-1}{8}, 0$)	$\frac{3}{4}$ $\frac{3}{4}$ $\frac{-1}{8}(1 - \sqrt{7}i)$ $\frac{-1}{8}(1 + \sqrt{7}i)$	(1, 0, 3, 0) (-2, 1, -3, 2) (-2, $-\sqrt{7}i$, 1, 0) (-2, $\sqrt{7}i$, 1, 0)	Saddle	Metric: eqn (5.54) Plane symmetric Phys. self-sim.
L_1 (0, 0, β , β^2)	β $1 + \beta$ -2β 0	(3, 0, 1, 0) (0, $1 + \beta$, β , $2\beta^2$) (0, 0, 1, 0) (0, 0, 1, 2β)	3-dim Saddle (if $\beta = 0$ then $L_1 = L_2$ is a saddle-node)	Violates WECs
L_2 (σ , 0, 0, $-\sigma^2$)	$-\sigma$ 2σ $1 - 3\sigma$ 0	(-1, 0, 1, 0) (1, 0, 2, 0) (σ , -2σ , 0, -3σ) (1, 0, 0, -2σ)	3-dim Saddle (if $\sigma = 0$ then $L_1 = L_2$ is a saddle-node)	Metric: eqn. (5.56) spherically symmetric Phys. self-sim.

where

$$K = X_1^2 X_2 + 2X_1^2 X_3 - 3X_1 X_2^2 + X_1 X_3^2 - X_2^3 + X_2^2 X_3 + X_2 X_3^2 - X_3^3 + 2X_2 X_4. \quad (5.30)$$

As was done in the finite KSS case the singular points located on the invariant boundary $\theta = 0$ [which is now the location of the infinite singular points for equations (5.22)-(5.25)] can be classified. It is important to note that the system (5.26)-(5.29) restricted to the invariant set $\Theta = 0$ is identical to that of the *finite* KSS case given in equations (4.5)-(4.8). Therefore, the location of the singular points and their classification is identical to that given in Table 4.2.

Returning now to the system (5.22)-(5.25) we see that the invariant hyperplanes $x_4 = 0$ and $x_2 = 0$ divide the phase space into four additional invariant sets:

$$I_1 = \{(x_1, x_2, x_3, x_4) | x_2 > 0, x_4 > 0\}, \quad (5.31)$$

$$I_2 = \{(x_1, x_2, x_3, x_4) | x_2 > 0, x_4 < 0\}, \quad (5.32)$$

$$I_3 = \{(x_1, x_2, x_3, x_4) | x_2 < 0, x_4 > 0\}, \quad (5.33)$$

$$I_4 = \{(x_1, x_2, x_3, x_4) | x_2 < 0, x_4 < 0\}. \quad (5.34)$$

As was the case in the *finite* KSS case, the function x_4 (curvature) is monotonic in each of these invariant sets. As a result all stable asymptotic behaviour is necessarily located on one of the invariant sets $x_2 = 0$ or $x_4 = 0$ (or at $x_4 = \pm\infty$). Each of these three cases will be studied individually when the global dynamics is considered. (In all cases we note that the classification of singular points (both finite and infinite) can be determined by considering the points listed in Tables 5.1 and 4.2 restricted to the invariant set being considered).

5.2.1 Subcase: $x_2 = 0$

We first consider the hyperplane $x_2 = 0$. In this case the system of equations (5.22) - (5.25) becomes:

$$\dot{x}_1 = x_1 v, \quad (5.35)$$

$$\dot{x}_3 = w_0 + x_1^2 + x_1 x_3 - x_3^2, \quad (5.36)$$

$$\dot{x}_4 = 0; \quad x_4 = w_0 = \text{const.} \quad (5.37)$$

This system is now a two-dimensional dynamical system in the variables x_1 and x_3 with parameter w_0 . The finite singular points are located (where they exist) at:

$$L_{1\pm} = (0, \pm\sqrt{w_0}), \quad (5.38)$$

$$L_{2\pm} = (\pm\sqrt{-w_0}, 0). \quad (5.39)$$

Each of these points is the intersection of the fixed curves (L_1 and L_2 respectively) with the plane under consideration; i.e., $x_2 = 0$ and $x_4 = w_0$.

We note here that the value $x_4 = 0$ is a bifurcation. We shall first consider the dynamics of the solutions when $w_0 < 0$ and $w_0 > 0$, and consider the dynamics at the bifurcation point second. We can see from Table 5.1 that when $w_0 < 0$ or $w_0 > 0$, the points $L_{1\pm}$ and $L_{2\pm}$ have both positive and negative eigenvalues when restricted to this case. Therefore, each is a two-dimensional saddle point. Further, from Table 4.2 we see that the infinite singular points are B_{\pm} , C_{\pm} , D_{\pm} , and E_{\pm} . Restricted to this invariant set we find that B_+ , D_- and E_- are sources; whereas B_- , D_+ and E_+ are sinks.

We now turn our attention to the dynamics of equations (5.35)-(5.36) at the bifurcation value of $w_0 = 0$. In this case we see that there is only one finite singular point, which is located at the origin, $(x_1, x_3) = (0, 0)$, i.e. the intersection of the two fixed curves L_1 and L_2 . This singular point is non-hyperbolic in nature, and as such its local properties can not be determined by examining the eigenvalues of the corresponding Jacobian matrix. In this case, however, there are three invariant lines: $x_1 = 0$, $x_1 = -2x_3$ and $x_1 = x_3$. The dynamics on each of these lines can be determined as follows:

- (i) on $I_1 : x_1 = 0: \dot{x}_3 = -x_3^2 < 0$.
- (ii) on $I_2 : x_1 = -2x_3: \dot{x}_3 = x_3^2 > 0$.
- (iii) on $I_3 : x_1 = x_3: \dot{x}_3 = x_3^2 > 0$.

Each of these three invariant lines then divide the 2-dimensional phase space into 6 additional invariant regions:

$$I_4 = \{(x_1, x_3) | x_3 > 0, 0 < x_1 < x_3\}: \quad \dot{x}_1 > 0$$

$$I_5 = \{(x_1, x_3) | x_3 < 0, -2x_3 < x_1 < 0\}: \quad \dot{x}_1 < 0$$

$$I_6 = \{(x_1, x_3) | x_1 > 0, 0 < x_1 < -2x_3\}: \quad \dot{x}_1 > 0$$

$$I_7 = \{(x_1, x_3) | x_1 < 0, x_3 < x_1 < 0\}: \quad \dot{x}_1 < 0$$

$$I_8 = \{(x_1, x_3) | x_1 > 0, -1/2x_1 < x_3 < x_1\}: \quad \dot{x}_3 > 0$$

$$I_9 = \{(x_1, x_3) | x_1 < 0, x_1 < x_3 < -1/2x_1\}: \quad \dot{x}_3 > 0$$

The result is that the point $(0,0)$ is a saddle. The asymptotic analysis is then completed by considering the singular points on the infinite boundary. As the quadratic portion of the vector field is unchanged by the differing values of the bifurcation parameter, the infinite singular points and the corresponding analysis is identical to that when $w_0 \neq 0$.

A bifurcation diagram, including all the phase portraits for each range of the parameter w_0 is given in Figure 5.1. As can be seen by these phase portraits all generic asymptotic behaviour (to the past and the future) is located on the infinite boundary. The exact solutions for each of these singular points (which are asymptotic states to past or future or are intermediate states) will be examined in section 5.4.

5.2.2 Subcase: $x_4 = 0$ - Plane Symmetry

The invariant set $x_4 = 0$ contains a subset of the asymptotic solutions for the system (5.22)-(5.25). As can be seen from equations (2.45) and (5.11), solutions which have w identically zero comprise the set of plane symmetric solutions. In this case, the system of ODEs (5.22)-(5.25) reduces to:

$$\dot{x}_1 = x_1(x_2 + x_3), \quad (5.40)$$

$$\dot{x}_2 = x_2(1 + x_3 - x_1 - x_2), \quad (5.41)$$

$$\dot{x}_3 = x_1^2 + x_3(x_1 + x_2 - x_3). \quad (5.42)$$

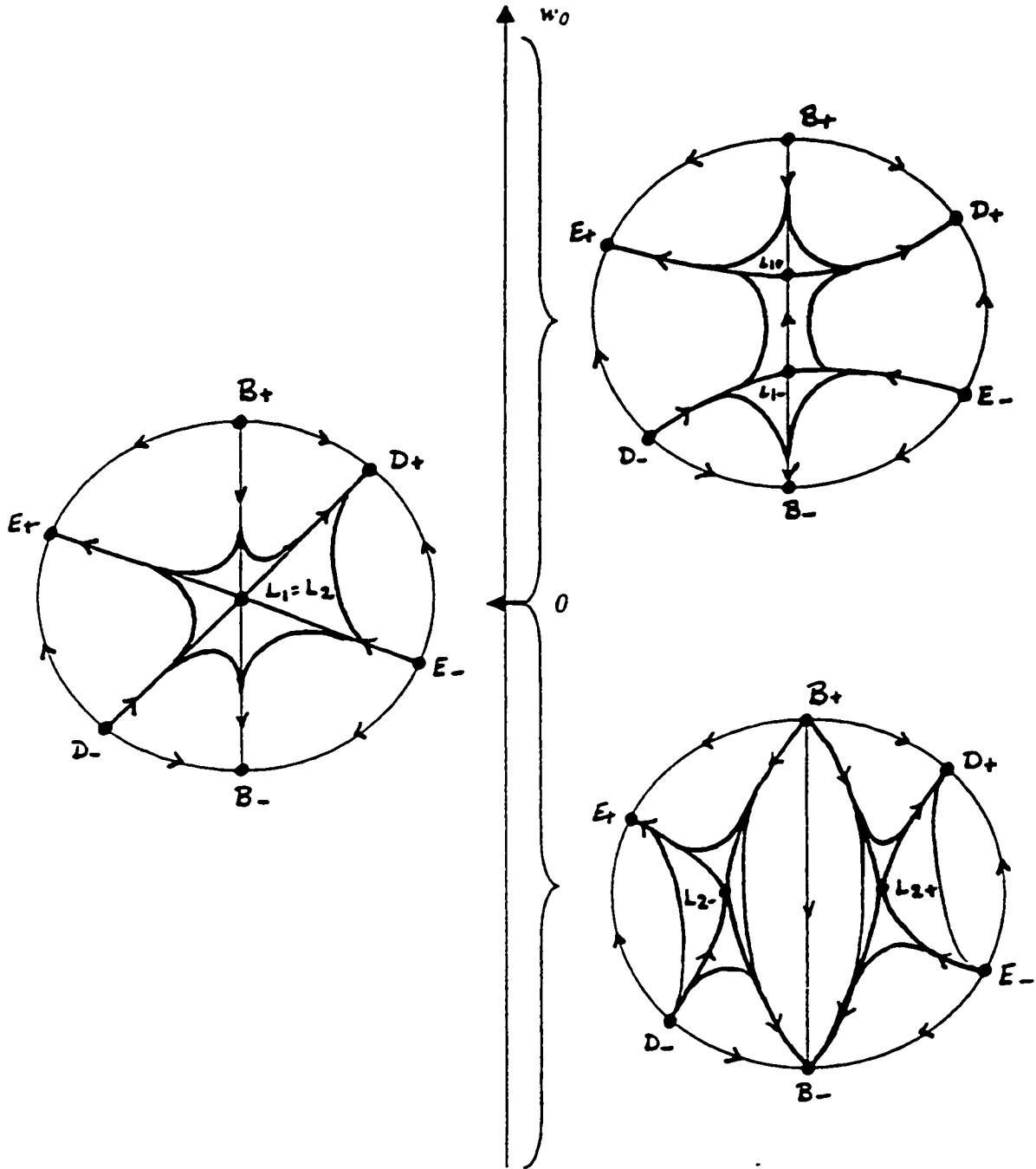


Figure 5.1: Phase portrait of the Poincaré transformation of system (5.35)- (5.36): The case of $w_0 < 0$ corresponds to spherically symmetric solutions, $w_0 = 0$ plane symmetric solutions, and $w_0 > 0$ hyperbolic symmetric solutions. The vertical direction represents the parameter space $w_0 \in \mathbb{R}$, where $w_0 = 0$ is the bifurcation value for the system.

The co-ordinate planes $x_1 = 0$ and $x_2 = 0$ are each invariant sets for this system, as are the sets $x_1 + 2x_3 = 0$ and $x_1 = x_3$.

The finite singular points in this case are given by Q_1, Q_2, Q_3 and $L_1 = L_2$. The local dynamics of each is determined by considering the sign of the eigenvalues of the Jacobian (see Table 5.1) restricted to this set $x_4 = 0$; i.e, those eigenvalues whose associated eigenvectors have the form $(c_1, c_2, c_3, 0)$. The points Q_1 - Q_3 are saddles in this three-dimensional set. The point $L = L_1 = L_2$ is non-hyperbolic. As was done when considering the non-hyperbolic points in Chapter 4, the Centre Manifold Theory will allow the point to be classified. The many invariant sets which include this point greatly simplify the analysis, and it is a straightforward matter to show that in the two dimensions which define the coordinate plane $x_2 = 0$ the point is a saddle and in the third direction it is a saddle-node. The infinite singular points are equivalent to those located and classified in Chapter 4. The dynamics on the infinite boundary are therefore equivalent, and are represented by Figures 4.10 and 4.11.

Before considering the global dynamics in this three-dimensional system, we shall consider the dynamics as restricted to the three invariant planes. Each of these planes will divide the phase space further, allowing for a simplification in the analysis when considering the entire space. Note that the $x_2 = 0$ invariant set has been completely analysed in the previous section. The dynamics are represented by the case $w_0 = 0$ in Figure 5.1. Therefore, we need only consider the planes $x_1 = 0$, $x_1 + 2x_3 = 0$ and $x_1 = x_3$.

Invariant Set: $x_1 = 0$

In the invariant set $x_1 = 0$, the system (5.40)-(5.42) reduces to:

$$\dot{x}_2 = x_2(1 + x_3 - x_2), \quad (5.43)$$

$$\dot{x}_3 = x_3(x_2 - x_3). \quad (5.44)$$

This system gives rise to dynamics in the $x_2 - x_3$ plane. The finite singular points are given by $L_1 = L_2 = (0, 0)$ and $Q_1 = (1, 0)$. Local analysis shows that the point $(1, 0)$ is a hyperbolic saddle point and the point $(0, 0)$ is non-hyperbolic, saddle-node in nature (determined, as in Chapter 4, through the use of centre manifold theory). Therefore,

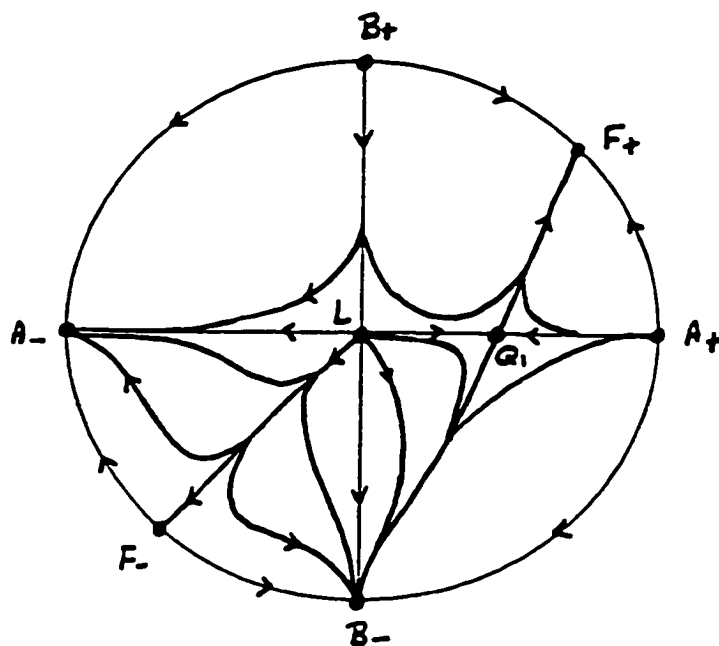


Figure 5.2: Phase portrait of the Poincaré transformation of system (5.43)- (5.44): i.e., plane symmetric solutions restricted to the invariant set $x_1 = 0$. The phase space is X_2 vs. X_3 .

no stable asymptotic behaviour is located in the finite part of the phase space and all asymptotically stable solutions in this subcase are located on the infinite boundary. The complete phase portrait, as compactified by the Poincaré transformation, is given in Figure 5.2.

The solutions in this case can, in fact, be determined completely as the system (5.43)-(5.44) can be integrated completely. The analytic solutions are given by:

- If $x_2 = 0$ then $\dot{x}_3 + x_3^2 = 0$; i.e.

$$x_2 = \text{const and } x_3 = (z + \text{const})^2.$$

- If $x_3 = 0$ then $\dot{x}_2 = x_1(1 - x_2)$; i.e.

$$x_3 = \text{const and } x_2 = (1 + \text{const} \cdot e^{-z})^{-1}.$$

- If $x_3 \neq 0$ then $\ddot{x}_3 + 2x_3\dot{x}_3 = \dot{x}_3 + x_3^2$; i.e.

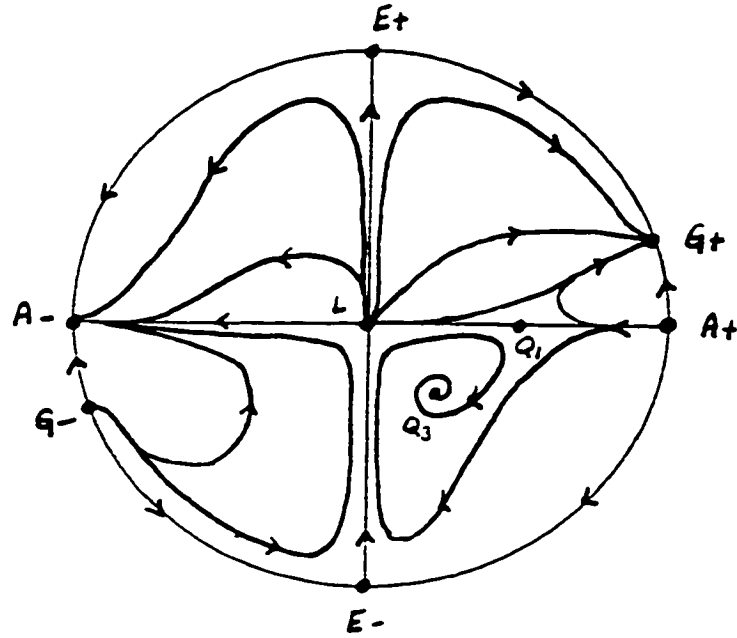


Figure 5.3: Phase portrait of the Poincaré transformation of system (5.45)- (5.46): i.e., plane symmetric solutions restricted to the invariant set $x_1 + 2x_3 = 0$. The phase space is X_2 vs. X_3 .

$$x_2 x_3 = \text{const. and } x_3 = e^{\xi} (\text{const.} + \text{const.} \xi)^{-1}.$$

Invariant Set: $x_1 + 2x_3 = 0$

In the invariant set $x_1 + 2x_3 = 0$, the system (5.40)-(5.42) reduces to:

$$\dot{x}_2 = x_2(1 + 3x_3 - x_2), \quad (5.45)$$

$$\dot{x}_3 = x_3(x_3 + x_2). \quad (5.46)$$

As a result the dynamics are located in a two-dimensional plane. The finite singular points are given by $Q_1 = (1, 0)$, $Q_3 = (1/8, -1/8)$ and $L_1 = L_2 = (0, 0)$. Local analysis determines that the point $(1, 0)$ is a saddle, $(1/8, -1/8)$ a spiralling sink and $(0, 0)$ a saddle-node (determined, as in Chapter 4, through the use of centre manifold theory). The phase portrait for this case, as compactified by the Poincaré transformation, is given in Figure 5.3.

Invariant Set: $x_1 = x_3$

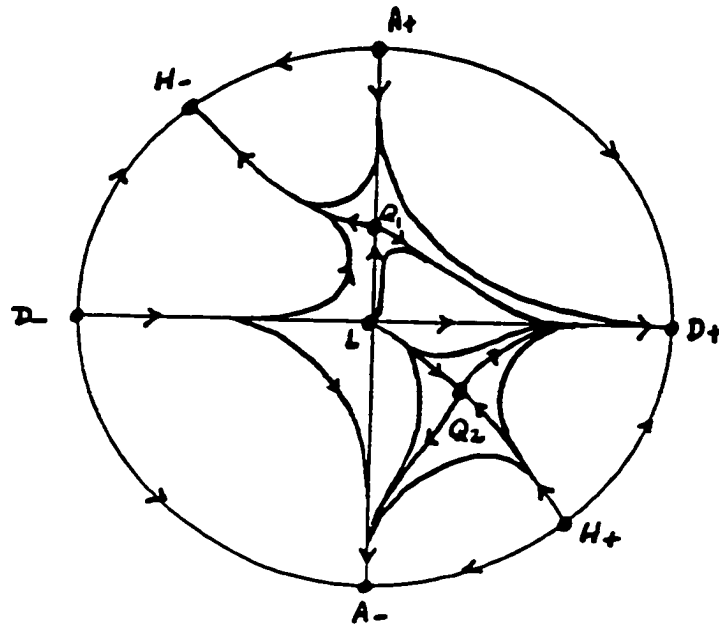


Figure 5.4: Phase portrait of the Poincaré transformation of system (5.47)- (5.48): *i.e., plane symmetric solutions restricted to the invariant set $x_1 = x_3$. The phase space is X_1 vs. X_2 .*

In the invariant set $x_1 = x_3$, the system (5.40)-(5.42) reduces to:

$$\dot{x}_1 = x_1(x_1 + x_2), \quad (5.47)$$

$$\dot{x}_2 = x_2(1 - x_2 - 2x_1). \quad (5.48)$$

As a result the dynamics are located in a two-dimensional plane. The finite singular points are given by $L_1 = L_2 = (0, 0)$, $Q_1 = (0, 1)$ and $Q_2 = (1, -1)$. Local analysis determines that the points $(1, 0)$ and $(1, -1)$ are saddles whereas $(0, 0)$ is a saddle-node (determined, as in Chapter 4, through the use of centre manifold theory). The phase portrait for this case, as compactified by the Poincaré transformation, is given in Figure 5.4.

Global Dynamics

The global dynamics can, once again, be determined through an investigation of the direction fields making use of the monotonicity principle. To simplify the global analysis, consider the full three-dimensional phase space divided into 16 invariant regions and labelled U_i so that U_{13} corresponds to the set $x_2 = 0$, U_{14} the set $x_1 = 0$,

Table 5.2: **Invariant regions of the space** (x_1, x_2, x_3) for the system (5.40)-(5.42) with corresponding monotonic functions. Note that the sets $U_{13}-U_{16}$ are not included here as they are two-dimensional invariant sets and their complete dynamics have been summarised in the phase portraits: Figures 5.1-5.4 .

Label	Definition of Region	Monotonic Function
U_1	$\{(x_1, x_2, x_3) x_1, x_2, x_3 > 0\}$	x_1 strictly increasing
U_2	$\{(x_1, x_2, x_3) x_1, x_2 > 0, x_1 + 2x_3 > 0\}$	$x_1 + 2x_3$ strictly increasing
U_3	$\{(x_1, x_2, x_3) x_1, x_2 > 0, x_1 + 2x_3 < 0\}$	$x_1 + 2x_3$ strictly decreasing
U_4	$\{(x_1, x_2, x_3) x_1 < 0, x_2 > 0, x_1 - x_3 < 0\}$	$x_1 - x_3$ strictly decreasing
U_5	$\{(x_1, x_2, x_3) x_1 < 0, x_2 > 0, x_1 - x_3 > 0\}$	$x_1 - x_3$ strictly increasing
U_6	$\{(x_1, x_2, x_3) x_1 < 0, x_2, x_3 > 0\}$	x_1 strictly decreasing
U_7	$\{(x_1, x_2, x_3) x_1 > 0, x_2 < 0, x_1 - x_3 < 0\}$	$x_1 - x_3$ strictly increasing
U_8	$\{(x_1, x_2, x_3) x_1 > 0, x_2 < 0, x_1 - x_3 > 0\}$	$x_1 - x_3$ strictly decreasing
U_9	$\{(x_1, x_2, x_3) x_1 > 0, x_2 < 0, x_3 < 0\}$	$x_1 - x_3$ strictly decreasing
U_{10}	$\{(x_1, x_2, x_3) x_1, x_2, x_3 < 0\}$	x_1 strictly increasing
U_{11}	$\{(x_1, x_2, x_3) x_1, x_2 < 0, x_1 + 2x_3 < 0\}$	$x_1 + 2x_3$ strictly increasing
U_{12}	$\{(x_1, x_2, x_3) x_1, x_2 < 0, x_1 + 2x_3 > 0\}$	$x_1 + 2x_3$ strictly decreasing

U_{15} the set $x_1 + 2x_3 = 0$ and U_{16} the set $x_1 = x_3$. In each of the remaining 12 regions of space a monotonic function has been identified. These regions, and their corresponding direction of monotonic change, are given in Table 5.2. Note that the sum of the sets U_i , $i = 1..16$ provides a decomposition of the complete phase space. As such, since each region is invariant under the system (5.40)-(5.42) the existence of strictly monotonic functions in the regions $U_1 - U_{14}$ ensures that the only possible asymptotic solutions are located on the boundaries (either finite or infinite). The finite boundaries are the sets $U_{13} - U_{16}$, or subsets thereof. As a result the global dynamics have been completely determined by the previous investigations. The only possible asymptotic states are, therefore, the singular points located at finite and infinite values.

5.3 Description of Asymptotic Solutions

In the qualitative analysis of the previous section, the asymptotic states of the governing system were described as singular points of the autonomous system of ODEs. The existence of other types of stable structures was ruled out by the existence of monotonic functions. Each of the physical solutions described by these singular points will now be given, restricting attention to those solutions which satisfy the energy conditions given by equations (5.19). Note that in Chapter 4 it was necessary to examine all the singular points since the physical space was not bounded by invariant sets, and the possibility existed that some solutions may satisfy the WECs while approaching a point which does not. In this present case, however, the boundaries of the regions which satisfy the WECs are, in fact, invariant sets; therefore we need only consider the solutions which lie in the regions satisfying the WECs. While some of the singular points being described are not structurally stable in all 4-dimensions, there are invariant regions in which they do act as attractors (either to the past or the future); in addition, these points act as intermediate attractors (repellers) for large classes of solutions. For these reasons the exact solutions for each of the singular points satisfying the WECs will now be given.

It is important to note that in this case of *infinite* KSS all asymptotic solutions which satisfy the WECs are necessarily *physically* self similar, satisfying at least one of the following criteria:

$$\text{Case I : } \quad x_3 = 0, \quad (5.49)$$

$$\text{Case II : } \quad x_1 = 0, \quad (5.50)$$

$$\text{Case III : } \quad x_4 + 2x_1x_3 + x_1^2 = 0. \quad (5.51)$$

Each of these cases of physical self-similarity is an invariant set of the governing system (5.22)-(5.25), and as such will be considered separately in section 5.4

Note: The singular points $Q_2, L_1, A_-, C_+, D_{\pm}, E_+, F_-, G_+$ and H_{\pm} do not satisfy the WECs.

5.3.1 Finite Singular Point Asymptotic States

Case 1: $Q_1 = (0, 1, 0, 0)$

In this case the metric is plane symmetric. By a suitable change of coordinates the metric and the energy density and pressure are given by

$$ds^2 = -dt^2 + t^2 dr^2 + s_0^2(d\theta^2 + \theta^2 d\phi^2) \quad (5.52)$$

$$\mu = p = 0. \quad (5.53)$$

Note: This solution is a vacuum.

Case 2: $Q_3 = (1/4, 1/8, -1/8)$

In this case the metric is plane symmetric. The metric and the energy density and pressure are given by

$$ds^2 = -a^2(r/t)^{1/4} dt^2 + b^2(t/r)^{3/4} r^{-2} dr^2 + \frac{(t + cr)^2}{16r^2} (d\theta^2 + \theta^2 d\phi^2) \quad (5.54)$$

$$\mu = \mu_0(t^3 r)^{-1/4} \quad p = (a^2/4 - \mu_0)(t^3 r)^{-1/4}. \quad (5.55)$$

Note: when the constant μ_0 is positive the WECs are satisfied

Case 3: $L_2 = (\beta, 0, 0, -\beta^2)$

In this case the metric is spherically symmetric, and the solutions are in the geodesic class. The metric and the energy density and pressure are given by

$$ds^2 = -a^2 dt^2 + b^2(t/r)^\sigma r^{-2} dr^2 + (\sigma \ln(\xi) + c)^2 (d\theta^2 + \sin^2 \theta d\phi^2) \quad (5.56)$$

$$\mu = \mu_0 t^{-2} \quad p = (2\sigma a^{-2} - \mu_0) t^{-2}. \quad (5.57)$$

Note that in this case only those non-isolated singular points with $\sigma \geq 0$ satisfy the energy conditions.

5.3.2 Infinite Singular Point Asymptotic States

Case 1: $A_+ : x_1 = x_3 = x_4 = 0$

In this case the metric is plane symmetric. The metric and the energy density and pressure are given by

$$ds^2 = -a^2 dt^2 + b^2(\ln(\xi) + c^2 r^{-2} dr^2 + s_0^2(d\theta^2 + \theta^2 d\phi^2)) \quad (5.58)$$

$$\mu = p = 0. \quad (5.59)$$

Note: This solution is a vacuum.

Case 2: $B_{\pm} : x_1 = x_2 = x_4 = 0$

In this case the metric is plane symmetric. The metric and the energy density and pressure are given by

$$ds^2 = -a^2(\ln(\xi) + c)^2 dt^2 + b^2 r^{-2} dr^2 + s_0^2(d\theta^2 + \theta^2 d\phi^2) \quad (5.60)$$

$$\mu = p = 0. \quad (5.61)$$

Note: This solution is a vacuum.

Case 3: $C_- : x_1 = x_2 = x_3 = 0$

In this case the metric is spherically symmetric. By suitable change of coordinates the metric and the energy density and pressure are given by

$$ds^2 = -dt^2 + r^{-2} dr^2 + (d\theta^2 + \sin^2 \theta d\phi^2) \quad (5.62)$$

$$\mu = p = \mu_0. \quad (5.63)$$

Note: This solution is a stiff fluid.

Case 4: $E_- : x_2 = x_4 = 0, x_1 + 2x_3 = 0$

In this case the metric is plane symmetric. The metric and the energy density and pressure are given by

$$ds^2 = -a^2 S^{-1} dt^2 + b^2 S^2 r^{-2} dr^2 + S^2(d\theta^2 + \theta^2 d\phi^2) \quad (5.64)$$

where $S = s_0(\ln(t/r) + c)^{-2}$, and

$$\mu = \frac{12s_0^2}{a^2(\ln(t/r) + c)^4} t^{-2}, \quad \mu + p = \frac{8}{a^2(\ln(t/r) + c)^2} t^{-2}. \quad (5.65)$$

Case 5: F_+ : $x_2 = x_4 = 0, x_2 = x_3$

In this case the metric is plane symmetric. By a suitable change of coordinates the metric and energy density and pressure are given by

$$ds^2 = -dt^2 + r^{-2}dr^2 + (d\theta^2 + \theta^2d\phi^2) \quad (5.66)$$

$$\mu = p = 0. \quad (5.67)$$

Note: This is a vacuum solution.

Case 6: G_- : $x_4 = 0, x_1 + 2x_3 = 0, x_2 = 3x_3$

In this final case the metric is plane symmetric. The metric and energy density and pressure are given by

$$ds^2 = -a^2S^{-1}dt^2 + b^2S^{-1}r^{-2}dr^2 + S^2(d\theta^2 + \theta^2d\phi^2) \quad (5.68)$$

where $S = s_0(\ln(t/r) + c)^{1/2}$, and

$$\mu = \frac{12s_0^2}{a^2(\ln(t/r) + c)^4}t^{-2}, \quad \mu + p = \frac{8}{a^2(\ln(t/r) + c)^2}t^{-2}. \quad (5.69)$$

5.4 Physical Self-Similarity for Infinite KSS

As was noted in the previous section, there are three special cases in which the solutions not only admit a "geometrical" kinematic self-similarity, but a physical one as well. Each of these three cases will now be examined separately.

5.4.1 Case I: $x_3 = 0$

As was the case for *finite* KSS, these solutions represent the geodesic solutions for the system; i.e., the solutions have zero acceleration. Since the governing equations impose the condition $x_4 = -x_1^2$ there can be no hyperbolically symmetric solutions in this class. The plane symmetric solutions are in the special case $x_1 = 0$. All other solutions will exhibit spherical symmetry.

For $x_1 \neq 0$ it follows from equations (5.22)-(5.25) that

$$e^{2\Psi} = \dot{S}^2 \quad (5.70)$$

and thus

$$2\dot{x}_1 + 2x_1^2 - 2x_1 + p_0 = 0 \quad (5.71)$$

Note that the governing equation for the evolution of the function S (5.71) is identical to the governing equation for the geodesic solutions in the case of finite KSS [i.e. see equation (3.11)] where α has been set to -1 . Therefore, the analysis, and solutions to equation (5.71) will be identical to that given in Section 3.1. The case $x_1 = 0$ corresponds to vacuum (plane symmetric) solutions (which will be given separately below), and for $x_1 \neq 0$ the solutions correspond to the spherically symmetric case, hence the metric can be written as

$$ds^2 = -a^2 dt^2 + \frac{\dot{S}^2}{r^2} dr^2 + S^2(d\theta^2 + \sin^2 \theta d\phi^2) \quad (5.72)$$

with

$$\mu = (2\dot{S} - p_0 S)(aS)^{-2} t^{-2} \quad (5.73)$$

$$p = p_0 t^{-2} \quad (5.74)$$

In this class of solutions the WECs (5.19) are satisfied *iff* $x_1 \geq 0$.

The special case $x_1 = 0$ includes all plane symmetric solutions in this class. The metric and physical properties are

$$ds^2 = -dt^2 + (c_1 \xi + c_2)^2 r^{-2} dr^2 + s_0^2(d\theta^2 + \theta^2 d\phi^2) \quad (5.75)$$

$$\mu = p = 0 \quad (5.76)$$

where c_1 and c_2 are constants.

5.4.2 Case II: $x_1 = 0$

The finite singular points and the equilibrium sets \mathbf{Q}_1 and \mathbf{L}_1 (as well as \mathbf{L}_2 for $\nu = 0$) are included in this class of solutions, as are the infinite singular points \mathbf{A}_\pm , \mathbf{B}_\pm , \mathbf{C}_\pm and \mathbf{F}_\pm .

The system (5.22)-(5.25) reduces to the three-dimensional system of autonomous ODEs:

$$\dot{x}_2 = x_2(1 - x_2 + x_3) \quad (5.77)$$

$$\dot{x}_3 = x_4 + x_3(x_2 - x_3) \quad (5.78)$$

$$\dot{x}_4 = 2x_2x_4 \quad (5.79)$$

Exact solutions can be found in the two invariant planes $x_2 = 0$ and $x_4 = 0$.

1. $x_2 = 0$: The solution is given by:

$$ds^2 = -e^{2\Phi} dt^2 + b^2 r^{-2} dr^2 + s_0^2 d\Omega^2 \quad (5.80)$$

with

$$\mu = -w_0 b^{-2} \quad \text{and} \quad p = w_0 b^{-2}. \quad (5.81)$$

The function Φ is defined by

(a) $w_0 > 0$ (spherically symmetric metric): $e^{2\Phi} = a^2(\xi^{\sqrt{-w_0}} + \xi^{-\sqrt{-w_0}})^2$

(b) $w_0 = 0$ (plane symmetric metric): $e^{2\Phi} = a^2(\xi + c)^2$

(c) $w_0 < 0$ (hyperbolically symmetric metric): $e^{2\Phi} = a^2 \cos^2(\sqrt{w_0} z)$

Note that in the case $w_0 > 0$ the WECs are not satisfied and $w_0 = 0$ corresponds to a vacuum solution.

2. $x_4 = 0$: The solution is given by:

$$ds^2 = -e^{2\Phi} dt^2 + e^{2\Psi} r^{-2} dr^2 + s_0^2(d\theta^2 + \theta d\phi^2) \quad (5.82)$$

with

$$\mu = 0 \quad \text{and} \quad p = 0, \quad (5.83)$$

a vacuum solution. The function Φ is defined as the following:

(a) if $x_2 = 0$: $e^{2\Psi} = b^2$, $e^{2\Phi} = a^2 \xi^2$

$$(b) \text{ if } x_3 = 0: e^{2\Psi} = b^2(\xi + c)^2, e^{2\Phi} = a^2$$

$$(c) \text{ if } x_2 x_3 \neq 0: e^{2\Psi} = b^2 e^{-x^2}, e^{2\Phi} = (i\sqrt{2\pi}\text{erf}(i\sqrt{2}z/2) + k)^2$$

Through the use of the monotonic function principle (with the function x_4), it is a straightforward matter to show that all solutions asymptote to solutions in one of the two cases listed above (i.e. $x_1 = 0$ or $x_3 = 0$).

5.4.3 Case III: $x_4 + 2x_1x_3 + x_1^2 = 0$

In this final class of physically self-similar solutions the system (5.22)-(5.25) reduces to the three-dimensional system of autonomous ODEs:

$$\dot{x}_1 = x_1(x_2 - x_3) \quad (5.84)$$

$$\dot{x}_2 = x_2(1 - x_2 + x_3) \quad (5.85)$$

$$\dot{x}_3 = x_3(x_2 - x_1 - x_3) \quad (5.86)$$

Through the use of various monotonic functions it can be shown that all asymptotic behaviour in this class of solutions is described by solutions in one (or more) of the invariant sets $x_1 = 0$, $x_2 = 0$, $x_3 = 0$ or $x_1 + 2x_3 = 0$, all of which have been previously discussed.

5.5 Summary

Through an extensive use of monotonic functions it was shown that all asymptotic solutions in this infinite class of KSS are necessarily located at singular points (either at finite or infinite values of the dependent variables). Unlike the analysis in Chapter 4, there was no need for the use of numerical analysis of the solutions to determine the dynamics.

The class of solutions which are also *physically* self-similar are again important in this analysis. It has been shown that in all cases in which the energy conditions are satisfied the asymptotic behaviour is necessarily "physically" self-similar.

Chapter 6

Anisotropic Fluids

In this chapter we shall generalise the perfect fluid solutions examined in the previous chapters to the case of an anisotropic fluid, in which stress energy tensor is given by

$$T_{ab} = \mu u_a u_b + p_{||} n_a n_b + p_{\perp} (g_{ab} + u_a u_b - n_a n_b), \quad (6.1)$$

where u^a is the comoving fluid velocity vector and n^a is a unit spacelike vector orthogonal to u^a (i.e., $u_a n^a = 0$). For the metric (1.17), \mathbf{n} is given by

$$\mathbf{n} = n^a \frac{\partial}{\partial x^a} = e^{-\psi} \frac{\partial}{\partial r}. \quad (6.2)$$

Using equations (1.4) - (1.6), it therefore follows immediately that

$$\mathcal{L}_{\xi} n_a = n_a \quad (6.3)$$

is satisfied identically, so that the form for \mathbf{n} is consistent with the similarity assumption. The scalars $p_{||}$ and p_{\perp} are the pressures parallel to and perpendicular to n^a , respectively, and μ is the energy-density. The perfect fluid case corresponds to the case in which $p_{||} = p_{\perp}$.

Fluids with an anisotropic pressure have been studied for many reasons (see the discussion in Coley and Tupper, 1994; hereafter denoted CT). For example, in several cases in which the stress-energy tensor is more general than that of a perfect fluid (due to, e.g., a two perfect fluid source, an imperfect fluid source or in the region of

interaction of two colliding plane impulsive gravitation waves), the energy-momentum tensor is formally of the form (6.1). In particular, a strong magnetic field in a plasma in which the particle collision density is low can cause the pressure along and perpendicular to the magnetic field lines to be unequal (Maartens et al., 1986). If the source of the gravitational field can be represented by the sum of a perfect fluid and a local magnetic field $H^a = Hn^a$ (as measured by u^a), then the stress-energy tensor can be written in the form (6.1) with

$$\begin{aligned}\mu &= \bar{\mu} + \pi \\ p_{\parallel} &= \bar{p} - \pi \\ p_{\perp} &= \bar{p} + \pi\end{aligned}\tag{6.4}$$

where $\pi = \frac{1}{2}\lambda H^2$ and λ is the magnetic permeability. Other possible sources of anisotropic stresses, in addition to cosmological magnetic and electric fields, include for example populations of collisionless particles like gravitons (Lukash and Starobinskii, 1974), photons (Press, 1976) or relativistic neutrinos (Doroshekevich et al., 1968), Yang-Mills fields (Darian and Künzle, 1995), axion fields in low-energy string theory (Green et al., 1987), long wavelength gravitational waves (Lukash, 1976), and topological defects like global monopoles, cosmic strings and domain walls (Barriola and Vilenkin, 1989; Vilenkin and Shellard, 1994; Stachel, 1980).

Most anisotropic models that have been studied are also spherically symmetric (see references cited in CT), and have applications especially in relativistic astrophysics (e.g., stellar models); in particular, static anisotropic spheres have received much attention (CT). In addition, such models with additional symmetries, including homothetic vectors and conformal Killing vectors, have also been studied (Maartens et al., 1986; CT, and references within).

For the metric (1.17) the Einstein field equations (EFEs) yield the following expressions for the physical variables:

$$\mu = \frac{W^1(z)}{r^2} + \frac{W^2(z)}{t^2}$$

$$\begin{aligned}
p_{\parallel} &= \frac{P_{\parallel}^1(z)}{r^2} + \frac{P_{\parallel}^2(z)}{t^2} \\
p_{\perp} &= \frac{P_{\perp}^1(z)}{r^2} + \frac{P_{\perp}^2(z)}{t^2}
\end{aligned} \tag{6.5}$$

where

$$\begin{aligned}
W^1(z) &= \frac{1}{S^2} - e^{-2\psi}[(1+y)^2 + 2y\dot{\phi}] \\
W^2(z) &= \frac{e^{-2\phi}}{\alpha^2} y[y + 2\dot{\psi}] \\
P_{\parallel}^1(z) &= -\frac{1}{S^2} + e^{-2\psi}(1+y)[1+y+2\dot{\phi}] \\
P_{\parallel}^2(z) &= -\frac{e^{-2\phi}}{\alpha^2} [2\dot{y} + 2\alpha y + 3y^2 - 2y\dot{\phi}] \\
P_{\perp}^1(z) &= e^{-2\psi} [2y\dot{\phi} + \dot{\phi}^2 + \ddot{\phi} - \dot{\phi}\dot{\psi}] \\
P_{\perp}^2(z) &= -\frac{e^{-2\phi}}{\alpha^2} [(\alpha-1)y + 2y\dot{\psi} + \dot{\psi} + \alpha\dot{\psi} + \dot{\psi}^2 + \ddot{\psi} - \dot{\phi}\dot{\psi}],
\end{aligned} \tag{6.6}$$

and where $y \equiv \dot{S}/S$, $z \equiv \ln \xi$ and $\dot{f} = df/dx$. The final EFE (that ensures that the Einstein tensor is diagonal) becomes

$$\dot{y} = y\dot{\phi} + (\dot{\psi} - y)(1+y). \tag{6.7}$$

Clearly there exist a variety of anisotropic fluid spherically symmetric kinematic self-similar spacetimes satisfying equations (6.5)-(6.7)

If we assume that the physical quantities also obey similarity conditions of the form

$$\begin{aligned}
\mathcal{L}_{\xi}\mu &= a\mu \\
\mathcal{L}_{\xi}p_{\parallel} &= b_{\parallel}p_{\parallel} \\
\mathcal{L}_{\xi}p_{\perp} &= b_{\perp}p_{\perp}
\end{aligned} \tag{6.8}$$

where a , b_{\parallel} and b_{\perp} are constants, then it can easily be shown that:

$$(i) \quad W^1 = 0 \quad \underline{\text{or}} \quad W^2 = 0$$

and

$$(ii) \quad P_{\parallel}^1 = 0 \quad \underline{\text{or}} \quad P_{\parallel}^2 = 0$$

and

$$(iii) \quad P_{\perp}^1 = 0 \quad \underline{\text{or}} \quad P_{\perp}^2 = 0.$$

The special subcases $W^i = 0$ with either $P_{\parallel}^i \neq 0$ or $P_{\perp}^i \neq 0$ ($i = 1, 2$) are not of physical interest. The special subcase $W^1 = P_{\parallel}^1 = P_{\perp}^1 = 0$ corresponds to the special subcase " $M_1 = 0$ ". Finally, the special subcase $W^2 = P_{\parallel}^2 = P_{\perp}^2 = 0$ is related to the special subcase " $M_2 = 0$ ", and the static models are included within this subclass of models.

As was seen in Chapter 3 all *static* spherically symmetric kinematic self-similar solutions belong to the subclass " $M_2 = 0$ ", regardless of the form of the stress-energy tensor, and, moreover, all such static spacetimes necessarily admit a *homothetic vector*. Consequently, no new static anisotropic solutions can be obtained that admit a proper kinematic self-similarity. Hence we shall concentrate here on the special subcase " $M_1 = 0$ ".

6.1 Geodesic Models

The geodesic case is characterised by $\dot{\phi} = 0$ and is equivalent to the special subcase " $M_1 = 0$ " considered in Chapter 3. In this model, equation (6.7) gives (for $S + \dot{S} \neq 0$)

$$e^{2\phi} = 1, \quad \dot{\psi} = \frac{\dot{S} + \ddot{S}}{S + \dot{S}} = \frac{\dot{y} + y^2 + y}{1 + y}, \quad (6.9)$$

whence the metric (1.17) becomes

$$ds^2 = -dt^2 + (S + \dot{S})^2 dr^2 + r^2 S^2 d\Omega^2. \quad (6.10)$$

Assuming the first of conditions (6.9), the second condition guarantees the resulting Einstein tensor is diagonal and hence the remaining EFEs simply yield the following expressions for μ , p_{\parallel} and p_{\perp} :

$$\begin{aligned} \mu &= W(z)t^{-2} \\ p_{\parallel} &= P_{\parallel}(z)t^{-2} \\ p_{\perp} &= P_{\perp}(z)t^{-2} \end{aligned} \quad (6.11)$$

(where we have now omitted the index "2" for convenience), so that equations (6.8) are automatically satisfied with $a = b_{\parallel} = b_{\perp} = -2\alpha$, where

$$\begin{aligned} W(z) &\equiv \frac{y}{\alpha^2(1+y)}(3y + 3y^2 + 2\dot{y}) \\ P_{\parallel}(z) &\equiv -(3y^2 + 2\alpha y + 2\dot{y})/\alpha^2 \\ P_{\perp}(z) &\equiv -\frac{(1+y)(2\dot{y} + 3y^2 + 2\alpha y) + 3y\dot{y} + \alpha\dot{y} + \ddot{y}}{\alpha^2(1+y)}. \end{aligned} \quad (6.12)$$

Equations (6.10) - (6.12) represent a class of anisotropic fluid solutions depending upon the arbitrary function $S(z)$.

We note that the following relationships result from the definitions given in equations (6.11):

$$\begin{aligned} P_{\perp} &= P_{\parallel} + \frac{\dot{P}_{\parallel}}{2(1+y)} \\ W &= \frac{-y[(2\alpha - 3)y + \alpha^2 P_{\parallel}]}{\alpha^2(1+y)} \end{aligned}$$

6.1.1 Perfect Fluid Models

In the perfect fluid case we have that $P_{\parallel} = P_{\perp}$, and hence from equations (6.12) we obtain the following differential equation for the function $y(z)$ [and hence $S(z)$] in the metric (6.10):

$$2\dot{y} + 3y^2 + 2\alpha y + \alpha^2 p_0 = 0. \quad (6.13)$$

In equation (6.13) p_0 is an arbitrary integration constant. In the perfect fluid case μ is obtained from equations (6.11) and (6.12) and we have that

$$p = p_0 t^{-2}, \quad (6.14)$$

and hence the significance of p_0 is that it constitutes a dimensional constant (appearing in the pressure) characterising the physical problem; this property is characteristic of self-similarity of the second kind (Barenblatt and Zel'dovich, 1972). Recall from Chapter 3 that these perfect fluid solutions (for $\alpha \neq 1$) cannot, in general, admit any homothetic vectors.

The perfect fluid solutions were studied in detail in Chapter 3; in fact, exact solutions were obtained and the qualitative properties of the whole class of models were studied. In particular, in the pressure-free case we obtain the exact dust solution of the Tolman family studied by Lynden-Bell and Lemos (1988) and Carter and Henriksen (1989), and we found that all solutions are asymptotic to exact, power-law (flat) FRW models (which admit a homothety).

6.1.2 Solutions with $S + \dot{S} = 0$

In the perfect fluid case it can be easily shown that the case $S + \dot{S} = 0$, which implies that $S = s_0 e^{-z}$, could be factored out of the analysis as it could not lead to a solution. For that reason, we consider it as a special case here. (This case is not contained in the geodesic models studied above.)

When $S = s_0 e^{-z}$ (i.e., $y = -1$), the EFEs yield

$$\dot{\phi} = 0, \quad (6.15)$$

whence we can choose coordinates so that $e^{2\phi} = 1$, and

$$\mu = s_0^{-2} e^{2z} r^{-2} + (1 - 2\dot{\psi}) \alpha^{-2} t^{-2} \quad (6.16)$$

$$p_{||}(z) = -s_0^2 e^{2z} r^{-2} + (2\alpha - 3) \alpha^{-2} t^{-2} \quad (6.17)$$

$$p_{\perp}(z) = -[(1 - \alpha)(1 - \dot{\psi}) + \dot{\psi}^2 + \ddot{\psi}] \alpha^{-2} t^{-2}. \quad (6.18)$$

The fluid described by these equations will further satisfy equation (6.8) in one of two cases. Either (i) $\alpha = 1$, and the solution admits a homothetic vector, or (ii) $\dot{\psi} = 1/2$, $\alpha = 3/2$.

In the first case, i.e. $\alpha = 1$, the solution is given by

$$ds^2 = -dt^2 + e^{2\psi} dr^2 + s_0 t^{-2} d\Omega^2, \quad (6.19)$$

with

$$\mu = (s_0^{-2} + 1 - 2\dot{\psi}) t^{-2} \quad (6.20)$$

$$p_{||} = -(s_0^{-2} + 1) t^{-2} \quad (6.21)$$

$$p_{\perp} = -(\dot{\psi}^2 + \ddot{\psi}) t^{-2}, \quad (6.22)$$

where the function $\psi(x)$ is arbitrary.

In the second case the solution is given by (after a coordinate redefinition)

$$ds^2 = -dt^2 + t^{-2/3}dr^2 + t^{4/3}d\Omega^2, \quad (6.23)$$

with

$$\mu = \mu_0 t^{-4/3} \quad (6.24)$$

$$p_{\parallel} = -\mu \quad (6.25)$$

$$p_{\perp} = 0, \quad (6.26)$$

where μ_0 is a constant. It can be easily shown that the metric (6.23) does not admit a proper homothetic vector. Curiously, cosmic strings satisfy “equations of state” of the form $\mu + p_{\parallel} = 0$, $p_{\perp} = 0$ (Vilenkin, 1981).

6.2 Special Cases

There are a variety of models which satisfy additional constraints. We consider here two such models.

6.2.1 Case A: Dimensional Constants

If we assume that $P_{\perp} = p_0$, a constant, then equations (6.12) yield

$$\dot{P}_{\parallel}(z) = 2(1+y)(p_0 - P_{\parallel}(z)). \quad (6.27)$$

This equation can be integrated to yield

$$P_{\parallel}(z) = p_0 + ce^{-2z}S^{-2}, \quad (6.28)$$

where c is an arbitrary constant. Using this expression for P_{\parallel} , we obtain

$$W(z) = \frac{y}{\alpha^2(1+y)} \left[y(3-2\alpha) - \alpha^2 p_0 - c\alpha^2 e^{-2z}S^{-2} \right], \quad (6.29)$$

and the differential equation

$$2\dot{y} + 3y^2 + 2\alpha y = -\alpha^2 p_0 - \alpha^2 c e^{-2z} S^{-2}. \quad (6.30)$$

Note that when $c = 0$ (i.e., $P_{\parallel} = P_{\perp} = p_0$, corresponding to a perfect fluid) equation (6.30) is related to equation (3.11) in Chapter 3.

If we had begun the analysis of this section with the assumption that $P_{\parallel} = p_0$, then the equations (6.12) automatically imply that $P_{\parallel} = P_{\perp} = p_0$, the perfect fluid case considered in Chapter 3.

The pressures p_{\parallel} and p_{\perp} are positive if the constants p_0 and c are non-negative. The energy conditions will constrain these constants further (for a given value of α) through (6.29).

6.2.2 Case B: Equations of State

We can also consider the subclass of solutions which satisfy equations of state of the form:

$$\begin{aligned} p_{\parallel} &= f_{\parallel}(\mu), \\ p_{\perp} &= f_{\perp}(\mu), \end{aligned} \quad (6.31)$$

for arbitrary functions f_{\parallel} and f_{\perp} . From equations (6.11), conditions (6.31) automatically yield

$$p_{\parallel} = c_{\parallel}\mu \quad \text{and} \quad p_{\perp} = c_{\perp}\mu, \quad (6.32)$$

where c_{\parallel} and c_{\perp} are constants. Substituting these conditions into the definitions (6.12) then yields

$$\mu = \mu_0 t^{-2} [S e^z]^{-2(1-c_{\perp}/c_{\parallel})} \quad (6.33)$$

and the differential equation for y :

$$2\dot{y} + 3y^2 + 2\alpha y = -\alpha^2 c_{\parallel} \mu_0 [S e^z]^{-2(1-c_{\perp}/c_{\parallel})}. \quad (6.34)$$

Once again we note that when $c_{\parallel} = c_{\perp}$ (i.e., the perfect fluid case), we recover equation (6.13) as expected.

A positive value for the constant μ_0 guarantees that the energy density is positive. If $|c_{||}| \leq \mu_0$ and $|c_{\perp}| \leq \mu_0$, the energy conditions are satisfied. The pressures are non-negative if $c_{||} \geq 0$ and $c_{\perp} \geq 0$.

6.3 Analysis of Special Cases

The behaviour of each of the special cases derived in section 6.2 can be studied qualitatively since each of the ordinary differential equations governing the model is autonomous.

The special cases A(dimensional constants) and B(equations of state) can be considered simultaneously using the following change of variables:

$$\nu = b[Se^z]^{-2n}, \quad (6.35)$$

where b is a non-negative constant. The resulting system is then

$$\dot{y} = -\frac{1}{2}(3y^2 + 2\alpha y + k + \nu) \quad (6.36)$$

$$\dot{\nu} = -2n\nu(1 + y). \quad (6.37)$$

Using these definitions, case A is characterised by $n = 1$, $k = \alpha^2 p_0$, and case B is characterised by $n = 1 + c_{\perp}/c_{||}$ and $k = 0$.

It is important to note that the invariant set $\nu = 0$ of equations (6.36)/(6.37) defines the perfect fluid solutions. We also note that $y = 0$ represents the static solutions. Each of these cases has been examined in detail.

If we consider only the case of positive pressures and positive energy density, we can impose the necessary (though not necessarily sufficient) condition that the parameters in our equations must satisfy $k \geq 0$, $n \geq 1$ and $\nu \geq 0$. With these restrictions, we find that there are at most three singular points at finite values. We note that $\nu = 0$ is an invariant set of the system (6.36)/(6.37), as is the set $\nu > 0$. As a result we need only consider the dynamics (and hence the singular points) in the half-plane $\nu \geq 0$.

Table 6.1: **Classification of Finite Singular Points for equations (6.36)-(6.37)**

	$\alpha^2 > 3k$		$\alpha^2 = 3k$	$\alpha^2 < 3k$
	$2\alpha - 3 \leq k$	$2\alpha - 3 > k$	$2\alpha - 3 \leq k$	$2\alpha - 3 < k$
	I	II	III	IV
Q_1	sink	sink	saddle-node	N/A
Q_2	source	saddle	($\equiv Q_1$)	N/A
Q_3	saddle	N/A	N/A	N/A

Summary of the nature of the finite singular points for the system (4.2)/(4.3). "N/A" indicates that the given point is not located in the physical region $\nu \geq 0$. The two cases (i) $\alpha^2 = 3k$, $2\alpha - 3 > k$ and (ii) $\alpha^2 < 3k$, $2\alpha - 3 \geq k$ are omitted since they do not give any real solutions for k and α .

The finite singular points (y_0, ν_0) are given by:

$$\begin{aligned} Q_1 &= \left(\frac{1}{3}(-\alpha + (\alpha^2 - 3k)^{1/2}, 0),\right. \\ Q_2 &= \left(\frac{1}{3}(-\alpha - (\alpha^2 - 3k)^{1/2}, 0),\right. \\ Q_3 &= (-1, 2\alpha - 3 - k). \end{aligned}$$

The nature of these singular points, which can be determined using standard techniques (Guckenheimer and Holmes, 1983), depends upon the relationship between the parameters α and k . The results are summarised in Table 6.1. Note that only those singular points which are located in the physical phase space are listed in this table. It is important to note that each of the cases I - IV is possible when considering the equations (6.36)/(6.37) in case A. In case B, however, we find that only the cases labelled (I) and (II) in table 6.1 yield consistent constraints on the parameter α .

We can complete the qualitative analysis of these two cases by considering the stability of the singular points at infinity. To perform the analysis at infinity, we apply the following Poincare transformation to our system (6.36)/(6.37) in order to compactify the phase space:

$$Y = \frac{y}{(1 + y^2 + \nu^2)^{1/2}}, \quad V = \frac{\nu}{(1 + y^2 + \nu^2)^{1/2}}. \quad (6.38)$$

In these new variables, the phase space has been compactified to the region $\Theta^2 = 1 - (Y^2 + V^2) \geq 0$, and all infinite points of the original system are found on the boundary $\Theta = 0$. The restriction that $\nu \geq 0$ implies that $V \geq 0$, and all finite singular points remain at finite values of Y and V and are of the same sign in the new coordinate system (Y, V) .

The transformed equations (6.36)/(6.37) are then given by:

$$Y' = \frac{1}{2}(4n-3)Y^2V^2 + \Theta\left[\frac{1}{2}Y + (2n-\alpha)V\right] - \frac{1}{2}\Theta^2[3Y^2 + kV^2] - \Theta^3\left[\alpha Y + \frac{1}{2}V\right] - \frac{1}{2}k\Theta^4, \quad (6.39)$$

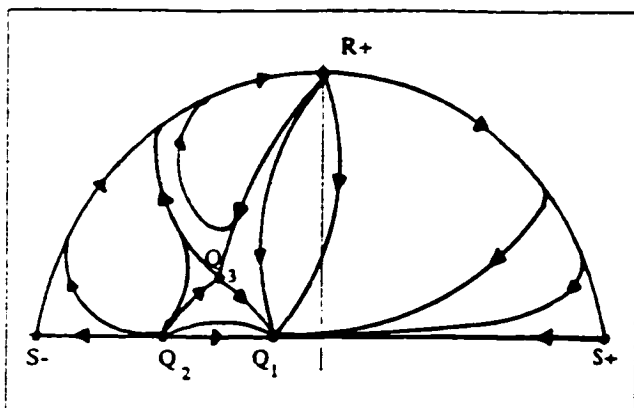
$$V' = -\frac{1}{2}(4n-3)Y^3V + \Theta YV\left[\frac{1}{2}V - (2n-\alpha)Y\right] + \frac{1}{2}\Theta^2 YV[k - 4n] - 2nV\Theta^3, \quad (6.40)$$

where $f' = \Theta \dot{f}$. There are four singular points at infinity located on the boundary $Y^2 + V^2 = 1$, which are given by

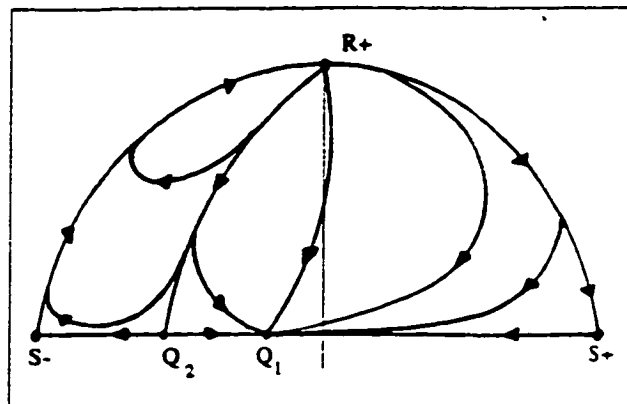
$$R_{\pm} = (0, \pm 1), \quad S_{\pm} = (\pm 1, 0). \quad (6.41)$$

The points S_{\pm} correspond to perfect fluid solutions, and R_{\pm} correspond to static solutions. A local stability analysis shows that the points S_{\pm} are both saddles. R_+ is a non-hyperbolic point containing both stable and unstable manifolds for all values of α and k . The stable manifold of R_+ lies in an elliptic sector of R_+ and corresponds to homoclinic orbits. The fixed point R_- is not in the physical phase space.

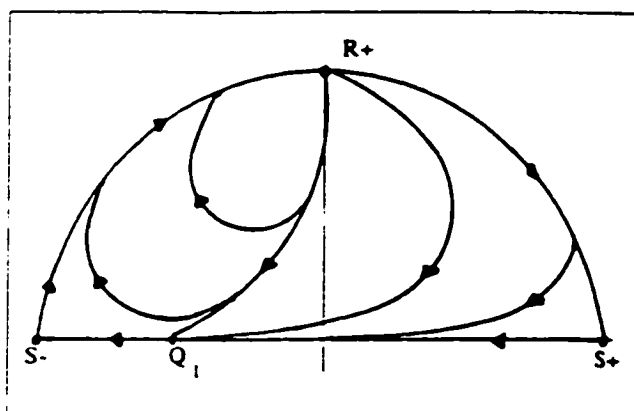
The phase portraits in the compactified phase space ($V^2 + Y^2 \leq 1, V \geq 0$) are given in Figures 6.1. From these portraits it is immediately evident that the only stable singular points (both to the past and the future) either lie in the $V = 0$ invariant set, occur at the infinite singular point R_+ , or occur at \mathbf{Q}_3 (when it exists in the phase space). Recall that the invariant set $V = 0$ represents the perfect fluid solutions studied previously, where in the equivalent “ $M_1 = 0$ ” case the solutions were shown to asymptote towards a flat FRW model. The fixed point R_+ has $y = 0$, and hence is a static solution. Finally, the fixed point \mathbf{Q}_3 has the property $y = -1$ (or $S + \dot{S} = 0$), which was examined in section 6.2. Since all of the solutions in the



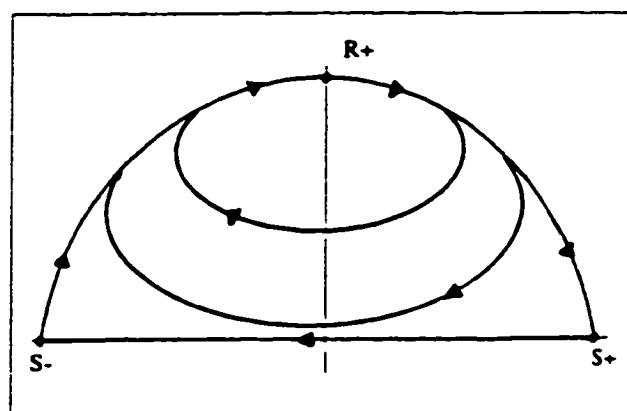
Case I



Case II



Case III



Case IV

Figure 6.1: Phase portraits for the system (6.39)/(6.40): for various ranges of values of α and k , where the particular cases are as listed in Table 6.1.

phase space, and in particular those asymptoting to the point Q_3 , have the property that $p_{\parallel} = P_{\parallel}(x)t^{-2}$, $p_{\perp} = P_{\perp}(x)t^{-2}$, and $\mu = W(x)t^{-2}$, by continuity so must the solution at Q_3 . Therefore the solution represented by the point Q_3 must be given by metric (6.23).

Consequently we see that in the analysis of the two cases considered in subsections 6.3.1 and 6.3.2 above the asymptotic behaviour is described by either a flat FRW perfect fluid model, a static model, or by that of metric (6.23). In all cases these exact asymptotic models admit a homothetic vector.

6.4 Discussion

We note that in the cases studied in this chapter the dynamics of the models is governed by a system of the form:

$$\dot{y} = -\frac{1}{2}(3y^2 + 2\alpha y) + f(\nu), \quad (6.42)$$

$$\dot{\nu} = -2n\nu(1 + y). \quad (6.43)$$

The variable ν is defined by equation (6.35) and the function $f(\nu)$ depends on the specific case being studied. In the cases considered in section 6.3 we had that:

$$f(\nu) = -\frac{1}{2}(\nu + \alpha^2 p_0): \text{ Case A: Dimensional Constants}$$

$$f(\nu) = -\frac{1}{2}\nu: \quad \text{Case B: Equations of State.}$$

The system (6.42)/(6.43) results whenever we impose the condition

$$P_{\parallel}(z) = -2\alpha^{-2}f(\nu). \quad (6.44)$$

In the cases examined in section 6.3 it was shown that all solutions necessarily asymptote to an exact solution admitting a homothetic vector. It is of interest to consider whether there are any possible asymptotic states for the geodesic anisotropic models which satisfy equation (6.44) that do *not* admit a homothetic vector.

As was the case in section 6.4, the perfect fluid solutions are located in the invariant set $\nu = 0$. The definition of ν requires that it be greater than or equal to zero. In the relevant phase space there are then (at most) three finite singular points of the system (6.42)/(6.43). These singular points, equivalent to those studied in section 6.4, are given by:

$$\begin{aligned} Q_1 &= \left(\frac{1}{3}[-\alpha + (\alpha^2 + 6f(0))^{1/2}], 0 \right) \\ Q_2 &= \left(\frac{1}{3}[-\alpha - (\alpha^2 + 6f(0))^{1/2}], 0 \right) \\ Q_3 &= (-1, f^{-1}(3/2 - \alpha)) \end{aligned}$$

The singular points Q_1 and Q_2 represent perfect fluid models, and Q_3 (as in section 6.4) is represented by the metric (6.23). In each case the model represented by the finite singular point admits a homothetic vector.

The only possibility for the asymptotic behaviour not to be governed by an exact homothetic model is then if (i) the model is represented asymptotically by a periodic orbit in the phase space, or (ii) the model is represented by a singular point at infinity not located on one of the coordinate axes $\nu = 0$ or $y = 0$.

In the first case we can impose necessary conditions for the existence of a periodic orbit. Any periodic orbit in a plane must necessarily enclose a singular point. As a result we must have that the point Q_3 is in the phase space in which case we necessarily have that $f^{-1}(3/2 - \alpha)$ is positive. The energy conditions requiring that the pressures and density are positive will result in the further condition that $f(\nu) \leq 0$, and therefore $\alpha \geq 3/2$ and $y \geq 0$. We consider the existence of a periodic orbit which encloses Q_3 by examining the horizontal and vertical isoclines of the system (6.42)/(6.43). The horizontal isoclines are located at (i) $\nu = 0$, an invariant line, and (ii) $y = -1$. The second case indicates that if there exists a periodic orbit about the point Q_3 then there must be vertical isoclines on either side of the line $y = -1$. Solving equation (6.43), we find that the vertical isoclines are given by

$$y_{\pm} = \frac{1}{3}(-\alpha \pm (\alpha^2 + 3f(\nu))^{1/2}). \quad (6.45)$$

Imposing the energy conditions $f(\nu) \leq 0$ and $\alpha \geq 3/2$, we find that the y -values of the vertical isoclines must satisfy

$$-1 \leq y \leq 0; \quad (6.46)$$

i.e., y_{\pm} cannot take on values less than -1 . Therefore, there can be no periodic orbits enclosing the point Q_3 if the energy conditions are to be satisfied.

If there is an asymptotic solution at infinite values of y and/or ν which is not homothetic then the corresponding singular point at infinity must be such that $y \neq 0$ or $\nu \neq 0$. This will occur when $\lim_{\nu \rightarrow \infty} f(\nu)\nu^{-2} \neq 0$. In such cases the infinite fixed point may represent a non-homothetic asymptotic solution. Therefore, geodesic models for which equation (6.44) and the energy conditions are satisfied will not admit a non-homothetic asymptotic solution whenever $\lim_{\nu \rightarrow \infty} f(\nu)\nu^{-2}$ is exactly zero.

6.5 Other Models

Additional anisotropic fluid models can be investigated. For example, we can consider the case in which the source is a combination of *a perfect fluid and a magnetic field* satisfying equations (6.4). Assuming $\bar{p} = (\gamma - 1)\bar{\mu}$ (where γ is a constant), in the geodesic case we can immediately derive the governing system as:

$$\dot{y} = -\frac{1}{2}(3y^2 + 2\alpha y) - \frac{1}{2}\alpha^2\eta, \quad (6.47)$$

$$\dot{\eta} = -4(1+n)y\eta - 4(n-1)(3-2\alpha)\alpha^{-2}y^2, \quad (6.48)$$

where $\eta \equiv -\alpha^{-2}(3y^2 + 2\alpha y + 2\dot{y}) = P_{||}$ and $n \equiv 1/\gamma$. The system (6.47)/(6.48) is of a similar form to equations (6.42) and (6.43) and can be analysed using similar techniques. In the special cases $\gamma = 1$ ($n = 1$) and $\alpha = 3/2$, equation (6.48) can be integrated immediately and exact solutions can be obtained. We note that at the equilibrium points of the system (6.47)/(6.48) $P_{||} = \text{constant}$ ($\dot{P}_{||} = 0$), and hence from equations (6.4), (6.11) and (6.12) we have that

$$\pi = \frac{1}{2}(p_{\perp} - p_{||}) = \frac{\dot{P}_{||}}{2t^2(1+y)} = 0; \quad (6.49)$$

hence these equilibrium points correspond to perfect fluid models.

However, in order to study the physics of this particular model we note that $\pi = \lambda H^2/2$ and equations (6.47) and (6.48) need to be supplemented by an additional differential equation (for H , derived from Maxwell's equations) and an assumption on the form of the magnetic permeability, λ .

Finally, we note that in the case in which $\pi = \text{constant} = \pi_0$ (with an unrestricted equation of state) it can be shown that the governing equations reduce to

$$\dot{y} = -\frac{1}{2}(3y^2 + 2\alpha y) - \alpha^2 \pi_0 \ln(\nu), \quad (6.50)$$

$$\dot{\nu} = -\nu(1 + y). \quad (6.51)$$

This system is of the same form as that of (6.42)/(6.43) with $f(\nu) = -\alpha^2 \pi_0 \ln(\nu)$ and with the constant $n = \frac{1}{2}$. Since (6.50)/(6.51) is of the same form we can immediately conclude that the only asymptotic states of the system necessarily admit a homothetic vector. Note that in this case $f(\nu)$ is not analytic at $\nu = 0$; however the physical phase space has $\nu > 0$.

Chapter 7

Discussion

7.1 Phase Space and Dynamics

In both the analysis of KSS of finite and infinite type the autonomous ODEs form a four-dimensional phase space. The existence of monotonic functions and invariant sets indicated that it was sufficient to examine the invariant sets of the shear-free solutions and the plane symmetric solutions (for the sake of determining the asymptotic behaviour). Each of these cases was examined in detail. The phase portraits for the shear-free solutions were completely determined by analytical means. The analysis of the plane symmetric solutions was made more complicated by the fact that the phase space is three-dimensional. In the case of the "infinite" KSS, the analysis was completed essentially using only the monotonicity principle. For the finite KSS case, however, there were several regions of the phase space for which no monotonic function was located. The behaviour in this case was, however, determined by a combination of numerical and analytic means.

In all cases, the asymptotic behaviour was found to be represented by simple singular points (either at finite or infinite values). The nature of the solutions represented by these points was determined with special attention paid to those solutions which satisfy the energy conditions since they will have more physical significance. We note that the saddle and saddle-node points were given equal importance as sinks

and sources in this analysis. Recalling that self-similar solutions are thought to be intermediate solutions of a larger class of solutions (Barenblatt and Zel'dovich, 1972) it is possible that the saddle points (representing possible intermediate asymptotic behaviour) may be as important physically as the sinks and sources.

7.2 Physical Self-Similarity

Throughout this thesis we have distinguished between the ideas of *geometric* and *physical* self-similarity. These two properties, while equivalent for perfect fluid solutions of the EFEs in the cases of self-similarity of the first kind (homothety), are not necessarily equivalent in the general case of kinematic self-similarity (Coley, 1997). The solutions for which both concepts of *physical* and *geometrical* self-similarity hold form invariant sets of the full four-dimensional system. In the coordinates of Chapter 4, these invariant sets (defined by either $x_3 = 0$ or $x_1 = 0$) are two-dimensional. However, integration allows for each to be reduced to a single differential equation which can be investigated. The results were given in Chapter 3 (see sections 3.1 and 3.2)

If we consider all the non-homothetic solutions for which the *total* energy and *total* pressure satisfy equations (1.8) [i.e., equations (1.16) and (1.17) are satisfied], so that the solution is both “physically” and “geometrically” self-similar, we find that the only possibilities are: (1) $M_1 = 0$ (where $a = b = -2\alpha$) and (2) $M_2 = 0$ (where $a = b = -2$). The exact solutions corresponding to each of these cases represent the most general spherically symmetric solutions that admit a kinematic self-similarity in the sense that all of equations (1.14), (1.15) *and* (1.20), (1.21) are satisfied [cf. Coley, 1997]. Again we note the fundamental importance of the solutions with $M_1 = 0$. In addition, we note that *all* physically acceptable solutions satisfying equations (1.20) and (1.21)) are necessarily asymptotic to an exact solution that admits a homothetic vector.

In Coley (1997), a set of integrability conditions (see equations (2.35)-(2.37) in

Coley (1997)) for the existence of a proper kinematic self-similarity in an irrotational perfect fluid spacetime was presented. For the models under consideration here, using the governing equations (2.60)-(2.63), these integrability conditions reduce to the following:

$$\frac{-2e^{-2\Psi}}{r^2} \left[\frac{e^{2\Psi}}{S^2} - (1+y)^2 - 3\dot{\Phi} - 2y\dot{\Phi} \right] = X \quad (7.1)$$

$$\frac{e^{-2\Phi}}{(\alpha t)^2} [3\alpha y + 4y^2 - y + 6y\dot{\Psi} + 3\dot{\Psi}] = X, \quad (7.2)$$

where

$$X = (m_1 W_1 + n_1 P_1) r^{-2} + (m_2 W_2 + n_2 P_2) (\alpha t)^{-2}, \quad (7.3)$$

and n_i and m_i are constants. We see that these integrability conditions are clearly satisfied in the two subcases $M_1 = 0$ and $M_2 = 0$. In the subcase $M_1 = 0$, we have that $m_1 = n_1 = 0$ and $m_2 = 3n_2 = -1$, and equations (7.1)/(7.2) contain all the solutions found in subsection 3.1. Likewise, in the subcase $M_2 = 0$, we have that $m_2 = n_2 = 0$ and $m_1 = -n_1 = 3$, and equations (7.1)/(7.2) contain all those solutions found in subsection 3.2. In fact, as was noted in the preceding paragraph, these two subcases correspond to the only possible solutions compatible with these integrability conditions.

Also in Coley (1997), a theorem was presented which states that given a “physically” kinematic self-similar solution with zero acceleration then the three spaces orthogonal to u^a are Ricci flat (i.e., ${}^3R_{ab} = 0$). Let us consider this theorem in the context of this thesis.

Given the metric (1.17), the Ricci tensor for the three spaces orthogonal to u^a can be calculated. If the solution admits a (non-homothetic) kinematic self-similarity then equations (2.60)-(2.63) allow the non-zero terms of ${}^3R_{ab}$ to be simplified. These non-zero terms are given as:

$${}^3R_{11} = 2y(x)\dot{\Phi}(x)r^{-2} \quad (7.4)$$

$${}^3R_{22} = e^{-2\Psi(x)} S^2(x) [2y(x) + y(x)\dot{\Phi}(x) + y^2(x) + 1] - 1 \quad (7.5)$$

$${}^3R_{33} = \sin^2(\theta) R_{22}. \quad (7.6)$$

Notice that the theorem summarised in the previous paragraph is verified since zero acceleration implies that $\dot{\Phi} = 0$ and “physical” self similarity then requires (from section 3.1) that $(1 + y)^2 = e^{2\psi(x)} S^{-2}(x)$.

On the other hand, from equations (7.4)-(7.6) it is easy to see that if ${}^3R_{11} = 0$ then either (a) $\dot{\Phi}(x) = 0$ or (b) $y(x) = 0$. Each of these cases have been examined in detail in Chapter three as they represent the only cases in which a single fluid model admits both “physical” and “geometrical” kinematic self-similarity. The conditions in each of these cases for which ${}^3R_{22}$ (and hence ${}^3R_{33}$) vanish is equivalent to the conditions required from the EFEs (see sections 3.1 and 3.2 respectively).

Thus, we can state the following result which complements the theorem of Coley (1997):

Given a perfect fluid spherically symmetric model which exhibits a non-homothetic kinematic self-similarity, the three spaces orthogonal to the fluid velocity are Ricci flat (i.e., ${}^3R_{ab} = 0$) **if and only if** the model is “physically” self-similar.

Two special cases that have not been considered in the thesis are those in which the kinematic self-similarity ξ is either parallel to or orthogonal to the fluid four-velocity u (see equation (1.16)). However, in a recent general analysis of irrotational perfect fluid spacetimes admitting a kinematic self-similarity (Coley, 1997) these two cases were explicitly investigated and we can deduce the appropriate results in the special case of spherical symmetry. In particular, it was shown that all such spacetimes admitting a kinematic self-similarity parallel to u^a are necessarily FRW spacetimes, and the existence of kinematic self-similar vectors in FRW spacetimes (in all cases, i.e., not just in the case in which ξ is parallel to u) was studied in detail therein. In the case in which ξ is orthogonal to u a number of consequences were obtained (Coley, 1997); however, we note that Ponce de Leon (1993) claims that in all spherically symmetric spacetimes in which there exists a vector field that satisfies equation (1.15) which is orthogonal to u , the resulting metric is singular.

While the entire four-dimensional space of solutions is not necessarily physically

self-similar, it is worthwhile to note that if the fluid is considered to be a non-interacting sum of two perfect fluids so that equations (3.3)-(3.4) are the density and pressure definitions for each fluid, then **all** solutions satisfy the condition of physical self-similarity, in that both of these perfect fluids will necessarily be self-similar.

7.3 Physical Considerations: Equation of State and Energy Conditions

As the solutions studied throughout this work are of physical interest it is important to consider which of the solutions satisfy relevant physical criteria. The first of these criteria is that of the energy conditions. Solutions of physical interest are normally assumed to satisfy energy conditions, the weakest of which is to demand that the energy density be positive, and allowing for negative pressure only if the sum of the pressure and density is always positive, i.e.

$$\mu \geq 0 \quad p + \mu \geq 0. \quad (7.7)$$

These conditions are the “Weak Energy Conditions” (WECs). The functional form for p and μ given in Chapter 2 (see equations (2.64) and (2.65)) create complications when investigating these WECs. In particular, we note that it is a straightforward matter to determine the conditions under which the WECs are satisfied at late time (i.e., $t^{-2} \rightarrow 0$) and at large r (i.e., $r^{-2} \rightarrow 0$). For intermediate values of r and t , however, the conditions become ambiguous as an interplay between the coefficients of r^{-2} and t^{-2} can occur. When the lower bound of the WECs found for large r and or large t define an invariant set of the dynamical system, however, the investigation of these physical conditions is greatly simplified since orbits (or solutions) can not pass through these sets. This is exactly the case that occurs when investigating the solutions with “infinite” KSS. In the finite case, however, the lower bound of the energy conditions is not an invariant set and solutions can cross these bounds at such

a time as to **not** violate the WECs. As such it is difficult to completely classify all solutions which satisfy the WECs for all time. We will, therefore, consider the WECs in the three following different cases; namely (i) physical self-similarity, (ii) two fluid model, and (iii) the single fluid model.

1. **Physical Self-similarity:** In the case of physical self-similarity we have seen that the form of the density and pressure simplifies to either (a) $\mu = W(\xi)r^{-2}$ and $p = P(\xi)r^{-2}$, or (b) $\mu = W(\xi)t^{-2}$ and $p = P(\xi)t^{-2}$ (the geodesic solutions). In each of these cases the WECs are easily determined. The one-dimensional phase space is then limited to the portion of the line which does not include solutions violating the WECs, and depending on the relationship between the dimensional constant which appears in the solutions and the various other constants (which determine the location of the singular points) the set of possible asymptotic behaviours is reduced.
2. **Two-Fluid Model:** In the two fluid model it is necessary from a physical viewpoint that **both** fluids individually satisfy the WECs. The WECs then become the combination of *each* of the conditions for the “physical” self-similar case. The constraints are now surfaces through which solutions of physical significance cannot pass. Passage through these surfaces would result in one (or both) of the fluids becoming “unphysical.”
3. **One-Fluid Model:** In the case of a single fluid, the functional form for μ and p complicate the investigation. It is possible to demand that each term in the definitions for p and μ (i.e. the coefficients of r^{-2} and t^{-2} respectively) must satisfy the WECs. This condition does not, however, identify all solutions which satisfy the WECs. It is possible that a solution crosses the boundaries determined by these conditions in such a way that the interplay between the two terms allows the overall result (be it the density or the sum of the density and pressure) to maintain its positive sign. In the cases considered in this thesis, however, each solution which passes through one (or more) of these boundaries

has asymptotic behaviour represented by one of the singular points. We have shown that for each of the singular points lying in the region of space where the WECs for either of the individual terms of the density and pressure are violated the *total* energy and pressure also violate the WECs (both at the exact solution represented by the singular point and all solutions which asymptote to that singular point). As a result, we can conclude that the solutions which satisfy the WECs must (necessarily) be represented by orbits which do not cross these boundaries.

In this investigation of the WECs we note that in general the boundary between physical and unphysical solutions is **not** an invariant set of the system. This differs from previous qualitative investigations within GR (see for example Coley and Wainwright,1992) where the boundary between the physical and unphysical was a “dynamical” as well as “physical” object, i.e. it defined an invariant set. In these cases the energy conditions provided an obvious manner in which to compactify the phase space. Note again that in the case of “infinite” KSS the necessary conditions for the WECs to be satisfied do indeed define invariant sets of the system.

We now turn our attention to the equation of state for the matter. We have shown that for an equation of state to exist, i.e., $p = f(\mu)$, we must necessarily have that the fluid is either (i) **physically** self-similar or (ii) the fluid is “dust”, i.e. $p = 0$ [which was studied by Carter and Henriksen (1989)], a subcase of the physically self-similar models. The equation of state will necessarily be linear, i.e. $p = (\gamma - 1)\mu$. In general, however, the solutions of the full system do not exhibit an equation of state.

In the case of physical self-similarity, the only possible solutions with an equation of state are located at the finite singular points of the system. In the case of the geodesic solutions examined in Section 3.1, these solutions are the flat FRW models, and as such necessarily admit a homothetic vector and a linear equation of state. In the second case of physical self-similarity with $M_2 = 0$ the solutions with an equation of state once again correspond to the finite singular points. These solutions are static, admitting a homothetic vector and a linear equation of state.

Again, if we consider the solutions as a non-interacting sum of perfect fluids, we see that it may be possible to have an equation of state for more general solutions than just those that are physically self-similar. In the case of the two-fluid model we demand that each fluid separately satisfy an equation of state. Once again, the functional form of the density and pressure would exclude all possibilities but the linear equation of state.

7.4 Remarks

We note that in the homothetic case, studied in detail previously (Cahill and Taub, 1971; Carr and Coley, 1998), the governing equations are not autonomous in the variables (and coordinates) utilised here. In Bogoyavlenskij (1985) a coordinate transformation was effected [see equations (3.9) in chapter IV - let us denote this by equations B(3.9)] which changed the form of the homothetic ($\alpha = 1$) spherically symmetric metric (1.17) [equation B(3.1)] to the conformally static form [equation B(1.1)] in which the resulting ODEs are in fact autonomous (in these coordinates). [See also Goliath et. al., 1998a and 1998b]

If we apply an analogous [to B(3.9)] transformation of coordinates of the following form in the non-homothetic case ($\alpha \neq 1$)

$$t = Re^{\alpha\tau}, \quad r = f(R)R^{1/\alpha}e^\tau, \quad (7.8)$$

where f is an arbitrary function of R , then the *kinematic self-similarity* is indeed of the form $\xi = \frac{\partial}{\partial\tau}$, and the self-similarity coordinate $\xi \equiv r(\alpha t)^{-1/\alpha} = f(R)\alpha^{-1/\alpha}$ is also a function of R alone. However, for $\alpha \neq 1$ the metric does not transform to as simple a form as in the homothetic ($\alpha = 1$) case. In any event, the resulting autonomous ODEs are equivalent to those studied in this paper [cf. equations (2.15)-(2.17)].

In subsection 3.1 the important subcase $M_1 = 0$ was studied. In this subcase the governing equations can be completely integrated, and the exact solutions obtained (containing the dimensional constant p_0) are a generalisation of the dust solutions of Lynden-Bell and Lemos (1988) and Carter and Henriksen (1989). The properties of

these solutions, including their asymptotic behaviour, were discussed in this thesis; in particular, it was shown that these solutions are asymptotic to exact (flat) FRW solutions (which are known to admit a proper homothety). This last property, that solutions are asymptotic to exact homothetic solutions, is true in more generality, as can be seen from the analysis of the equilibrium points at finite values (see below). The subcase $M_1 = 0$ in the case $\alpha = 0$ was studied in subsection 3.2.

The special subcase $M_2 = 0$ was studied and the exact solutions were exhibited in the static subcase. Again we note that these static solutions necessarily admit a homothetic vector. The subclass of solutions in the subcase $M_2 = 0$ necessarily contain all static metrics which admit a kinematic self-similarity, although there are solutions in this special subcase which are not static. The result that all static metrics admitting a kinematic self-similarity are contained in the subcase $M_2 = 0$ and necessarily admit a homothetic vector is not dependent on any assumptions regarding the matter.

Finally, coordinate transformations can be made in all cases ($\alpha = 1$, $\alpha = 0$, α finite but not 1 or 0, and " $\alpha = \infty$ "; where α is assumed to be non-negative) in order for the kinematic self-similarity to be put into a canonical form. In the homothetic case, ξ is given by (1.12) with $\alpha = 1$ and $\beta = 0$, and the metric is given by (1.13). It is informative to write out the metric in these canonical coordinates in the non-homothetic cases. Defining $\bar{t} = (\alpha t)^{1/\alpha}$ in equation (1.12) we obtain

$$\xi = \bar{t} \frac{\partial}{\partial t} + r \frac{\partial}{\partial r}. \quad (7.9)$$

In these coordinates, (1.13) is given by

$$ds^2 = -e^{2\Phi(r/\bar{t})} \bar{t}^{2(\alpha-1)} d\bar{t}^2 + e^{2\Psi(r/\bar{t})} dr^2 + r^2 S^2(r/\bar{t}) d\Omega^2. \quad (7.10)$$

Under the transformation $\bar{t} \rightarrow a\bar{t}$, $r \rightarrow ar$ we see that (3.14) is equivalent to

$$ds^2 = -e^{2\bar{\Phi}(r/\bar{t})} \bar{t}^{2(\alpha-1)} d\bar{t}^2 + a^2 e^{2\Psi(r/\bar{t})} dr^2 + a^2 r^2 S^2(r/\bar{t}) d\Omega^2, \quad (7.11)$$

or

$$ds^2 = -a^{2\alpha} e^{2\Phi(r/\bar{t})} \bar{t}^{2(\alpha-1)} d\bar{t}^2 + a^2 e^{2\Psi(r/\bar{t})} dr^2 + t^2 \bar{S}^2(r/\bar{t}) d\Omega^2. \quad (7.12)$$

In the case $\alpha = 0$, we can define $\bar{t} = e^t$ in equation (1.12), so that ξ is again given by equation (3.13). Under this redefinition we find that (1.13) is equivalent to (3.15) with α set equal to zero. Lastly, in the “infinite” case, we find that under the definition $\bar{t} = e^t$ the similarity vector (1.12) is transformed to (3.13), and the metric (1.13) takes on the same form as (3.15) (where 1 is “neglected” with respect to α (i.e., $\alpha \gg 1$) and α can then be rescaled to 1; i.e., the first term in equation (3.15) contains the term r^2).

7.5 Brief comments on future work

Throughout this thesis attention has been paid on the asymptotic states of solutions to the EFEs. As a result of this work several questions have been raised, each of which identify areas for future work. Briefly, these questions and future work include:

1. It has been conjectured that self-similar models play an important role in the asymptotic behaviour of more general models. It would be interesting to investigate whether the self-similar (homothetic or kinematic) models studied in this thesis, and in particular the spherically symmetric models, do indeed play such a role in a more general class of models. This would involve investigating the local stability of the KSS and/ or homothetic class of solutions with respect to the system of PDEs which govern the more general class of models.
2. It has also been conjectured, both by Barenblatt and Zel’dovich (1972) in the Newtonian case and Henriksen and Carter (1989) in the relativistic case, that KSS solutions may correspond to *intermediate* asymptotics. It is of interest to determine if this is in fact the case. Each of the asymptotic states of the system of equations studied in this thesis indicates that the long term behaviour of KSS solutions have higher symmetry; e.g., in the case of the physically valid solutions, all solutions asymptote to solutions which admit a self-similarity of the first kind. This raises the question as to whether the dynamics of the

governing equations for which the KSS vector field exists “forces” the asymptotic solutions to admit a higher symmetry.

3. From a purely mathematical viewpoint, the task of locating the asymptotic solutions in this thesis has illustrated that lack of tools available when analysing three-dimensional phase spaces qualitatively. There are a wide range of questions which remain unanswered in this area. In particular, it may be possible to further develop the techniques utilised throughout sections 4.2 and 5.2.2.

Appendix A

Investigation of Eigenvalue Algebra

In section 4.2 the classification of the points \mathbf{R}_{\pm} are determined by examining the signs of the eigenvalues. Since the eigenvalues can not be determined in closed form, properties of the roots of polynomial are exploited to determine the signs. A review of the derivation is given below.

First, note that if λ_i is a real root then it can be zero *iff* the constant term of the quartic equation, namely $e(\alpha)$ is identically zero. Therefore we have zero real eigenvalues in the following cases:

$$\mathbf{R}_+ \quad \alpha = \sqrt{2} - 1 \quad \text{and} \quad 3;$$

$$\mathbf{R}_- \quad \alpha = 0$$

The **imaginary** roots with zero real part can be found by solving the characteristic equation (4.30) when λ is replaced by κi , i.e. solve the equation

$$a(\alpha)d(\alpha)^2 - b(\alpha)c(\alpha)d(\alpha) + b(\alpha)^2e(\alpha) = 0 \tag{A.1}$$

for α . For \mathbf{R}_+ the only real positive solutions to this equation occur when α is 3 and $\sqrt{2} - 1$ (as found when locating the real bifurcation values) and at

$$\alpha = r_1 \approx 1.067836956 \tag{A.2}$$

found numerically. There are no real positive solutions in the case of \mathbf{R}_- .

For a general n^{th} order polynomial

$$P(\lambda) = \sum_{i=0}^n p_i \lambda^i \quad (\text{A.3})$$

the roots $\{\lambda_i | i = 0..n\}$ necessarily satisfy the relations:

$$\sum_{i=0}^n \lambda_i = \frac{-p_{n-1}}{p_n}, \text{ and} \quad (\text{A.4})$$

$$\prod_{i=0}^n \lambda_i = (-1)^n \frac{p_0}{p_n}, \quad (\text{A.5})$$

and it immediately follows from equation (A.5) that when we only consider the **real** part of the roots:

$$n \text{ even} : \quad \text{Sign}(\prod_{i=0}^n \lambda_i) = \text{Sign}(\prod_{i=0}^n \text{Re} \lambda_i) \quad (\text{A.6})$$

$$n \text{ odd} : \quad \text{Sign}(\prod_{i=0}^n \lambda_i) = -\text{Sign}(\prod_{i=0}^n \text{Re} \lambda_i) \quad (\text{A.7})$$

Applied to the point \mathbf{R}_+ we then have

$$\frac{b(\alpha)}{a(\alpha)} < 0 \quad \forall \alpha \geq 0 \quad \rightarrow \sum_{i=1}^4 \text{Re}(\lambda_i) < 0 \quad \forall \alpha \geq 0 \quad (\text{A.8})$$

$$\frac{e(\alpha)}{a(\alpha)} \geq 0 \quad \forall \alpha \geq 3, \quad \rightarrow \prod_{i=1}^n \text{Re}(\lambda_i) \geq 0 \quad \forall \alpha \geq 3, \quad (\text{A.9})$$

$$(\text{A.10})$$

It then follows immediately that either two of the eigenvalues are positive or *no* eigenvalues are positive $\forall \alpha \geq 3$.

To determine which of these cases applies we consider the eigenvalues when α is large (i.e. $\alpha \rightarrow \infty$). In this case the quartic characteristic equation is

$$2(4\lambda + \alpha)(4\lambda + 3\alpha)(8\lambda^2 - 2\lambda\alpha + \alpha^2) \quad (\text{A.11})$$

so the eigenvalues (at large α) are:

$$\lambda_1 = -\alpha/4 \quad \lambda_2 = -3\alpha/4 \quad \lambda_{3,4} = \alpha \pm \sqrt{7}i$$

implying that $\forall \alpha \geq 3$ there is exactly 2 eigenvalues with positive real part and 2 with negative real parts. Therefore in the range $\alpha \in (3, \infty)$ the point \mathbf{R}_+ is a saddle.

To examine the nature of this point in the range $\alpha \in [0, 3)$ we consider each of the eigenvalues separately. When the n_{th} term of a polynomial, (A.3), is not zero the roots will be continuous if each of the terms of (A.3) have continuous coefficients. In the case of \mathbf{R}_+ the term $a(\alpha)$ has no roots in the domain $\alpha \in [0, \infty)$, therefore, since each of the remaining coefficients is continuous we necessarily have that the eigenvalues will each be continuous functions of α . The values for each eigenvalue are calculated numerically for values of the parameter α from 0 to 3. Since the real parts of the eigenvalues can only become zero at $\sqrt{2} - 1$, 3 and τ_1 we focus attention in these regions. The plot of the functions for λ_i , $i = 1..4$ are given in figures 4.5, 4.6, and 4.7. As can be seen in all regions (except at the bifurcation values) this point is a saddle (i.e., has both positive and negative eigenvalues).

Note that the three eigenvalues labelled λ_1 , λ_2 and λ_3 are representative of the dynamics in the invariant set $x_4 = 0$, therefore when constrained to this invariant set and in the region $\alpha \in (\tau_1, 3)$ all three are negative. For all other values of α there are both positive and negative eigenvalues.

This analysis is then repeated for the point \mathbf{R}_- where

$$\frac{b(\alpha)}{a(\alpha)} > 0 \quad \forall \alpha \geq 0 \quad \rightarrow \sum_{i=1}^4 Re(\lambda_i) > 0 \quad \forall \alpha > 0 \quad (\text{A.12})$$

$$\frac{e(\alpha)}{a(\alpha)} < 0 \quad \forall \alpha \geq 0, \quad \rightarrow \prod_{i=1}^n Re(\lambda_i) \leq 0 \quad \forall \alpha > 0, \quad (\text{A.13})$$

$$(\text{A.14})$$

It then follows immediately that either only one eigenvalue is positive or exactly one eigenvalue is negative $\forall \alpha \geq 0$. Once again the exact condition is determined by considering α very large (i.e. $\alpha \rightarrow \infty$). In this case the characteristic equation becomes

$$2(\lambda + \alpha)(\lambda + \alpha)(\lambda^2 - \lambda\alpha + \alpha^2) \quad (\text{A.15})$$

so the eigenvalues (for large α) are:

$$\lambda_1 = \lambda_2 = -\alpha \quad \lambda_{3,4} = 1/2(\alpha \pm \sqrt{3}\alpha i)$$

implying that $\forall \alpha \geq 0$ there is exactly 1 eigenvalue with positive real part and 3 with negative real parts. Therefore in the range $\alpha \in (0, \infty)$ the point \mathbf{R}_- is a saddle. The eigenvalues labelled λ_1 , λ_2 and λ_3 are again representative of the dynamics in the invariant set $x_4 = 0$, therefore when constrained to this invariant set there are both positive and negative eigenvalues.

References

- Aulbach B., 1984, Continuous and Discrete Dynamics near Manifolds of Equilibria, Lecture Notes in Mathematics, No. 1058 (Springer)
- Barenblatt G E and Zel'dovich Ya B, 1972, Ann Rev Fluid Mech, **4**, 285
- Barenblatt G E, 1952, Prikl Mat Mekh, **16**, 67
- Barriola and Vilenkin, 1989, Phys Rev Letts, **63**, 341
- Benoit P M and Coley A A, 1996, Proc 6th Canadian Conf on General Relativity and Astrophysics (Fields Institute Communication Series 15) ed S P Braham, J D Gegenberg and R J McKellar (Providence, RI: AMS)
- Benoit P M and Coley A A, 1998, Class Quan Grav, **15**, 2397
- Benoit P M and Coley A A, 1999, to appear in J Math Phys,
- Bogoyavlenskij O J, 1985, Methods in Qualitative Analysis of Dynamical Systems in Astrophysics and Gas Dynamics (Heigelberg: Springer)
- Cahill M E and Taub A H, 1971, Commun Math Phys, **21**, 1
- Carot and Sintes, 1994, Class Quantum Grav, **11**, L125
- Carr B J and Coley A A, 1998, Class Quan Grav, **15**,
- Carr B J and Koutras A, 1993, Astrophys J, **405**, 34

- Carr B J and Yahill A, 1990, *Astrophys J*, **360**, 330
- Carter B and Henriksen R N, 1989, *Ann Phys Paris*, **14**, 47
- Carter B and Henriksen R N, 1991, *J Math Phys*, **32**, 2580
- Coley A A and Tupper B O J, 1986, *J Math Phys*, **27**, 406
- Coley A A and Tupper B O J, 1994, *Class Quan Grav*, **11**, 2553
- Coley A A and Wainwright J, 1992, *Class Quan Grav*, **9**, 651
- Coley A A, 1997, *Class Quantum Grav*, **14**, 87
- Eardley D M, 1974, *Commun Math Phys*, **37**, 287
- Eardley D M, 1974, *Phys. Rev. Lett.* **33**, 442.
- Ellis G F R, 1971, *Relativistic Cosmology General Relativity and Cosmology*, XLVII (Corso 1969) ed R Sachs (New York: Academic)
- Goliath M, Nilsson U S, and Uggla C, 1998a, *Class Quan Grav*, **15**, 2841
- Goliath M, Nilsson U S, and Uggla C, 1998b, *Class Quan Grav*, **19**, 167
- Guckenheimer J and Holmes P, 1983, *Nonlinear Oscillations, Dynamical Systems, and Bifurcations of Vector Fields* (Wiley)
- Henriksen R N, 1989, *Mon Not R Astron Soc*, **240**, 917
- Henriksen R N, Emslie A G and Wesson P S, 1983, *Phys Rev D*, **27**, 1219
- Henriksen R N and Patel K, 1991, *Gen Rel Grav*, **23**, 527
- Ibenez and Sanz, 1982, *J Math Phys*, **23**, 1964
- Ikeuchi S, Tomisaka K and Ostriker J P, 1983, *Ap J.*, **265**, 583
- LeBlanc V G, Kerr D and Wainwright J, 1995, *Class Quantum Grav*, **12**, 513

- Lynden-Bell D and Lemos J P S, 1988, *Mon Not R Astron Soc*, **233**, 197
- Maartens R and Maharaj S D, 1986, *Class Quant Grav*, **3**, 1005
- Maartens R, Mason D P and Tsamparlis M, 1986, *J. Math. Phys.* **27**, 2987.
- Ori A and Piran T, 1990, *Phys Rev D*, **42**, 1068
- Ovsiannikov, 1982, *Group Analysis of Differential Equations*, (London: Academic)
- Penstone M V, 1969, *Mon Not R Astron Soc*, **144**, 425
- Ponce de Leon J, 1993, *Gen Rel Grav*, **25**, 865
- Schwartz J, Ostriker J P and Yahill A, 1975, *Astrophys J*, **202**, 1
- Sedov L I, 1959, *Similarity and Dimensional Methods in Mechanics* (New York: Academic)
- Sedov L I, 1967, *Similarity and Dimensional Methods in Mechanics* (New York: Academic)
- Tavakol R, 1997, in *Dynamical Systems in Cosmology*, ed. Wainwright and Ellis, (Cambridge: University Press)
- Taylor G I, 1950, *Proc Roy Soc London*, **A201**, 175
- Vilenkin and Shellard, 1994
- Wainwright and Ellis, 1997, *Dynamical Systems in Cosmology* (Cambridge: University Press)
- Wesson P S, 1979, *Astrophys J*, **228**, 647
- Wiggins S, 1990, *Introduction to Applied Nonlinear Dynamical Systems and Chaos* (Springer)

Yano K, 1955, The Theory of Lie Derivatives (Amsterdam: North Holland)

Zel'dovich Ya B and Kompaneets A S, 1950, Izd Akad Nauk SSSR, Moskow, 61

Zel'dovich Ya B and Raizer Yu P, 1963, Physics of Shock Waves and High Temperature Phenomena (New York: Academic)